Geothermometry of selected Montana hot spring waters
by Michael Bernard Kaczmarek

A thesis submitted to the Graduate Faculty in partial fulfillment of the requirements for the degree of
MASTER OF SCIENCE with concentration in Geology
Montana State University
© Copyright by Michael Bernard Kaczmarek (1974)

Abstract:
The base temperature of hot-water dominated hydro-thermal systems can be quantitatively estimated using two different methods. One method uses the concentration of dissolved silica in the discharge wasters in equilibrium with respect to quarts. The other method is based on the ha, K, and Ca concentrations in the discharge waters in equilibrium with solid mineral phases in the wall rocks. Experimental studies and practical applications of these two hydrogeothermometers have been largely limited to the temperature range of 200 to 360°C. This paper presents some results of application of both methods in the temperature range 15 to 150°C.

Dissolved silica calculated base temperatures are reliable for undiluced thermal waters in the temperature range studied. Sources of error are cold water dilution of thermal waters and assimilation of silica from amorphous silica in wall rocks.

Base temperatures calculated from Na, K, and Ca concentrations in discharge waters are generally inaccurate. Errors in the calculated temperatures result from the fact that net water/rock reactions in the temperature range 15 to 150°C may be significantly different from those in the range 200 to 360°C, Net water/ rock reactions for the temperature range 15 to 150°C are presented here and the importance of E-mica versus kaolinite mineral phase stability is discussed.

The hydrogeology of six Montana and one Idaho hot springs is presented herein. Base temperatures are calculated for each hydrothermal system and are evaluated as to their reliability. Suggestions are made for further research on application of the Na-K-Ca hydrogeothermometer in the temperature range 15 to 150°C.

In presenting this thesis in partial fulfillment of the requirements for an advanced degree at Montana State University, I agree that the Library shall make it freely available for inspection. I further agree that permission for extensive copying of this thesis for scholarly purposes may be granted by my major professor, or, in his absence, by the Director of Libraries. It is understood that any copying or publication of this thesis for financial gain shall not be allowed without my written permission.

Signature Michael B Kacymarek

Date June 17, 1974

GEOTHERMOMETRY OF SELECTED MONTANA HOT SPRING WATERS

by

Michael Bernard Kaczmarek

A thesis submitted to the Graduate Faculty
in partial fulfillment of the requirements for the degree

of

MASTER OF SCIENCE

with concentration in

Geology (Earth Sciences)

Approved:

Milton J. Edw
Head, Major Department

Robert A. Chadwick
Chairman, Examining Committee

F. Goering
Graduate Dean

MONTANA STATE UNIVERSITY
Bozeman, Montana

August, 1974

N378
K115
cop. 2

VITA

Michael Bernard Kaczmarek was born on May 7, 1945 in Missoula Montana. His parents are Bernard Kaczmarek (deceased) and Wilma Osmond Kaczmarek. He is married to the former Helen Phyllis Gruel of Portage, Montana and they have two children, Jennifer and John.

Michael graduated from Shelby High School in Shelby, Montana, in May of 1963. He entered Montana State University in Bozeman, Montana, in the fall of that year. After receiving his Bachelor of Science degree in Earth Sciences (Geology option) from that institution in August of 1968, he began four years of active duty as an officer in the Army Corps of Engineers.

Following their marriage on April 12, 1969; Michael and Helen lived 15 months in Sattahip, Thailand, and two years in Fort Lewis, Washington. Michael returned to Montana State University in August of 1972 where he has since held a Graduate Teaching Assistantship while working towards the degree of Master of Science.

ACKNOWLEDGEMENTS

The author is much indebted to his advisor, Dr. Robert A. Chadwick, for his helpful advice and review of this manuscript. Dr. Ray Woodriff of the Montana State University Chemistry Department and Dr. Murray Klages of the Montana State University Plant and Soils Science Department have been especially helpful in assisting in spectrochemical analysis and X-ray diffraction identification of rock and mineral composition.

Funding of the field work making this project possible was provided by the Montana Power Company, and much assistance was kindly provided by many members of the Montana State University Earth Sciences Department.

Most of all, the author would like to thank his wife, Helen, for her unselfish support and patience through two years of study and a second child. Without her firm support, this thesis would not have been completed.

TABLE OF CONTENTS

	Page
INTRODUCTION	1
Purpose and Scope	1
Location and Physiography	2
Methods of Investigation	2
Previous Work	4
PHYSICAL CHARACTERISTICS OF HOT SPRINGS	5
Hydrothermal Systems	5
Heat Sources	5
Temperature	9
Geohydrology	10
Reservoir Fluid Phases	13
Vapor Versus Liquid	15
CHEMICAL CHARACTERISTICS OF HOT SPRINGS	17
Application	17
General Conditions	17
Source of Dissolved Solids	18
Soluble Element Equilibria	18
Soluble Mineral Equilibria	19
Mineral Phase Equilibria	21
Hydrologic Effects	23
An Example	24
GEOTHERMOMETRY	27
Qualitative Indicators	27
Dissolved Silica Hydrogeothermometer	28
Na-K-Ca Hydrogeothermometer	32
MONTANA HOT SPRINGS	40
Hot-Water System Subtypes	40
Relative Economic Potential	40
Representative Hot Springs	42
The Boulder Batholith	44
Alhambra Hot Springs	52
Boulder Hot Springs	54
Helena Hot Springs	57
Puller Hot Springs	59
Hunters Hot Springs	61
Big Spring	66
Salmon Hot Springs	69

Page

HYDROGEOCHEMICAL INTREPRETATIONS 71
Dilution Effects 71
Dissolved Silica Interpretation 75
Na-K-Ca Temperature Interpretation 82
Water-Rock Reactions 87
Evaluation of Net Reactions 94
Mineral Stability 97
Conclusions 103

BASE TEMPERATURES. 106
Range 106
Control 107
Geothermal Gradient 109

SUMMARY. 114

APPENDIX I 117

APPENDIX II. 124

APPENDIX III 130

REFERENCES CITED 133

LIST OF TABLES

		Page
Table I	Chemical and modal composition of rocks in the Butte Quartz Monzonite	47
Table II	Heat flow	51
Table III	Thermal water data.	77

LIST OF FIGURES

		Page
Figure 1	Regional geology and hot spring locations	3
Figure 2	Sketch of Model Hydrothermal system	6
Figure 3	Phase diagram for Ca and K minerals at 260°C	26
Figure 4	Dissolved silica in equilibrium with quartz in thermal water	29
Figure 5	LogK* vs $10^3/T$.	33
Figure 6	Regional geology of Boulder Batholith	45
Figure 7	Geology of the Alhambra Hot Springs area.	53
Figure 8	Preliminary geologic map of the Boulder Hot Springs area.	55
Figure 9	Geology of the Helena Hot Springs area	58
Figure 10	General geology of Pullers Hot Springs area, Ruby River basin.	60
Figure 11	Regional geology; Hunters Hot Spring area.	63
Figure 12	Geology of the Big Spring area, Toston	67
Figure 13	Geology of the Salmon Hot Springs area	70
Figure 14	Log($Ca^{\frac{1}{2}}$/Na) and log($Ca^{\frac{1}{2}}$/K) vs reciprical of temperature	90
Figure 15	Stability relations of the phases in the system K_2O-Al_2O_3-SiO_2-H_2O at 25°C (298.15°K)	98
Figure 16	Stability relations of the phases in the system K_2O-Al_2O_3-SiO_2-H_2O at 127°C (400°K)	98
Figure 17	Heat flow in the western United States	110

ABSTRACT

The base temperature of hot-water dominated hydrothermal systems can be quantitatively estimated using two different methods. One method uses the concentration of dissolved silica in the discharge wasters in equilibrium with respect to quartz. The other method is based on the Na, K, and Ca concentrations in the discharge waters in equilibrium with solid mineral phases in the wall rocks. Experimental studies and practical applications of these two hydrogeothermometers have been largely limited to the temperature range of 200 to 360°C. This paper presents some results of application of both methods in the temperature range 15 to 150°C.

Dissolved silica calculated base temperatures are reliable for undiluted thermal waters in the temperature range studied. Sources of error are cold water dilution of thermal waters and assimilation of silica from amorphous silica in wall rocks.

Base temperatures calculated from Na, K, and Ca concentrations in discharge waters are generally inaccurate. Errors in the calculated temperatures result from the fact that net water/rock reactions in the temperature range 15 to 150°C may be significantly different from those in the range 200 to 360°C. Net water/rock reactions for the temperature range 15 to 150°C are presented here and the importance of K-mica versus kaolinite mineral phase stability is discussed.

The hydrogeology of six Montana and one Idaho hot springs is presented herein. Base temperatures are calculated for each hydrothermal system and are evaluated as to their reliability. Suggestions are made for further research on application of the Na-K-Ca hydrogeothermometer in the temperature range 15 to 150°C.

INTRODUCTION

Purpose and Scope

Subsurface temperature of geothermal hot-water systems is a critical factor in determining the potential for power production in geothermal areas. Geochemistry of surface hot spring discharge waters is often a useful tool in estimating subsurface water temperatures. The two best chemical indicators (hydrogeothermometers) of subsurface temperatures in hot-water systems to date are dissolved silica content (Fournier and Rowe, 1966) and Na-K-Ca atomic ratios (Fournier and Truesdell, 1973). This paper discusses the application of the dissolved silica and Na-K-Ca hydrogeothermometers for estimating subsurface temperature of Montana hot-water systems. Salmon Hot Spring in Idaho is also discussed to provide an additional example of a specific geochemical relationship.

This paper presents a general overview of geology and geochemistry of hot spring areas in Montana. The six Montana hot spring areas examined in detail herein are representative of all of the types of hot-water geothermal systems (hydrothermal systems) currently known to exist in Montana. Montana hot springs are classified in this paper on the basis of the hydrologic nature of their subsurface flow systems as determined by local geology, and this classification scheme is presented in conjunction with the silica and Na-K-Ca hydrogeothermometers as a general method to further evaluate the economic potential of hydrothermal systems. Possible relations between hot springs in the western United States and regional tectonic features are explored in an attempt to establish guides to

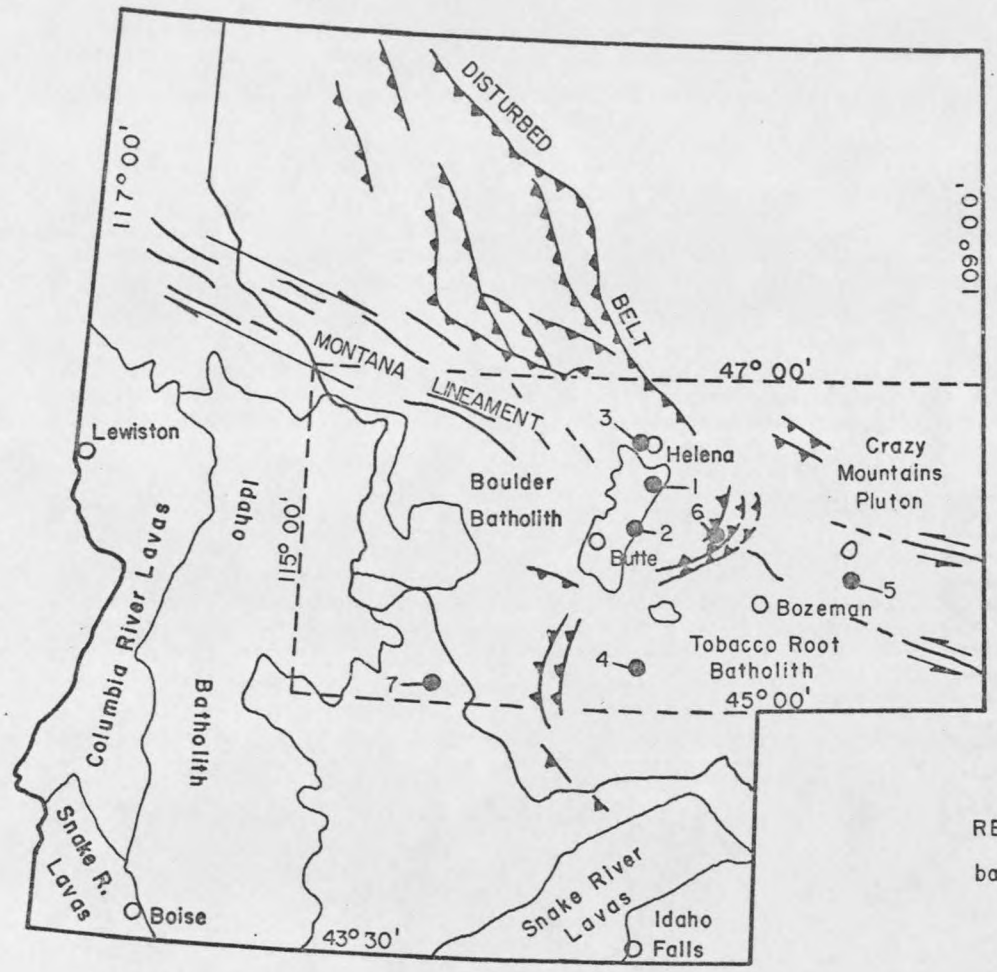
the occurence at depth of a commercially exploitable geothermal system.

Location and Physiography

Figure 1 depicts the general area investigated and shows the locations of the individual hot springs. The six representative Montana hot springs and the one Idaho hot spring lie within the Northern Rocky Mountains physiographic province except for Hunters Hot Springs, which is in the Great Plains physiographic province. Specifically, Alhambra, Boulder, and Helena Hot Springs discharge from Late Cretaceous quartz monzonite rocks of the Boulder batholith; Pullers Hot Springs discharges from Quaternary and Tertiary sediments in the intermontane Ruby River Valley, Hunters Hot Springs issues from Late Cretaceous sediments on the extreme southwestern flank of the Crazy Mountains Basin, and Big Spring near Toston discharges from deformed and faulted Amsden carbonates along the margin of an intermontane basin comprising the Townsend Valley. Salmon Hot Spring in Idaho issues from Tertiary age Challis Volcanics extruded through Tertiary sediments at the southern end of the intermontane Salmon Basin.

Methods of Investigation

Methods of investigation for this study were twofold and consisted of: (1) field mapping of surface geology of hot spring areas, and (2) field analysis of hot spring water for dissolved silica and laboratory analysis of hot spring waters for sodium, potassium, calcium, magnesium, and chloride concentrations. Appendix I describes analytical methods. Field studies were conducted from June 1973 through September 1973. Mapping was accomplished on



HOT SPRINGS INDEX

1. Alhambra
2. Boulder
3. Helena
4. Pullers
5. Hunters
6. Big Spring
7. Salmon

Study area boundary

Geologic province boundary

Basement structural trend

Thrust fault

2 Hot Spring location

SCALE
1:5 000 000
approximately 1 inch to 80 miles

REGIONAL GEOLOGY AND HOT SPRING LOCATION
based on Geologic Map of North America by the
USGS 1965

FIGURE 1

U.S. Geological Survey topographic quadrangles where coverage was available and on U.S. Department of Agriculture aerial photos, U.S. Forest Service base maps, and county land maps in other areas. Existing geologic maps from various sources were used to the extent available.

Previous Work

Excellent summaries of hot spring chemistry and geothermometry are provided by Ellis (1970), Mahon (1970), Tonani (1970), and White (1970). Known Montana hot spring locations and temperatures are summarized by Balster and Groff (1972). Thermal gradient measurements from oil and gas drill holes in the plains of eastern Montana are contoured on AAPG geothermal gradient maps of portions of the United States (AAPG 1973). Waring (1965) summarizes all literature referring to Montana and Idaho hot springs to that date including references to descriptions of Montana hot springs by Lewis and Clark (1814) and Mullan (1855). Significant early contributions are a tabulation of hot springs in the Montana Territory including six chemical analyses of waters by Peale (1886) and an excellent study of hot spring vein mineralization at Boulder Hot Springs by Weed (1900). Other early references provide brief descriptions of Montana hot springs and a few chemical analyses: Clark (1886), Weed and Pirsson (1896), Weed (1904, 1905), and Perry (1934). More recent contributions have been made in the field of heat flow studies by Blackwell (1969), Blackwell and Baag (1973), and Blackwell and Robertson (1973). Various workers too numerous to cite here have contributed to the knowledge of basic geology in Montana hot spring areas and will be referred to individually.

PHYSICAL CHARACTERISTICS OF HOT SPRINGS

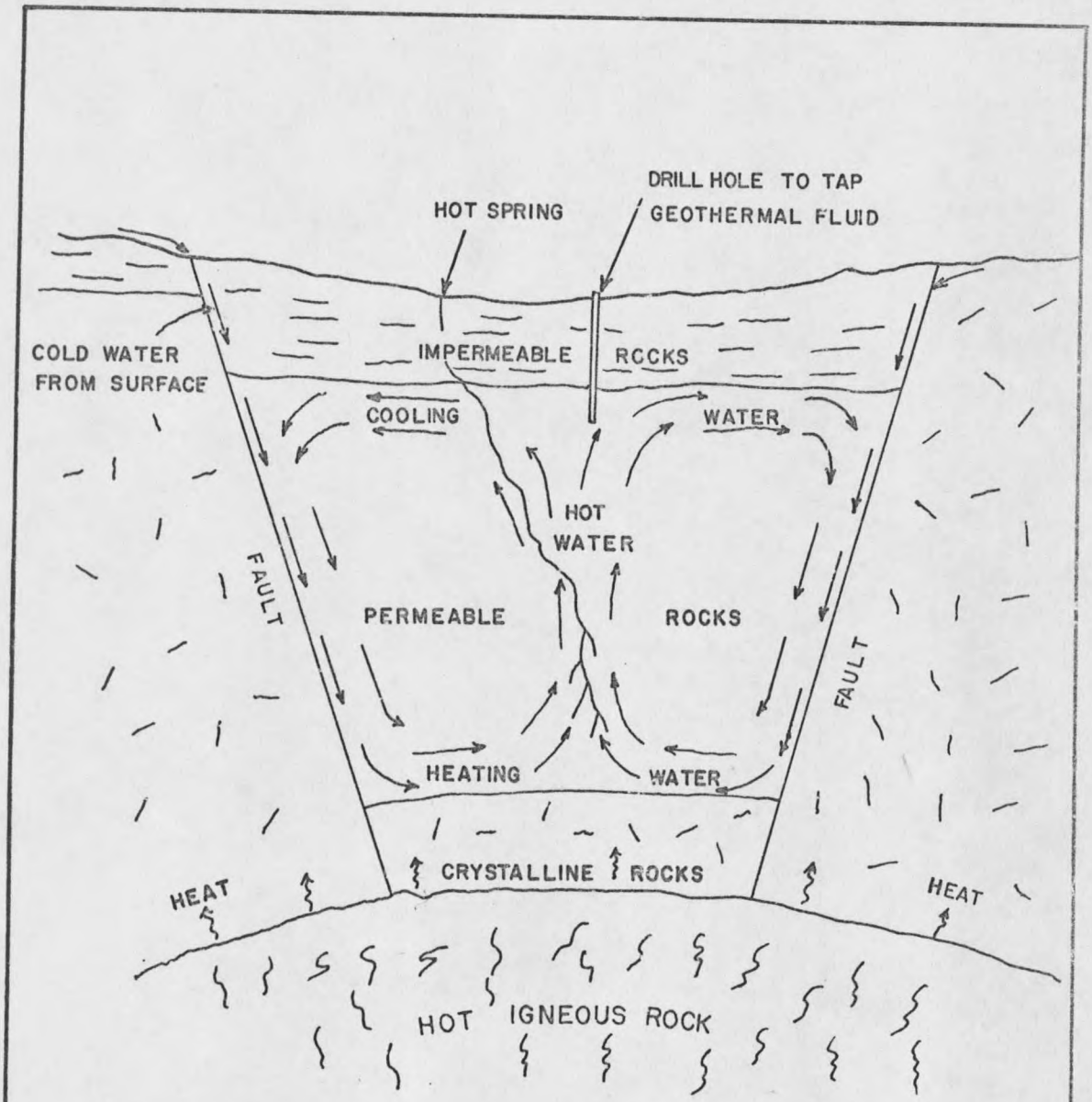
Hydrothermal Systems

Hot spring areas as well as geysers and fumaroles are the surface expression of geothermal systems which involve circulating waters; i.e., hydrothermal systems. A hydrothermal system (Figure 2) includes zones of convective upflow of hot water as well as marginal zones of convective down-flow of cold recharge waters or recirculated thermal waters. Thus, the essential elements of a hydrothermal system discharging through a hot spring consist of a heat source, a circulation system, a source of recharge water, and the discharge system feeding the hot spring (Elder, 1965).

Heat Sources

Proposed sources of heat for hydrothermal systems include decay of radioactive elements, heat of friction along active faults, deep circulation of ground water and heating in equilibrium with the geothermal gradient, and heating of deep ground water by a cooling intrusive rock body. Proposed mechanisms to transfer heat from the source to the thermal water include derivation of geothermal water primarily from condensation of juvenile volcanic steam, heating of deep meteoric ground waters by heat transfer from juvenile volcanic steam (steam heating), and heating of deep circulating meteoric ground water due to conductive heat transfer from a cooling intrusive body.

Studies by Blackwell (1969) show that heat generation due to decay of radioactive elements in the earth's crust is not sufficient to support a hydrothermal system. A study of the San Andreas Fault by Henyey (1968) indicates



SKETCH OF MODEL HYDROTHEMAL SYSTEM

CROSS-SECTIONAL VIEW

AFTER

J. Eric Schuster (1973)

FIGURE 2

that heat generated by friction along active faults also is not adequate to produce hydrothermal systems.

Many hot springs probably result from deep circulation of meteoric waters in confined aquifers where the waters adjust to subsurface temperatures along the geothermal gradient, especially in areas of higher than normal regional heat flow. Hot springs of this type are discharging from low temperature hydrothermal systems in which the water temperature is a product of the geothermal gradient times the depth of circulation. Discharge of the heated water from depth must be fairly rapid to prevent heat loss back to the country rocks as the water ascends. Deep circulation of meteoric ground water in this type of system typically occurs in permeable fault zones or vertically deformed sedimentary aquifers.

It is necessary to explain the high temperatures and high dissolved solids concentration of some thermal waters in terms of a localized high-temperature heat source. The most acceptable model for a localized high-temperature heat source which satisfies geophysical and geochemical data for known geothermal areas and which is compatible with current geologic concepts is a cooling(?) rock body in the upper crust. Three mechanisms for heat transfer from a cooling magma or hot intrusive rock body to circulating thermal waters have been proposed.

Derivation of thermal waters primarily from condensation of juvenile volcanic steam has been considered possible by most early investigators of thermal waters. However, comparisons of the chemistry of surface ground water with deep thermal water by White (1957b) and comparisons

of the O^{18}/O^{16} ratios of surface ground water with deep thermal waters by Craig (1963) and White (1968), as summarized by White (1970), indicate that at least 90 to 95 percent by mass of the water recharging most hydrothermal systems consists of local meteoric water. Similarly, it can be reasoned that if only about 5 percent of thermal water by mass is from juvenile sources, heating of deep meteoric ground water by juvenile volcanic steam or supercritical juvenile water would not be significant enough to explain the total heat flow of most hydrothermal systems (White, 1970). Though the isotopic evidence indicates a predominately meteoric origin for thermal waters, one might postulate that deep circulating meteoric ground water coming in contact or near contact with a cooling intrusive rock body may change temporarily to steam which in turn could transfer heat to the circulating ground water. However, thermodynamic considerations (James, 1968) render this concept invalid.

White (1968, 1970) and White, Muffler, and Truesdell (1971) suggest that heat from an intrusive body may be conducted through the surrounding country rocks where it is transferred to deep meteoric ground waters circulating through the heated country rocks without formation of a vapor phase. Circulation in the hydrothermal system may then result from thermal convection and flow along piezometric gradients intrinsic to the hydrologic system. Mathematical treatments by White, Muffler, and Truesdell (1971) and theoretical considerations presented by Tonani (1970) make this concept appear to be the most likely of the three presented here for a heat transfer mechanism

transferring heat from a cooling intrusive body to deep ground water.

Temperature

Perhaps the most important characteristic of a hydrothermal system in terms of potential geothermal energy production is temperature. Temperature in a hydrothermal system increases with depth until a "base" temperature is reached (White, 1961 and Bovarrson, 1964) beyond which no significant increase of temperature with depth occurs. Under current geothermal technology, most turbines are designed for an absolute operating pressure of 5 kg/cm^2. Utilization of steam pressures lower than 5 kg/cm^2 requires construction of disproportionately larger turbines resulting in increased installation costs per unit of plant capacity and higher operational cost due to the less efficient utilization of the energy. The saturation pressure of steam is 5 kg/cm^2 at 150°C and thus geothermal reservoirs with a base temperature of less than 150°C are not currently of economic interest for power production. Reservoirs with base temperatures of 150 to 200°C may be economically developable where permeability is high and sufficient volume exists. Reservoirs with base temperatures above 200°C are especially attractive.

Hansen (1964) describes a process whereby low-temperature thermal waters might be used for geothermal power generation. Low-temperature thermal water is circulated through a closed heat exchange unit where heat is transferred at a constant temperature from the thermal water to a low boiling temperature working fluid. The vaporized working fluid is used to drive a turbine, condensed, and

recycled to the heat exchanger in a closed circuit. This process could utilize water as a working fluid, however, the high heat of vaporization of water would make the process inefficient. Use of a volatile liquid such as freon may increase efficiency 2:1 over water (Hansen, 1964).

Theoretically, low-temperature thermal water over any range of temperature could be used in this process by building larger heat exchange units for lower temperature water. In practice, the available volume of thermal water and the construction costs of heat exchange units versus amortization will limit the temperature of utilization of thermal water to a practical minimum yet to be determined. Thus, even in utilization of low-temperature thermal water reservoir base temperature will continue to be a critical consideration in geothermal resources development.

Geohydrology

Hydrothermal systems may exist in an almost infinite variety of geologic settings. Regardless of the details of the local geology of a hydrothermal system, the physical geology of any individual hydrothermal system determines critical factors including boundary conditions and reservoir porosity and permeability. Boundary conditions dictated by geologic structure determine the extent and volume of a hydrothermal system. Volume and potential production can be estimated if stratigraphic units of known hydrologic properties can be identified and correlated with structure. Identification of fault zones and permeable aquifers may also facilitate recognition and location of potential zones of maximum production.

The existence of an impermeable cap formation may con-

fine a hydrothermal system under static pressure thereby allowing a liquid water phase to exist at reservoir base temperatures sufficient to generate steam when the static pressure is released by means of a drill hole penetrating the cap formation. Confinement of a hydrothermal system under static pressure greatly reduces boiling and heat loss accompanying boiling and is probably a necessary condition for an economically exploitable reservoir. Consequently, a permeable aquifer overlain by an impervious formation constitutes the most favorable geologic setting for geothermal steam production, and structural or stratigraphic traps of this nature accompanied by high heat flow are the objectives of geothermal exploration.

An impervious cap may consist of any type of normally low-permeability rock strata such as siltstone or shale. Normally permeable sandstones and carbonates may act as impermeable cap formations if they are well cemented. In addition, the existence of self-sealing hydrothermal systems should not be overlooked.

Facca and Tonani (1967) suggest that silica deposition may be an important mechanism of self-sealing at depth, and calcium carbonate deposition and argillization may act as shallow sealing mechanisms. Silica deposition is the most likely sealing mechanism at depth where steam loss from boiling waters with temperatures above 150 to 180°C results in supersaturation of water with silica and subsequent silica precipitation. At lower temperatures near the surface, heating of descending recharge water causes loss of CO_2 and subsequent precipitation of calcite. Vapor from ascending boiling waters may include H_2S and CO_2

which react with atmospheric oxygen and water, respectively, to form acids which in turn cause argillization of wall rocks. The Geysers field in California and Wairakei and Waiotapu in New Zealand are cited as examples. White, Muffler, and Truesdell (1971) point out that silica self-sealing is probably not significant in hydrothermal systems with base temperatures below 150°C due to lack of silica concentrations sufficient to result in supersaturation even with steam loss, and that self-sealing is most extensive where water temperatures decrease most rapidly during discharge of water from the hydrothermal reservoir.

Facca (1969) describes the detection of self-sealed areas by geophysical means in volcanic reservoir rocks in South America and the United States. Self-sealed areas appear as magnetic low anomalies due to oxidation of magnetite to hematite during the hydrothermal alteration producing the sealed zone. The alteration and the increased temperature result in low resistivity. Thus magnetic lows correlating with low resistivity indicate self-sealed areas whereas magnetic highs correlating with low resistivity indicate unsealed areas of thermal water circulating in unaltered rocks with unoxidized magnetite content.

The magnitude of trapped heat available for geothermal power exploitation is determined by the reservoir dimensions and temperature; however, the productivity is determined by the reservoir permeability and recharge volume (Facca and Tonani, 1961). Thus hot-water systems in permeable sedimentary or volcanic rocks may have more potential for steam production than systems in open channels in fractured or faulted massive rocks such as granite where

the reservoir volume or water supply is limited. Similarly, hydrothermal systems in sedimentary or volcanic strata with permeabilities that are too low will not provide satisfactory steam production despite adequate reservoir base temperatures (Brown, 1970).

Reservoir Fluid Phases

Wells penetrating hydrothermal systems may yield dry or superheated steam with little or no associated liquid water. Examples are The Geysers steam field, California and the Larderello steam field, Italy. Most hydrothermal systems yield hot water when penetrated by drill holes as at Wairakei, New Zealand and Steamboat Springs, Nevada. Part of the water flashes to steam due to decreasing pressure as the hot water rises up the drill hole. The result is a mixture of hot water and steam at the surface. Steam may comprise 10 to 20 percent of the total mass flow (White, Muffler, and Truesdell, 1971). Other hydrothermal systems may yield only hot water and negligible steam due to base temperatures which are inadequate for steam generation or barely above the boiling point at the hydrostatic pressure of the system. In systems of this type, increasing hydrostatic pressure with depth in the reservoir limits boiling to the upper 20 to 30 feet below the water surface; however, conduction of heat from the ascending thermal water into the wall rocks probably cools the water to the point where no boiling occurs in the system at all. As an alternative, such a system could be pictured as a column of water under normal hydrostatic pressure and everywhere at its boiling point. Either gentle boiling with minimal steam separation or conductive heat loss to the wall rocks would maintain water temperature in the

system near the boiling temperature. Conductive heat loss to the wall rocks is more probable where discharge water is not boiling.

The presence of liquid water as the continuous fluid phase in reservoirs of hydrothermal systems yielding a mixture of water and steam at the surface is evident from drill hole studies; however, the nature of the continuous fluid phase in the reservoirs of hydrothermal systems yielding dry steam has been subject to debate. Elder (1965) and James (1968) propose that two phases exist in reservoirs of hydrothermal systems yielding dry steam and suggested a boiling liquid phase in the lower parts of the reservoir and a vapor phase in the upper part of the reservoir. This continues to be a valid concept today.

Tonani (1970) shows that the fundamental phase to which heat is initially transferred in the system is a liquid regardless of the nature of the exchange mechanism. Tonani (1970) further stresses the necessity of convective flow to permit formation of a vapor phase. Convective flow reduces static pressure and temperature along streamlines thus allowing steady state steam formation to occur. Steam formed in this manner must either condense in the uppermost part of the reservoir to maintain thermodynamic and mechanical equilibrium or must escape from the system as a surface manifestation. If steam should form under static conditions without flow in spite of reservoir pressure staying at a static value or increasing to maintain a single liquid phase, phreatic or volcanic explosions would occur according to Tonani (1970).

White, Muffler, and Truesdell (1971) further support

this concept with a mathematically balanced model of a hydrothermal system in which liquid and vapor coexist as described above. In this model, heat in hot country rocks contiguous to a cooling igneous body is transferred to deep meteoric ground water circulating as a liquid phase in the hot country rocks. Heating of the water raises the vapor pressure above static pressure in the reservoir. Steam forms and begins to migrate upward. Confinement of the migration of this steam without circulation would result in either higher static pressure or failure of the confining media and phreatic explosion. Above a pressure of about 30 atmospheres, the rising steam is supersaturated, and expansion during ascent results in some condensation (James, 1968). Ultimately, build-up of the condensation water scrubbed from the steam by the porous media raises the water surface in the reservoir to a level where pressure is reduced to 30 atmospheres. At this pressure, steady state formation of dry steam at maximum enthalpy occurs at the water surface and changes in temperature result in only small changes in enthalpy (White, Muffler, and Truesdell, 1971 and James, 1968). This seems to be roughly the case at Larderello (James, 1968) and at The Geysers (White, Muffler, and Truesdell, 1971) where dry steam is produced at maximum enthalpy in the upper portions of the hydrothermal systems penetrated by drill holes.

Vapor Versus Liquid

The early observation that some systems yield dry steam while others yield a mixture of steam and water or just water at the surface resulted in the initial classi-

fication of hydrothermal systems as "vapor-dominated" or "hot-water" systems respectively (White, 1970). The preceding section on reservoir fluid phases supports the validity of this fundamental distinction between types of hydrothermal systems. The concept of vapor-dominated and hot-water systems is necessary to the understanding of the chemical nature of surface hot spring discharges because of the profound difference in the solubility of nonvolatile elements in hot water versus steam.

CHEMICAL CHARACTERISTICS OF HOT SPRINGS

Application

Dissolved solids in geothermal water may precipitate as minerals resulting in severe scaling in drill holes, transmission lines, steam separators, and holding tanks. High concentrations of dissolved solids in some geothermal waters pose serious problems in disposing of discharge water from geothermal installations without causing water pollution. Thermal water high in dissolved solids concentration is extremely corrosive to most metals used in casing, pipes, pumps, and tanks. A knowledge of the chemical characteristics of geothermal water is necessary in all phases of design for utilization of geothermal resources. Moreover, dissolved constituents in geothermal wastewater may be economically recoverable as saleable by-products.

This paper is primarily concerned with the application of hot spring chemistry to estimating subsurface temperatures for hot-water type hydrothermal systems. Only two hydrogeothermometers are currently believed to be of quantitative value in estimating subsurface or reservoir temperatures. These are dissolved silica concentrations and Na-K-Ca atomic ratios. Other hydrogeochemical information may provide qualitative guides to subsurface temperatures and will be discussed under geothermometry.

General Conditions

Surface discharge water from hot-water systems is nearly always neutral to alkaline and is characterized by high contents of silica and alkali chlorides where it is undiluted by local ground water. Surface discharges from

vapor-dominated systems are generally neutral to acid and low in chloride and dissolved solids since the only chlorides with sufficient volatility to transfer Cl in low-pressure steam are HCl and NH_4Cl which are minor constituents in most hot springs. Other dissolved solids are similarly insoluble in steam due to low volatility. Acid conditions in surface discharges from vapor-dominated systems result from the reaction of H_2S gas with atmospheric oxygen to form sulfuric acid. Additional acidity may result from CO_2 being dissolved in the surface condensate waters if Ca is not present to buffer the system. Acid springs of the first type are typical of vapor-dominated system discharge and are termed acid-sulfate springs. Neutral springs low in Cl and dissolved solids may be indicative of discharge from vapor-dominated systems with a high content of NH_3 gas which buffers the waters at a neutral pH.

Source of Dissolved Solids

Ellis and Mahon (1964 and 1967) conducted experimental studies which demonstrated that the source of dissolved constituents in thermal water is the wall rock in the hydrothermal system and that water-rock reactions fall into three main types as follows: (1) soluble element reactions controlling Cl, B, I, and Cs; (2) soluble mineral reactions controlling SiO_2, F, Mg (in some cases), SO_4, and Ca; and (3) mineral phase equilibria reactions controlling Na, K, Al, Li, and Rb, and Mg (in some cases).

Soluble Element Equilibria

Soluble elements do not react to form secondary minerals, and since they are minor constituents in most rocks,

their concentrations in water may be largely controlled by available supply in high-temperature systems. Where reservoir temperatures are so high the solubility of these elements in the thermal waters exceeds the supply of elements in the wall rocks, changes in soluble element content in discharge waters may be related to changes in available supply in reservoir rocks of differing composition. Thus, iso-chloride contours or contours of Cl/B ratios in spring discharges across an area may be correlated with reservoir rock types with which the waters are reacting at depth. This may be used as a method of detecting different types of reservoir rocks in different parts of the reservoir where reliable reservoir temperature estimates are available from the SiO_2 or Na-K-Ca hydrogeothermometers. Conversely, if the chemical composition of the reservoir rocks can be interpolated from geologic evidence, iso-chloride or Cl/B ratio contours may be useful in detecting high temperature zones or sources of high temperature water, especially when correlated with geophysical data such as resistivity. Ratios of Cl with other soluble elements may be used similarly.

Soluble Mineral Equilibria

Ellis and Mahon (1964 and 1967) were able to relate concentrations of SiO_2, F, Mg, SO_4, and Ca in thermal water directly to the solubilities of quartz, fluorite, chlorite, anhydrite, and calcite respectively. Concentrations of SiO_2 increase with increasing temperature whereas concentrations of F, SO_4, Ca and Mg decrease with increasing temperature. The solubility of quartz in water will be discussed under Geothermometry in this paper. Although

Ellis and Mahon (1964 and 1967) attribute Mg concentration in thermal water to mineral-solution equilibrium with chlorite, Ellis (1970) states that Mg concentration in thermal water is controlled by mineral phase equilibrium involving chlorite where thermal waters are neutral to alkaline. In contrast, it appears that the high Mg concentrations of 1 to 40 ppm (Davis and DeWiest, 1970) common in cold shallow ground waters are the result of the solution of carbonate rocks. Similarly, as the pH of thermal waters decreases, the equilibrium concentrations of Mg increase in a manner parallel to Ca suggesting that Ca and Mg concentration are in equilibrium with carbonate minerals and that this equilibrium is dependent on a minimum concentration of dissolved CO_2. Once the CO_2 concentration in the thermal water drops below this undetermined concentration, the Mg concentration becomes controlled by equilibrium with chlorite which is a stable mineral phase over the entire temperature range of 25 to 260°C (Garrels and Christ, 1965 and Ellis, 1970).

When the Mg concentration is in equilibrium with chlorite, constant growth of chlorite in its wide stability range depletes Mg from the thermal waters. This is in good agreement with data presented by Ellis (1970) which shows high-temperature thermal waters typically contain less than several ppm Mg in solution. Muffler and White (1969) show that at high temperatures (up to 360°C) Mg strongly favors solid phase equilibrium with chlorite and also illite mica and montmorillonite. White, Craig, and Begemann (1963) suggest that at lower temperatures hydrolysis of Mg cations prevents them from reacting in sili-

cate structures (and possibly in carbonate structures as well) resulting in higher concentrations of Mg in lower temperature waters. This combination of factors indicates that neutral to alkaline thermal waters should be low in Mg concentration.

Concentration of Ca tends to decrease with increasing temperature because Ca is dissolved by H_2CO_3 which depends on the solubility of CO_2 in the thermal water. As water temperature increases, the vapor pressure of CO_2 increases. The CO_2 in solution as H_2CO_3 is driven from solution as a volatile gas and Ca is precipitated. If the CO_2 concentration at any temperature is above 0.1 molal (Ellis, 1970) due to static or hydrostatic reservoir pressure sufficient to maintain a vapor pressure for CO_2 which allows this concentration, Ca will precipitate as calcium carbonate. If the CO_2 concentration at any temperature is below 0.1 molal, Ca concentration will be in equilibrium with a silicate and a calcium silicate mineral will form (Ellis, 1970). Thus, thermal water with high CO_2 concentration is likely to precipitate calcite during ascent and boiling whereas thermal water low in CO_2 content may begin to assimilate Ca during ascent as additional CO_2 is dissolved by water in the upper parts of the system. The formation of a calcium silicate mineral below a critical minimum CO_2 concentration in the thermal water also indicates the capability of Ca to compete with other cations in silicate reactions.

Mineral Phase Equilibria

Ellis and Mahon (1964) demonstrated that the concentrations of Na, K, Al, and Rb in solution in thermal water

is controlled by the equilibrium of these elements with specific mineral suites and that the solution concentrations represent an aqueous phase coexisting with the solid phase of the mineral assemblage. Additional work by White (1965), Ellis and Mahon (1967), Hemley (1967), and White (1968) demonstrated that specific mineral suites controlling Na, K, Al, Li, and Rb concentration in solution are in mutual phase equilibrium within specific temperature-dependent stability fields. These temperature-dependent stability fields were found to be relatively independent of pressure changes, and the general system in which partitioning of elements between solid and liquid phases occurs was established as K_2O-Na_2O-Al_2O_3-SiO_2-H_2O. An infinite number of combinations of stable mineral suites containing K-feldspar, K-mica, albite, paragonite, and quartz in various relative amounts can be formed from this system to control the solution concentration of Na and K as well as the other above listed elements in neutral to alkaline water.

Thus, plots of atomic Na/K ratios vs temperature for various natural geothermal waters and various experimental water-rock reactions vary widely depending on the mineral suite in equilibrium with the thermal solution as shown by Ellis and Mahon (1964 and 1967), Hemley (1967), and White (1965 and 1968). In order to apply the atomic Na/K ratio as a hydrogeothermometer, the composition of the reservoir wall rocks must be known. For example, if K-feldspar (a common mineral in most reservoir wall rocks) is present without albite, atomic Na/K ratios will be lower for a given temperature than for K-feldspar with albite

present, and if albite is controlling solution composition in the absence of K-feldspar, atomic Na/K ratios will be higher (Fournier and Truesdell, 1970).

Hydrologic Effects

The preceding section states that reservoir rock composition establishes the mineral suites initially controlling alkali concentrations in thermal waters. The extent to which the initial mineral suite continues to control solution composition depends on the nature of the flow conducting the thermal water to the surface.

Water moving slowly and homogeneously will tend to impose a new composition on the rocks above the first point of boiling; however, the rock mineral system will buffer these changes. Significant changes in the water solution composition during ascent by homogeneous flow are primarily the result of concentration of constituents due to steam loss during boiling. Concentration causes saturation and temperature-dependent growth of minerals required to keep the water solution concentration in equilibrium with stable mineral phases as the temperature decreases. Thus, the composition of water discharged at the surface from a hydrothermal system in which slow homogeneous flow is prevalent is basically in equilibrium with the primary mineral assemblage in the unaltered wall rock. If the upward flow is sufficiently slow, the stable mineral assemblage last in equilibrium with the water may impart a solution composition equivalent to a lower temperature than exists at depth in the reservoir. Also, solution composition may represent equilibrium with new mineral suites if the wall rock composition changes in the upper part of the

reservoir or discharge system.

Where the water is rising rapidly such as when channelled in fissures, the water has more limited contact with the wall rock and boils vigorously because of the more rapid ascent. In this type of flow condition, buffering by the wall rock is minimal and the water tends to deposit secondary minerals about the flow zone which grow primarily as the result of changes in pH (Ellis, 1970) and as the result of saturation due to steam loss. Alkali concentrations in discharge water under rapid flow conditions will more closely represent alkali concentrations at equilibrium with reservoir mineral assemblages at depth and at reservoir temperature. Regardless of the nature of the discharge flow in the system, it is still necessary to know the specific mineral assemblage present at depth in order to relate the atomic Na/K ratio of the discharge water to reservoir temperature.

An Example

Ellis (1970) presents an example of a hydrothermal system initially at chemical equilibrium with reservoir country rocks and traces the sequence of alteration minerals that would result in theory from ascent of the thermal water both by slow homogeneous flow and by rapid fissure type flow. This example is based on the Broadlands, New Zealand hydrothermal system and demonstrates the combined effects of flow, temperature change, and pH change on mineral phase stability and chemical equilibrium in the thermal water.

The thermal water is initially in equilibrium with albite, K-feldspar, K-mica, calcite, warakite, and chlorite

at 260°C as shown on the phase diagram on Figure 3. As the water ascends by slow homogeneous flow, a slight steam and CO_2 loss causes temperature to drop and pH to rise. The water composition point moves out of the K-mica stability field into that for K-feldspar and wairakite. Quartz and calcite both begin to precipitate due to steam loss and CO_2 loss respectively and continue to precipitate throughout ascent of the thermal water. Chlorite remains stable throughout the temperature range. Continued temperature decrease moves the water composition into the K-feldspar stability field due to change of the phase boundaries with temperature change and K-feldspar grows to bring water composition back onto the two feldspar equilibrium line. Further steam loss would advance the same trends except that epidote would be favored over wairakite at lower temperatures.

If ascending flow of the same thermal water were to take place by fissure flow accompanied by rapid steam loss and little continued water-rock reaction, the secondary minerals would result primarily from changes in water pH and from saturation conditions resulting from steam loss. The main minerals to be deposited in the flow fissure in this example would be K-feldspar, calcite, and quartz. Wairakite would also form at the level of first boiling followed by epidote at decreased temperatures, and chlorite would form throughout the system.

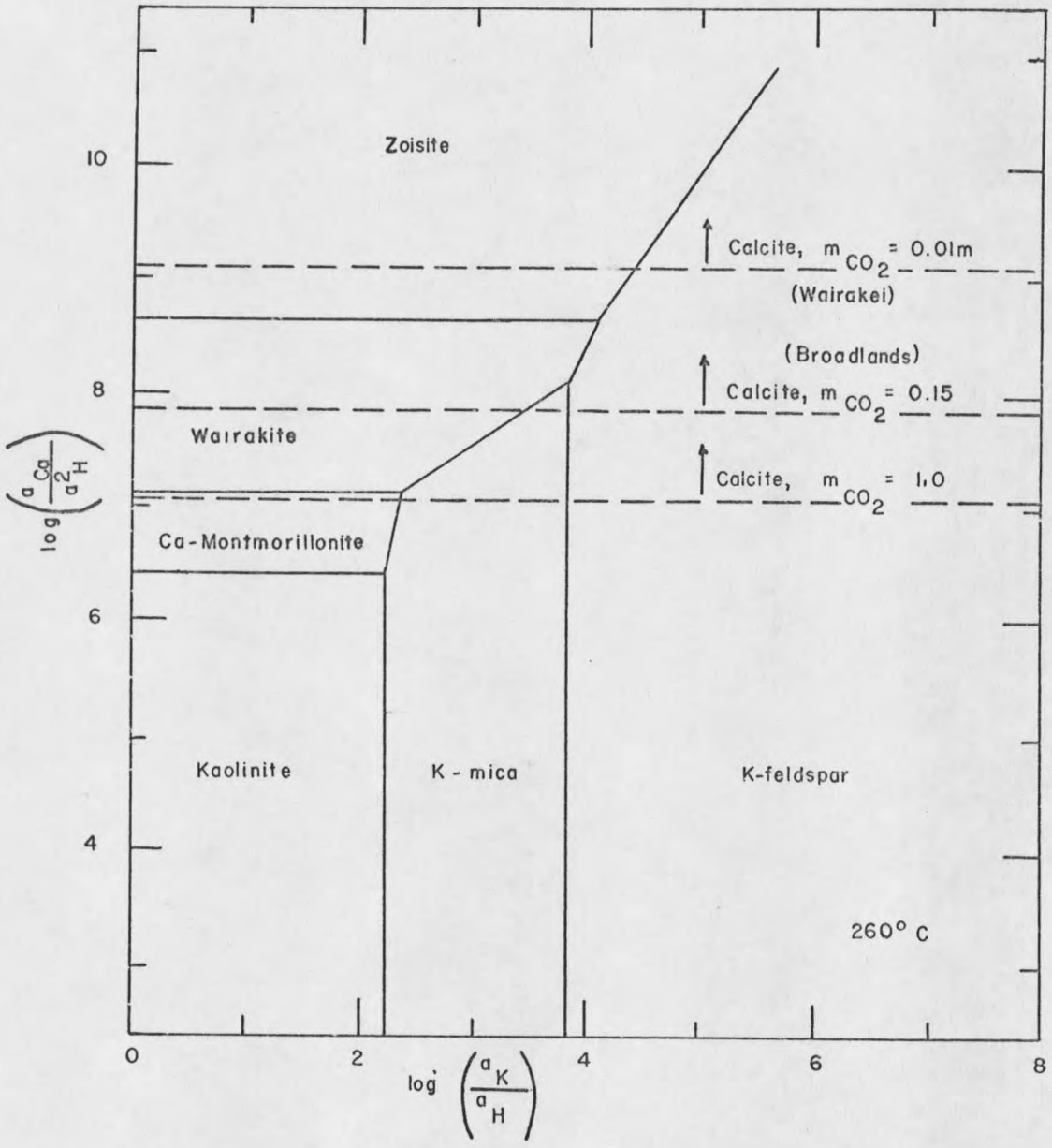


FIGURE 3. Phase diagram for Ca and K minerals at 260° C. From Ellis (1970).

GEOTHERMOMETRY

Qualitative Indicators

Quantitative estimates of reservoir temperatures can be made from dissolved silica concentrations and from Na, K, and Ca concentration ratios. Certain other dissolved solids and gases may be used as general indicators of reservoir temperatures during preliminary evaluation of a hydrothermal system. The Na/K atomic ratio is a qualitative indicator of temperature when wall rock composition is unknown. The concentration of Ca and HCO_3 tends to decrease with increasing temperature and increase with decreasing temperature. The concentration of Mg is uniformly low over a wide range of temperature from at least 60 to 260°C. Magnesium concentration begins to increase for temperatures below 60°C. High temperature reservoirs usually discharge water with high $Cl/(HCO_3 + CO_3)$ ratios whereas $Cl/(HCO_3 + CO_3)$ ratios are generally lower in lower temperature waters (Fournier and Truesdell, 1970).

Direct precipitation of silica as siliceous sinter is a reliable indicator of reservoir temperatures above 180°C. Precipitation of siliceous sinter in shallow thermal pools, sheet flow areas, or in geyser discharge may be due to evaporative concentration of silica and is not a good qualitative indicator of temperature.

Because of the inverse solubility of calcite with increasing temperature, active travertine deposition by discharge water is a strong indicator of low subsurface temperature if no assimilation of calcium carbonate from surface rocks by cooled discharge water is occuring.

Dissolved Silica Hydrogeothermometer

The dissolved silica concentration in surface discharge water from hot-water hydrothermal systems can be used to estimate quantitatively reservoir temperatures at depth. The temperature-dependent solubility of the mineral quartz in water has been established by Kennedy (1950), Krauskopf (1956), and Morey et al (1962) over a wide range of temperatures. For a pH less than 8.5, the solubility of quartz in water is independent of gas pressures, other dissolved constituents, and other mineral assemblages. The solution equilibrium of quartz in water plotted vs temperature from Fournier and Truesdell (1970) is shown by curve B on Figure 4. The solution equilibrium of amorphous silica in water vs temperature from Iler (1955) is shown for contrast. Amorphous silica includes both glass and opal in this report.

Fournier and Rowe (1966) were able to demonstrate that in certain hydrothermal systems the dissolved silica concentration in the discharge water can be related to equilibrium with quartz at reservoir temperatures. A correction must be made for the concentrating of dissolved silica in the water due to steam loss as the water ascends from the reservoir. Additional studies by Mahon (1966) and Fournier and Truesdell (1970) indicate that dissolved silica in most hydrothermal water is in equilibrium with quartz at reservoir temperatures. By using a curve corrected for steam loss due to irreversible adiabatic expansion at constant enthalpy, curve A on Figure 4 from Fournier and Rowe (1966), dissolved silica concentration in discharge water can be used to estimate quantitatively the

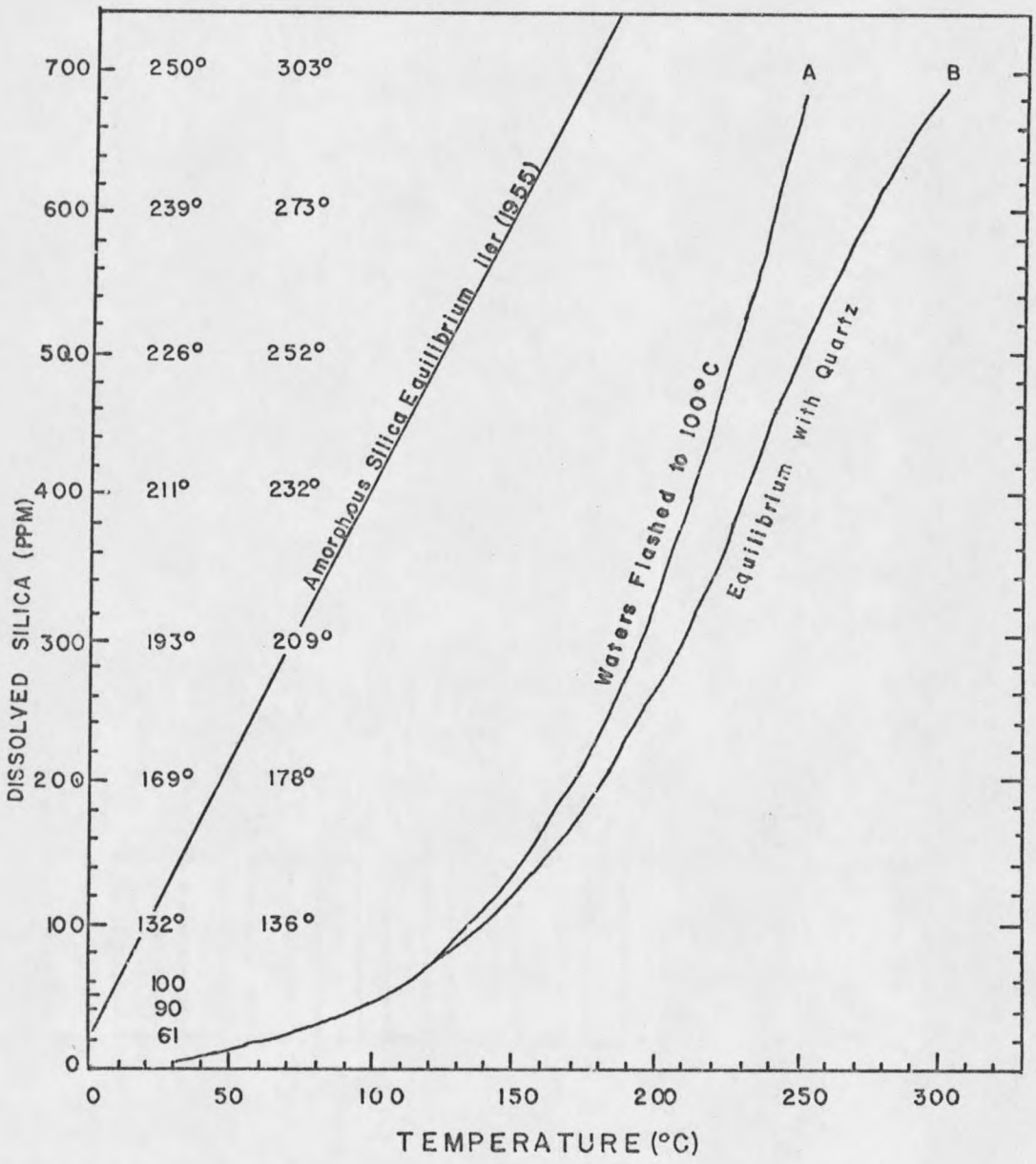


Fig. 4. Dissolved silica in equilibrium with quartz in thermal water.

reservoir temperature. It is important to note that analysis of silica content in discharge water should distinguish between colloidal particles of silica and truly dissolved silica. Appendix I describes analytical techniques employed in this study and discusses the distinction between dissolved monosilicic silica and colloidal and polymerized amorphous silica in water.

The dissolved silica hydrogeothermometer of Fournier and Rowe (1966) is based on the following assumptions: (1) silica is in equilibrium with quartz at reservoir temperature, (2) ascending water cools by irreversible adiabatic cooling at constant enthalpy due to steam loss, i.e., no heat is lost to wall rocks or by separation of gases other than steam, (3) no silica precipitation due to supersaturation is occurring, and (4) no mixing with dilute ground water is occurring.

Each of the preceding assumptions provides a possible source of error in applying dissolved silica geothermometry to thermal water. In water passing through wall rocks containing significant amounts of volcanic glass or opal, dissolved silica may be in equilibrium with amorphous silica. Estimated reservoir temperatures will be much too high due to the higher solubility of amorphous silica in water (Figure 4). Dissolved silica in equilibrium with quartz at reservoir temperatures less than 210°C will be undersaturated with respect to amorphous silica at the surface discharge (Fournier and Rowe, 1966) and may dissolve additional silica from amorphous silica present in the discharge system, again resulting in high estimated reservoir temperatures.

Water ascending from the reservoir may not cool entirely by steam loss. Cooling may be due to conduction of heat into the wall rocks or may be due to loss of gases such as CO_2 and H_2S. Cooling by conduction or by gas separation will not concentrate silica in solution. If cooling is conductive, curve B on Figure 4 would give better estimated reservoir temperatures since it represents the temperature-dependent equilibrium of dissolved silica with quartz without any water loss by steam separation. Dissolved silica equilibrium for some thermal waters may fall between curves A and B on Figure 4 where cooling is partially conductive and partially due to steam separation. Equilibrium for silica in gassy thermal waters would also fall between the curves A and B.

White, Muffler, and Truesdell (1971) indicate that cooling of quartz-saturated water will result in relatively rapid precipitation of quartz down to about 180°C. Quartz precipitation below 180°C will be relatively slow compared to the rate of discharge from most systems. Thus estimated reservoir temperatures based on the dissolved silica content of thermal waters discharged at the surface from hydrothermal systems with actual reservoir temperatures above 180°C may be too low due to precipitation of silica in the flow channels of the ascending water. Estimated reservoir temperatures over 180°C must be regarded as minimum reservoir temperatures based on this criterion.

Shallow and surface cold ground waters have low dissolved silica content due to the relatively low solubility of quartz at low temperatures. Data from White (1957b), White, Hem, and Waring (1963), and Davis and DeWiest (1970)

indicate that although ground water may contain from 5 to 40 ppm silica in temperate regions, only 5 to 15 ppm silica is derived from quartz and since amorphous silica rapidly recrystallizes to quartz, shallow ground waters in non-volcanic terrains in temperate regions contain from 5 to 15 ppm silica on the average. Thus, dilution of thermal waters by shallow ground water decreases dissolved silica concentration and results in low estimated reservoir temperatures based on either curve A or B of Figure 4.

Na-K-Ca Hydrogeothermometer

Fournier and Truesdell (1973) have derived an empirical curve of atomic Na/K ratios vs temperature which is corrected for CO_2 content and pH effects expressed as the competition of Ca with Na and K in silicate reactions. The empirical curve (Figure 5) is based on a graphic solution for a straight line curve most representative of an atomic Na/K ratio vs temperature plot of all known natural thermal waters, experimentally reacted thermal waters, and natural cold waters. It is accurate to within $\pm$ 15 to 20°C centigrade for all data with increasing accuracy for temperatures above 200°C. The main significance of this empirical curve is that it permits estimation of reservoir temperatures based on alkali ratios without knowledge of the specific mineral suites controlling solution composition. This is an important tool for waters above 180°C where the silica based estimated reservoir temperatures may not be accurate.

The empirical curve of Fournier and Truesdell (1973) is based on a number of assumptions and approximations. Experimental studies by Orville (1963) and Hemley (1967)

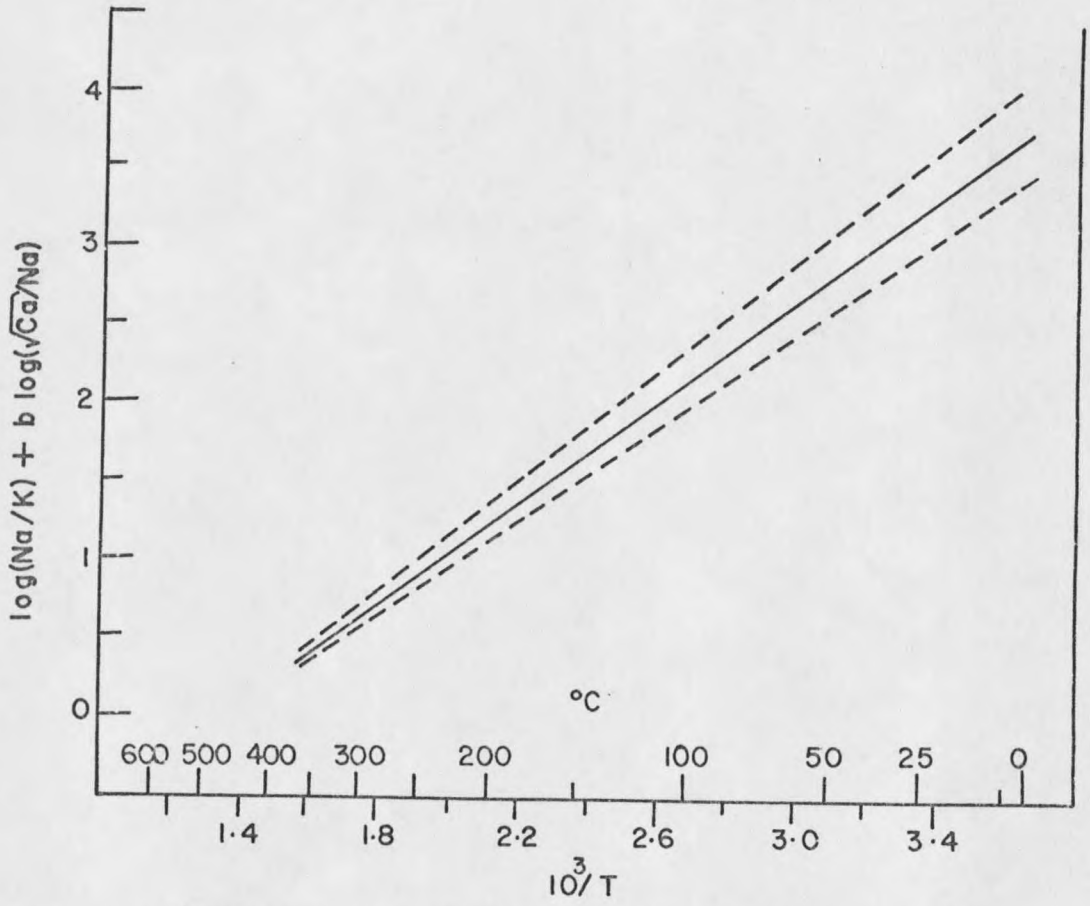


Fig.5. Log K^* vs 10/T. From Fournier and Truesdell. Dashed lines show +15° C and −15°C with respect to the middle curve. Use curve as follows: 1. Calculate log $(\sqrt{Ca}/Na)$; 2. If negative b = 1/3, If positive b = 4/3; 3. Where b = 4/3, if T ≥ 100°C recalcate using b = 1/3.

show that the equilibrium constant, K_{eq}, for the reaction

$$K^+ + \text{Na-feldspar} = \text{K-feldspar} + Na^+$$

is the same for albite and K-feldspar as isolated reactants as it is for albite and K-feldspar in the presence of muscovite and quartz, implying that K_{eq} is approximately the same for the entire system K_2O-Na_2O-Al_2O_3-SiO_2-H_2O and can be written as

$$K_{eq} = (\text{K-feldspar})(Na^+)/(\text{Na-feldspar})(K^+)$$

where the parenthesis denote activities of the inscribed species.

The actual purity of solid phases in natural systems is not known, nor are the activity coefficients for the aqueous species. Evaluation of K_{eq} at a specific equilibrium temperature is impossible and it is necessary to assume that: (1) solid phases are pure, and (2) activity coefficients for aqueous Na and K are equal and cancel each other. Based on these two assumptions, K_{eq} is approximately equal to molal (atomic) Na/K. Even though the activity coefficients of aqueous Na and K in the range of thermal water temperatures differ greatly in reality, molal concentrations of Na and K plotted as Na/K ratios vs temperature result in approximately straight lines when plotted as described in the following paragraphs, so assumption (2) can be used.

Based on the two assumptions made by Fournier and Truesdell (1973), K_{eq} is approximately equal to the atomic Na/K ratio at a given temperature. The relation of K_{eq} to temperature is given by the van't Hoff equation,

$$d \log K_{eq} / d \log (1/T) = -\bar{H}_T / 4.5758$$

where T is the absolute temperature and $\bar{H}_T$ is the standard heat of reaction at a given temperature. Because $\bar{H}_T$ varies only slightly with temperature, a plot of experimentally determined K_{eq} values plotted as $\log K_{eq}$ vs 1/T yields a nearly straight line that can be interpolated and extrapolated. Since K_{eq} is approximated by the atomic Na/K ratio, a plot of molal concentrations of Na and K as log(Na/K) vs 1/T represents the approximate relation between temperature and equilibrium of solid phase mineral suites with thermal water for the system K_2O-Na_2O-Al_2O_3-SiO_2-H_2O. This relation does not imply that K_{eq} or atomic Na/K ratios will not vary according to changes in mineralogy. Changes in mineralogy result in changes in the molar concentrations of K-feldspar and Na-feldspar to which K_{eq} is equated.

Fournier and Truesdell (1973) were able to show that the concentrations of Na and K in water are influenced by the aqueous concentration of Ca due to competition of Ca with Na and K in silicate reactions. Most natural low-temperature waters contain such low Na concentrations that changes in Na are evident in response to changes in Ca concentrations. Changes of Na concentration in response to changes in Ca concentration can best be shown by fixing K concentration and writing a generalized equation for all possible Na-K-Ca silicate reactions. The generalized equilibrium constant for all possible Na-K-Ca silicate reactions takes the form

$$\log K^* = \log(Na/K) + b(\log(Ca^{\frac{1}{2}}/Na))$$

where K^* is the approximate equilibrium constant and b depends on the stoichiometry of the reaction.

This equation is based on the assumptions that: (1) excess silica is present due to the presence of quartz, chalcedony, or cristobalite in the wall rocks, (2) aluminum is conserved in solid phases, i.e., so little aluminum is present in solution relative to other cations as to be negligible, and (3) hydrogen ions involved in hydrolysis cancel out due to decomposition of hydroxyl-bearing minerals for formation of other hydroxyl-bearing minerals. This last assumption may not be valid but cannot be avoided in practice because subsurface temperature and CO_2 partial pressure data would be required to correct for pH effects and hydrogen ion activity at depth.

Fournier and Truesdell (1973) calculate that in the equation for $\log K^*$, b = 0 where K_{aq} exchanges for Na_{aq} and b = 2 where $K_{aq} + Ca_{aq}$ exchanges for $3Na_{aq}$. A plot of $\log K^*$ vs $10^3/T$ for all natural thermal waters, experimental thermal waters, and natural cold waters using b = 0 and b = 2 yields points plotted at two extremes. If data points for any one water sample are tied together by a vertical tie line, b = 1 lies half way between the points for b = 0 and b = 2 and b = 1/2 lies one-fourth the distance from the b = 0 to the b = 2 point. Using this graphic method, Fournier and Truesdell (1973) plotted a straight line intersecting tie lines for all waters at about the same relative position along each tie line.

This graphically derived empirical curve for $\log K^*$ vs $10^3/T$ (Figure 5) passes through points $10^3/T = 1.70$, $\log K^* = 0.560$ and $10^3/T = 3.20$, $\log K^* = 3.031$ where $\log K^*$ is

plotted on a logarithmic scale. The average value of b for this line is about 1/3 for points above 100°C and is about 4/3 for points below 100°C. Using b = 4/3 and b = 1/3, most data points fall within ± 15 to 20°C of the empirical curve using plots based on measured temperature, fluid inclusion temperatures, geothermal gradient temperatures (oil well waters), and silica estimated temperatures.

Fournier and Truesdell (1973) suggest use of the empirical curve on Figure 5 to estimate temperature of last rock-water equilibrium as follows:

> "(1) express the concentrations of dissolved species in units of molality. (2) Using molality values, calculate $\log(Ca^{\frac{1}{2}}/Na)$. If this number is negative, calculate logK* for b = 1/3, and use (Figure 5) to estimate temperature. (3) If $\log(Ca^{\frac{1}{2}}/Na)$ is positive, calculate logK* for b = 4/3, and determine whether the temperature estimated from (Figure 5) is greater or less than 100°C. If greater than 100°C, recalculate logK* using b = 1/3, and use that value to estimate the temperature. Otherwise, use b = 4/3 to estimate the temperature."

Use of the empirical curve on Figure 5 as above will give estimated reservoir temperatures corrected for Ca competition with Na and K in silicate reactions and does not require a knowledge of the composition of the wall rocks in the hydrothermal system. The accuracy of reservoir temperatures estimated from this curve is better for temperatures over 200°C as shown by the tighter grouping of data points above 200°C on Figure 6 in Fournier and Truesdell (1973). The inherent accuracy is ± 15 to 20°C for any reservoir temperature estimate based on this curve.

Sources of error in estimating reservoir temperatures by using Figure 5 are: (1) dilution of thermal water by shallow ground water, (2) continued reaction of ascending thermal water with the wall rocks, and (3) different net reactions resulting from different reservoir conditions than assumed in establishing $\log K^*$ for Figure 5.

The relative absolute amounts of Na and K in thermal waters and shallow ground waters normally differ by such an order of magnitude that dilution of thermal water by shallow ground water does not significantly change the atomic Na/K ratio of the thermal water. However, the square root factor of Ca used in calculating the approximate K^* value may result in incorrect estimated reservoir temperatures due to ground water dilution where the Ca content of the thermal water is large relative to the Na content. Dilution of the Ca concentration will result in estimated reservoir temperatures that are higher than the actual reservoir temperature.

Continued reaction of ascending thermal water may result in assimilation of Ca if the thermal water is initially low in Ca content. This will result in estimated reservoir temperatures being too low. On the other hand, precipitation of calcite from Ca-rich thermal waters during ascent or in the discharge spring will result in estimated reservoir temperatures being too high. Continued water-rock reaction of ascending thermal waters may also result in a last equilibrium with wall rocks at temperatures significantly lower than actual reservoir temperatures.

The fact that the data used by Fournier and Truesdell

(1973) in deriving the empirical curve on Figure 5 correlates well with temperature suggests that the assumptions regarding hydrogen ion participation and stoichiometry of the net reactions are valid in most cases. However, acid pH conditions at depth may permit hydrogen ion participation in the net silicate reactions resulting in a different approximate equilibrium constant and in as yet undetermined effects on estimated reservoir temperatures. Since the important consideration in any case is the Ca content, changes in pH dictated by silicate hydrolysis reactions would cause decreasing solubility of calcite and lower Ca content in solution as pH increased, possibly resulting in estimated reservoir temperatures being high, whereas changes in pH dictated by partial pressures of CO_2 would cause an increase in calcite solubility as CO_2 content increased and subsequently lower estimated reservoir temperatures.

MONTANA HOT SPRINGS

Hot-Water System Subtypes

All of the hot springs studied in Montana for this project are discharging from hot-water hydrothermal systems. Montana hydrothermal systems can be categorized on the basis of the presence or absence of a confining cap formation in the reservoir structure and on the basis of reservoir aquifer characteristics. Reservoir aquifers may consist of rock types in which flow is predominately through an ideally homogeneous porous medium which can be defined in terms of pore size, pore distribution, and permeability; or the reservoir aquifer may transmit water primarily through open channels such as fractures, joints, solution conduits or caverns, and other fissure openings typical of shear zones and faults in massive, brittle rock. The four possible categories of hydrothermal systems in Montana based on the above criteria are:

(1) confined reservoir,
porous aquifer

(2) confined reservoir,
fractured rock or solution channel aquifer

(3) unconfined reservoir,
porous aquifer

(4) unconfined reservoir,
fractured rock or solution channel aquifer

Relative Economic Potential

The four categories of Montana hydrothermal systems are listed above in general order of decreasing economic potential. The presence of a stratum confining a hydrothermal reservoir is necessary for the existence of a li-

quid or vapor phase at pressures currently required to drive steam turbines economically. Confined geothermal reservoirs have more potential for power production than unconfined reservoirs.

Assuming adequate pressure and temperature exist in a reservoir, it is still necessary for the liquid phase to move through the reservoir aquifer to a drill hole rapidly enough to support production demands. Production from a reservoir, either confined or unconfined, depends on the aquifer permeability and can be defined in terms of the hydraulic conductivity of the aquifer. Hydraulic conductivity describes the permeability of the aquifer and measures its capacity to transmit a unit volume of water per unit area of aquifer in a given period of time.

Aquifers with large, interconnected pores will have relatively high hydraulic conductivity as is typical of medium to coarse, well-sorted, uncemented sandstones with rounded grains. Aquifers with small, poorly interconnected pores such as found in fine sediments or in poorly-sorted sandstones with angular grains and close packing arrangements will have relatively low hydraulic conductivity. The hydraulic conductivity of aquifers in which water is transmitted in fractures or solution channels is determined by the size, number, and interconnection of the open channels conducting water and is usually relatively high where sufficient channels are present. Water volume is usually relatively low per unit of reservoir volume in this type of aquifer. This is because the open channels transmitting the water occupy little of the total aquifer volume resulting in an aquifer with low porosity and high

permeability.

A geothermal reservoir may contain large volumes of liquid water in a porous aquifer at pressure and temperature adequate for economic steam production; however, if the hydraulic conductivity of the reservoir aquifer is too low, the geothermal water will not move to a production drill hole rapidly enough to produce steam in quantities sufficient to drive a turbine. A comparison of the economic potential for power generation of the four possible categories of Montana hydrothermal systems can be made on the basis of potential geothermal water production if reservoir base temperatures are assumed to be the same for all four categories. The hydraulic conductivities of the reservoir aquifers can be used as an index to the rate of water (or steam) production. The geologic structure and aquifer pore characteristics can be used as an index to the volume of water available in the reservoir.

Category 1 systems with high hydraulic conductivity are the most attractive economically. Category 1 systems with low hydraulic conductivity may be less attractive than category 2 systems even though the category 2 systems may have less total reservoir volume. The same general criteria apply to category 3 and 4 systems for assessing space heating, irrigation, and heat exchange power generation potential. Thus, the four categories of hydrothermal systems listed above ore in general order of descending economic potential excluding aquifers with low hydraulic conductivities in category 1 and 3 systems.

Representative Hot Springs

Geologic evaluation of all known Montana hot springs

for this study reveals that Montana hot springs are discharging from category 1, 2, and 4 hydrothermal systems, but not from any known category 3 hydrothermal systems. Chemically, Montana hot spring discharge waters are neutral to alkaline. A few spring discharges are slightly acidic (pH of 6.0 to 6.5) probably because of undersaturation with Ca. The specific hot springs chosen for detailed evaluation in this paper are representative of all hydrothermal system categories and hot spring water chemical types that are known to exist in Montana and represent a wide range in base temperatures.

Alhambra, Boulder, and Helena Hot Springs discharge neutral to alkaline waters from category 4 hydrothermal systems in evidently unconfined, fractured igneous rock aquifers with limited reservoir volume. Pullers Hot Springs discharges neutral waters from what is probably a category 2 hydrothermal system consisting of a fractured metamorphic rock aquifer confined by relatively impervious lacustrine clay-shales and silt-shales and has limited reservoir volume potential. Hunters Hot Springs discharges alkaline waters from a category 1 hydrothermal system consisting of sandstone(?) aquifers confined by marine clay-shales and has a large potential reservoir volume. Big Spring at Toston discharges slightly acidic water from a category 4 hydrothermal system consisting of cavernous or permeable limestones bounded by impermeable orthoquartzite and shale and has moderate potential reservoir volume due to local structural conditions. Salmon Hot Springs in Idaho discharges slightly acidic water from what is probably a category 4 hydrothermal system consist-

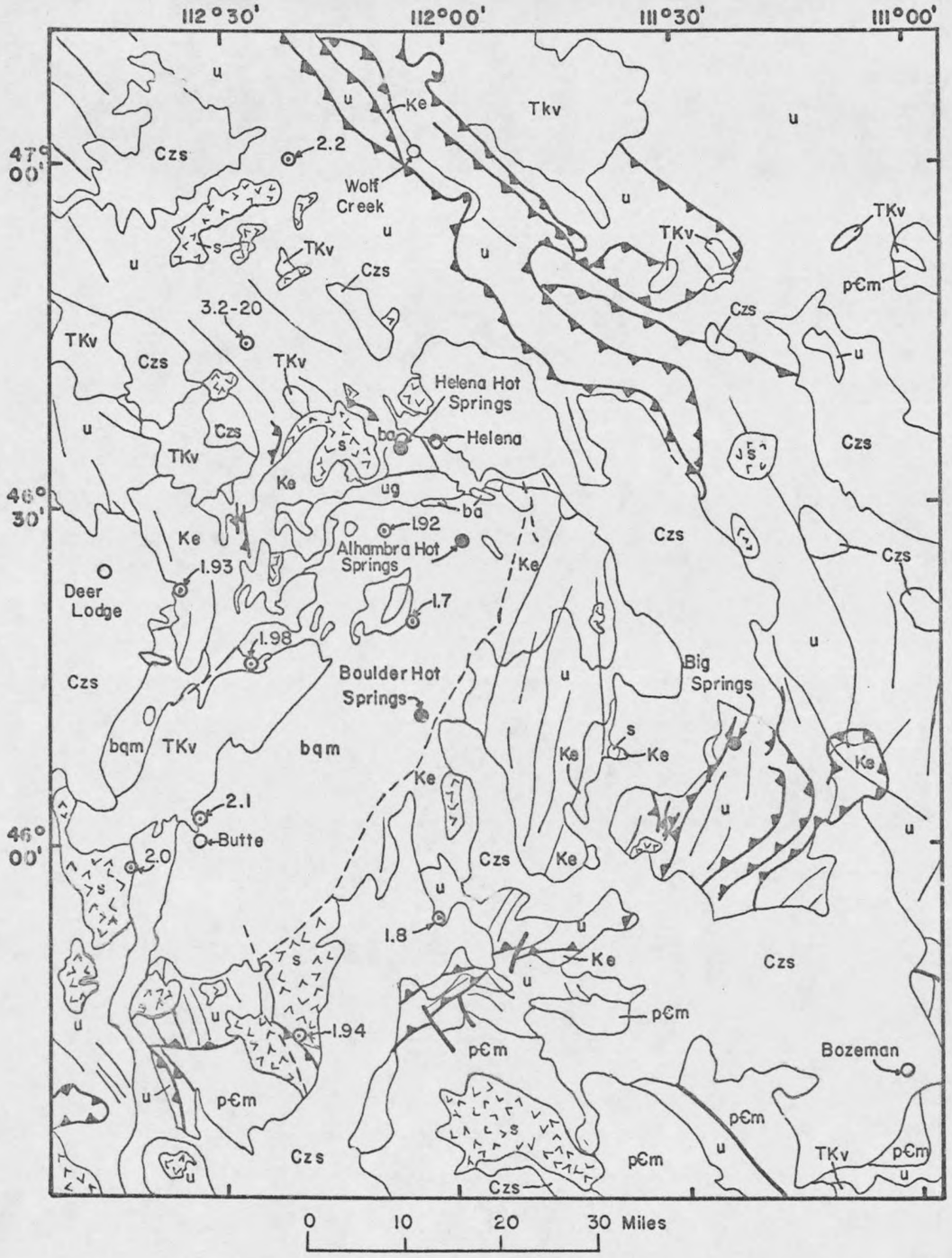
ing of an unconfined fractured volcanic rock aquifer with limited reservoir potential. There is also a possibility that this system may be receiving water at depth from confined Tertiary valley sediments. The hydrothermal system categories, water chemistry, and estimated reservoir temperatures for the above hot springs are listed in Table III.

The Boulder Batholith

A significant portion of this study is devoted to investigating application of the Na-K-Ca hydrogeothermometer in evaluating Montana hot springs. Alhambra and Boulder Hot Springs represent two extremes of thermal water chemistry which typify the various factors affecting application of the Na-K-Ca hydrogeothermometer. Both of these hot springs discharge from hydrothermal systems in the Butte Quartz Monzonite of the Boulder batholith. A short but pertinent description of the geology of the Boulder batholith is presented here to provide the reader with an overview of the lithologic and structural framework in which Alhambra and Boulder Hot Springs exist.

Klepper (1973) describes the Boulder batholith (Figure 6) as a northeast trending calkalkaline composit body containing at least 15 separate plutons; most of which are quartz monzonite or granodiorite in composition. Tilling, Klepper, and Obradovich (1968) provide K-Ar dates for the batholith indicating emplacement of the plutons between about 78 and 68 million years (m.y.) ago. Tilling (1973) observes that the multiple-intrusion hypothesis for the batholith requires at least two chemically and isotopically distinct magma sources.

About 75 to 80 percent of the exposed area of the



EXPLANATION

Czs

Cenozoic Sediments

TKv

Post–Batholith Tertiary Volcanics

ba

Biotite Adamellite of Knopf (1963)

s

Satellite Plutons, Various Ages and Compositions

bqm

Butte Quartz Monzonite and Related Facies

ug

Unionville Granodiorite

Ke

Elkhorn Mountains Volcanics – Late Cretaceous

u

Mesozoic, Paleozoic, and Precambrian Belt Rocks

p€m

Precambrian Crystalline Metamorphic Rocks

Geologic Contact

Thrust Fault

Steep Fault

Fold Axis

Fault–Controlled Intrusive Contact

2.2 Heat Flow Measurement

Regional Geology of the Boulder Batholith

Figure 6

After Klepper, and Robinson, and Smedes (1971)

batholith consists of a single large pluton, the Butte Quartz Monzonite, most of which crystallized during the period from 75 to 70 m.y. ago, in Late Cretaceous time (Tilling, Klepper, and Obradovich, 1968). Main stage Butte Quartz Monzonite is crosscut by younger alaskite, aplite, and quartz monzonite pegmatite bodies. These are present as irregular pods, lenses, and random dikes with blended contacts which are apparently late stage residual differentiates formed in situ. These were cut by later sharply defined dikes and sheets which show dilation offset and joint control as the result of still later intrusion of the same late stage differentiates into completely solidified quartz monzonite (Smedes, 1966). Tilling, Klepper, and Obradovich (1968) place the age of the late-stage felsic rocks at 70 to 75 m.y. old or essentially contemporaneous with cooling of the Boulder batholith. Other igneous rocks associated with the Butte Quartz Monzonite include quartz latite dikes and plugs which are contemporaneous with part of the Lowland Creek volcanics of Eocene age, dated as 50 m.y. old by Smedes and Thomas (1965), and rhyolite intrusive and extrusive rocks thought to be younger than the Lowland Creek volcanics, (Rupple, 1961; Smedes, 1962; and Smedes, 1966). Other post batholith deposits include joint controlled quartz veins and chalcedony veins. Some of the chalcedony veins appear to be of hydrothermal origin.

Rocks of the Butte Quartz Monzonite range in composition from 20 to 48 percent plagioclase, 15 to 45 percent K-feldspar, 15 to 40 percent quartz, less than 1 to 12 percent biotite, less than 1 to 8 percent hornblende, and

TABLE I

CHEMICAL COMPOSITION

Butte Quartz Monzonite

from Smedes, Klepper, and Tilling (1973)

SiO_2	64.92	TiO_2	.52
Al_2O_3	15.46	P_2O_5	.18
Fe_2O_3	1.81	MnO	.09
FeO	2.70	H_2O+	.59
MgO	2.05	H_2O-	.12
CaO	4.24	CO_2	.06
Na_2O	3.06	BaO	.09
K_2O	3.94	S	.05

MODAL COMPOSITION

	Butte Quartz Monzonite			Alaskite-Aplite	
	1	2	3	4	5
Plagioclase	38.5	39.0	30.8	---	---
K-feldspar	22.6	26.6	33.6	3.0	50.0
Quartz	23.7	25.8	26.4	77.0	50.0
Biotite	7.6	8.0	4.4	0.6	---
Amphibole	5.0	---	3.1	---	---
Chlorite	1.4	Tr	0.9	---	---
Accessories	1.2	0.6	0.8	---	---
Secondary kaolinite	---	---	---	19.4	---

1. Smedes, Klepper, and Tilling (1973)
2. Alhambra Hot Springs Sample 1
3. Boulder Hot Springs Sample 2
4. Alhambra Hot Springs Sample 2
5. Boulder Hot Springs Average Aplite Composition

less than 1 to 3 percent accessory minerals including magnetite, sphene, zircon, and apatite (Becraft, Pinckney, and Rosenblum, 1963). Modes of 19 additional samples of Butte Quartz Monzonite presented by Smedes (1966) fall generally within this range. Representative chemical and modal composition for Butte Qaurtz Monzonite after Smedes, Klepper, and Tilling (1973) is shown in Table I. Modal compositions for rocks adjacent hydrothermal systems as shown by the author in Table I fall within the range of composition for the Butte Quartz Monzonite.

Alaskite, which is associated with the Alhambra hydrothermal system, varies widely in composition but consists in general of at least one-third quartz; one-third to one-half potassium feldspar; plagioclase; less than 1 percent biotite; and trace amounts of zircon, apatite, hematite, magnetite, pyrite, and tourmaline.

The regional tectonic setting of the Boulder batholith is depicted on Figure 6. The northeast trending Boulder batholith lies between the Idaho batholith to the west and the Montana Disturbed Belt to the east. The north end of the batholith terminates just south of the Montana Lineament. The Montana Lineament is a major west-trending tectonic feature marked by a left-lateral echelon fold system just north of the Boulder batholith and by tear faults west of the vicinity of the batholith. Klepper, Robinson, and Smedes (1971) and Smedes, Klepper, and Tilling (1973) show the batholith bounded on the south by a right-lateral tear thrust zone (Figure 6) which may project back to a west-trending linear tectonic zone in the Idaho batholith.

Smedes (1966) states that batholith emplacement was

controlled by a preintrusion northeast-trending fault along the eastern flank of the batholith. Klepper, Robinson, and Smedes (1971) suggest the possibility of similar emplacement controls along the concealed western flank of the batholith on the east margin of the Deer Lodge Valley. Joints in the batholith intruded by alaskite, aplite, and pegmatite exhibit diffuse orientation suggesting they are cooling joints. Barren joints display a dominant northeast trend regardless of main stage magma cooling contacts and were probably formed due to recurrence of regional stresses similar to those producing prebatholith structures (Smedes, 1966).

The thickness of the Boulder batholith has been subject to debate. Hamilton and Myers (1967) suggested a maximum thickness of 5 kilometers for the batholith and interpreted geologic mapping evidence and geophysical data to indicate that the batholith is "in effect a gigantic mantled lava flow.... only a few kilometers thick." Using more refined interpretations of gravity data from Biehler and Bonnini (1969); rock density measurements from Knopf (1963); and aeromagnetic data from Johnson, Henderson, and Tyson (1965); Klepper, Robinson, and Smedes (1971) concluded that the batholith has steep contacts on all sides and is at least 15 kilometers thick. Although the arguments of Klepper and his associates are not conclusive, they present persuasive evidence that the Boulder batholith was intruded transgressively from below as an extensive pluton with steep sides and is at least 3 times thicker than the 5 kilometers proposed by Hamilton and Meyers (1967).

Heat flow in the Boulder batholith at present is the result of the total combined heat flow of about 2.0 microcalories/cm^2sec (heat flow unit or HFU) from the mantle and radiogenic heat production in the batholithic rocks (Blackwell and Robertson, 1973). Western Montana, including the Boulder batholith, is in an area of abnormally high heat flow called the Cordilleran Thermal Anomally Zone (CTAZ) by Blackwell (1969) along the axis of the Cordilleran Mountain chain of the western United States. Average heat flow in the CTAZ is about 2.2 HFU compared to normal heat flow of about 1.4 HFU for stable platform areas of continents (Roy, Blackwell, and Decker, 1972). Heat flow values in the vicinity of the Boulder batholith are lowest for sites farthest removed from areas of Mesozoic and Cenozoic intrusive activity (Blackwell and Robertson, 1973); however, the youngest igneous rocks in this area are the quartz latites of the Lowland Creek volcanics, dated as approximately 50 m.y. old (Smedes and Thomas, 1965). Calculations by Blackwell (oral communication, 1973) based on the method of Jaeger (1957) indicate that the thermal effect of these igneous events has long since dissipated.

Heat flow values from Blackwell and Robertson (1973) are shown on Figure 6 for the Boulder batholith area. Thermal conductivity, thermal gradient, and heat flow values are summarized on Table II. Heat flow measurements were made in drill holes either in the Butte Quartz Monzonite (Unionville and Jefferson City) or in rocks underlain by the Butte Quartz Monzonite at shallow depth (Silver Bow, Elk Park, and Deer Lodge) with the excep-

TABLE II

HEAT FLOW

from Blackwell and Robertson (1973)

Locality	K 10^{-13} cal / cm sec °C	Geo Grad (°C/km)	Heat Fl 10^{-6} cal / cm^2 sec	Geologic Unit
Butte	6.62	31.9	2.1	Butte Quartz Monz.
Deer Lodge	7.4	24.2	1.93	Elkhorn Mts. Volc.
Elk Park	7.4	27.9	1.98	Lowland Crk. Volc. & Butte Quartz Monz.
Jefferson City	8.3	21.0	(1.7)	Butte Quartz Monz.
Lincoln			2.2	Belt Supergroup
Marysville		3.2-19.5		Belt Supergroup & Cenozoic Intrusives
Silver Bow	(5.0)	38.9	(2.0)	Lowland Crk. Volc.
Silver Star	6.4	30.1	1.94	Rader Crk. pluton
Unionville	7.3	26.3	1.92	Unionville Granodiorite and Butte Quartz Monzonite
Whitehall	7.8	19.8	1.8	Belt Supergroup

K = Thermal conductivity

10^{-6} cal/cm^2 sec is one Heat Flow Unit (HFU)

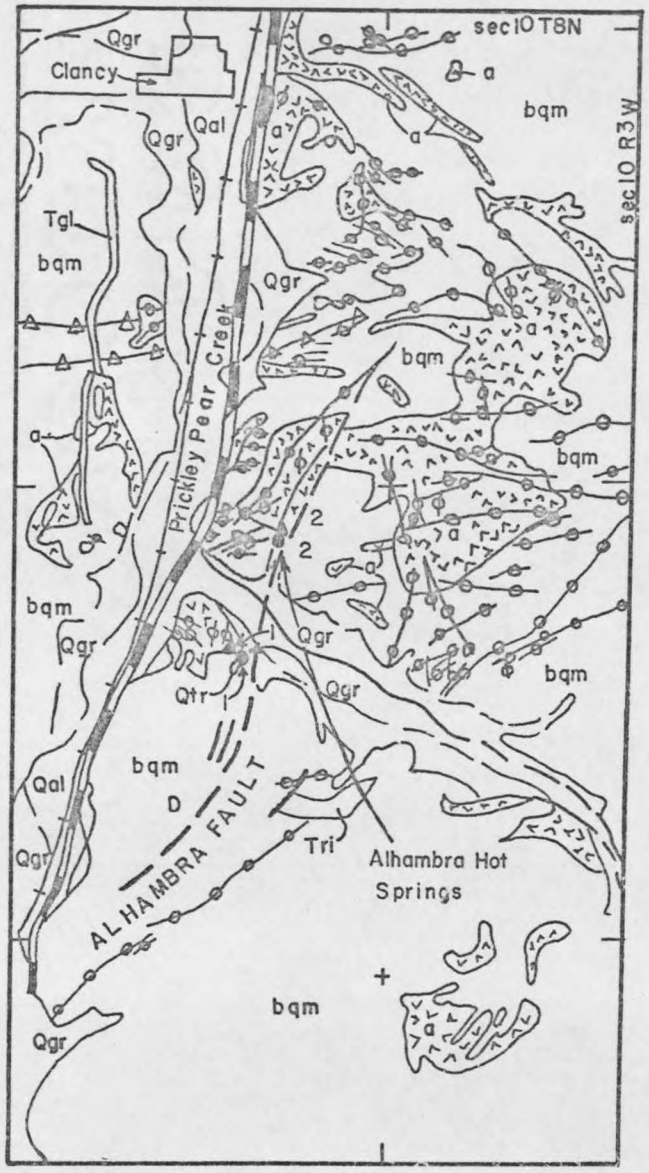
() indicates tentitive value

tions of Silver Star in the Rader Creek pluton and Whitehall in the Precambrian Belt Supergroup strata. Heat flow measurements were made at a depth range of 150 to 600 meters which is supposedly below the depth of surface thermal effects. An exception is the Jefferson City measurement which was made in shallow holes (50 to 170 meters) on top of a steep hill. The low value of 1.7 HFU for Jefferson City is not considered reliable. Additional data are needed for verification (Blackwell and Robertson, 1973).

Alhambra Hot Springs

Alhambra Hot Springs (Figure 7) consists of 4 main springs and a number of seeps discharging hot water (50 to 54°C) from the Alhambra fault zone where it crosses the Warm Spring Creek valley in the NE¼ of section 16, T8N, R3W of the Clancy quadrangle. The Alhambra fault is a slightly sinuous fault trending roughly N25E and is about 1 mile long. Smedes (1966) describes displacement along the fault as hingelike with the hinge on the north end. The west side of the fault dropped down relative to the east side. Smedes (1966) states that the displacement of the base of an alaskite sheet on the west side of the fault is 40 feet downward near the north end of the fault and about 200 feet downward at the south end.

The Alhambra hydrothermal waters appear to circulate in fractured and sheared Butte Quartz Monzonite rocks in and adjacent to the Alhambra fault which comprise an evidently unconfined aquifer. Cold surface water draining into the depression along the southern one-half of the fault and shallow ground water in the alluvium along Warm



GEOLOGY OF THE ALHAMBRA AREA

Geology by Harry W. Smedes (1966)

EXPLANATION

- Qal — Recent alluvium
- Qtr — Recent travertine deposit
- Qgr — Quaternary terrace gravels
- Tri — Tertiary flow-banded rhyolite intrusive
- Tql — Tertiary quartz latite dike
- a — Cretaceous alaskite of Boulder batholith
- bqm — Cretaceous Butte Quartz Monzonite
- Geologic contact
- U / D — Fault
- Chalcedony vein or vein zone
- Metalliferous quartz vein
- ▲ 1 — Fresh quartz monzonite
- ▲ 2 — Altered alaskite sample
- ● 1 — Main hot spring
- ● 2 — Low volume hotspring

0 — 1/2 — 1 Mile

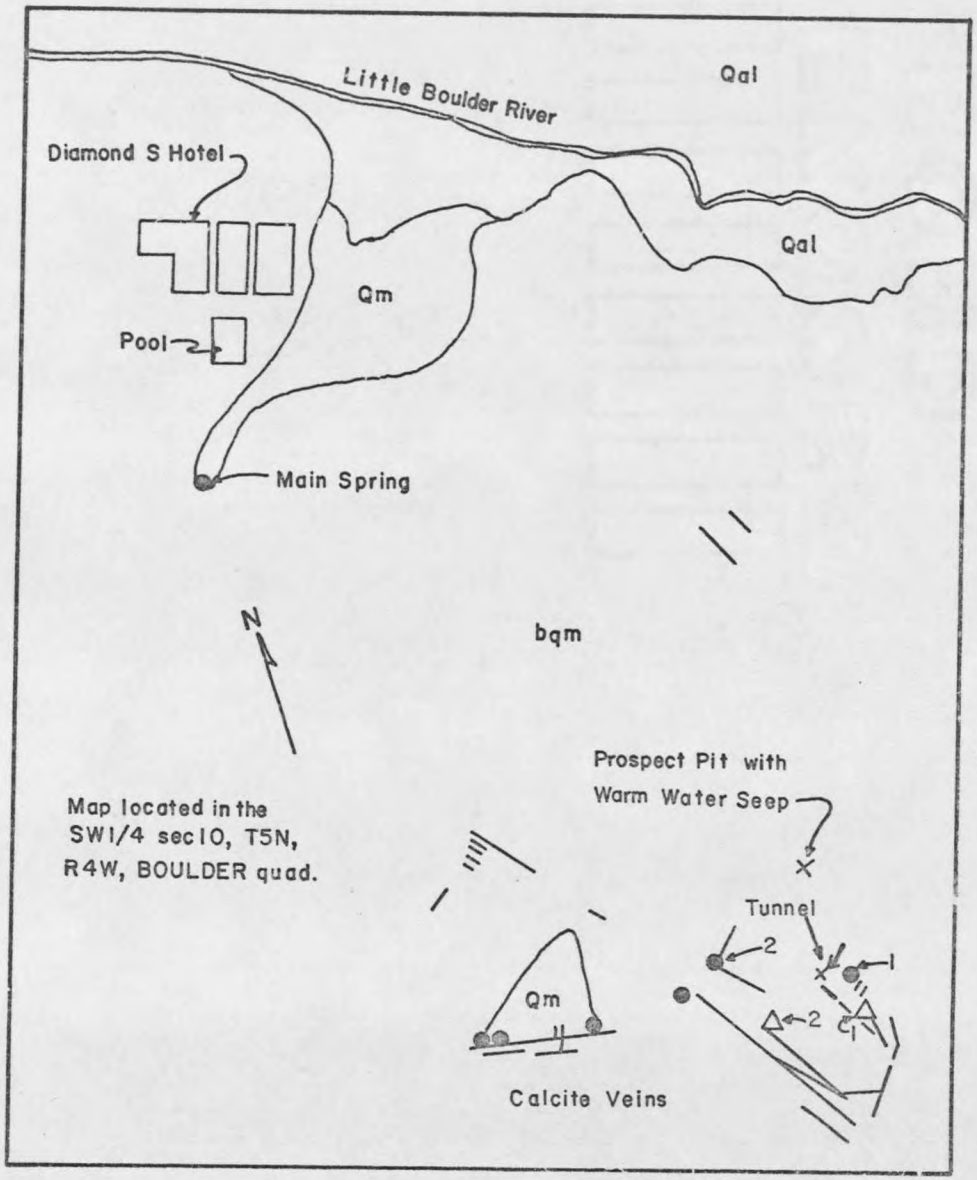
FIGURE 7

Springs Creek upstream from the fault may provide recharge for the system. The wall rock of the hydrothermal system is primarily a light-gray, medium to coarse-grained, locally porphyritic, quartz monzonite. The downfaulted alaskite and aplite sheet on the west side of the fault has been extensively altered by the hydrothermal waters in the area adjacent to the fault zone. Samples of the quartz monzonite and alaskite-aplite were collected at the locations indicated on Figure 7. No hydrothermally altered quartz monzonite is exposed in or near the hot spring discharges due to alluvial and colluvial cover.

An ancient travertine deposit at least 10 feet thick is present at the main spring south of Warm Springs Creek. The springs do not currently deposit any significant amounts of material. Small coatings of siliceous material (opal?) are present on the walls of the collection box at the spring. Smedes (1966) states that the springs are currently depositing silica. The collection system obscures the main spring discharge; however, the author estimates a discharge in excess of 500 gallons per minute.

Boulder Hot Springs

Boulder Hot Springs is located in the Boulder batholith in the SE¼ of section 10, T5N, R4W of the Boulder quadrangle. The Boulder hydrothermal system discharges thermal waters ranging in surface temperatures from 41.5 to 74.5°C from a number of springs in Butte Quartz Monzonite as shown on Figure 8. The main spring discharges appear to be joint controlled; however, an old test pit penetrating altered bedrock about 200 feet downhill from the nearest major joint discharging thermal water contains



PRELIMINARY GEOLOGIC MAP

of the

BOULDER HOT SPRINGS AREA

Based on W.H. Weed (1900)

EXPLANATION

Qm — Recent bog and marsh soil

Qal — Quaternary alluvium

bqm — Cretaceous Butte Quartz Monzonite including Alaskite and Aplite

——— Geologic contact

——— Calcite vein

1 ● Hot Spring Discharge, number indicates water sample collected

1 △ Vein sampled here

2 △ Wall rock sampled here

Caved adit – hot water filled

0 100 200 300 400 500 Feet

FIGURE 8

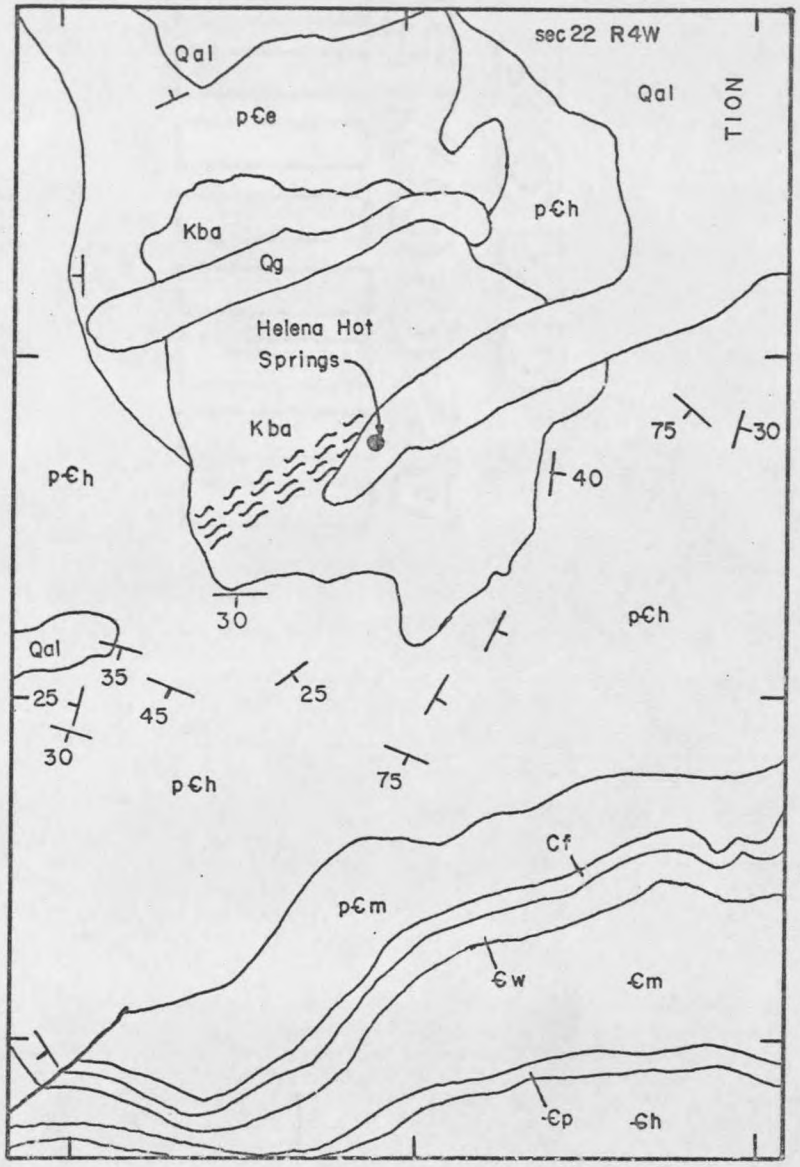
a thermal water seep which fills the pit to within 6 to 8 feet of the ground surface. The joints discharging thermal water are filled with calcite-chalcedony veins; however, in the tunnel shown on Figure 8 the thermal water is currently depositing silicate minerals and no calcite. Discharge from this system ranges from less than 1 gallon per minute in some springs to over 1000 gallons per minute (author's estimate) in the largest spring.

Although the country rocks near the hydrothermal system are saturated with thermal water as seen in the test pit and tunnel (Figure 8), the largest volume of the circulation probably takes place in the more permeable channels of the joint system. Thus, the hydrothermal reservoir may be limited in effective volume due to low porosity wall rocks although the hydraulic conductivity of the "aquifer" is high. The hydrothermal reservoir is unconfined although some self-sealing has occurred in the discharge part of the system due to vein deposition. The system may be recharged from surface waters in Beaver Creek to the west or Farnham Creek to the south. These waters are topographically higher than the hot springs discharges. Recharge water from these sources flowing through the local joint system to depth would provide a source of head in the hydrothermal system and a reasonable steady state source for the large volume of water being discharged from the potentially low-volume reservoir of the Boulder hydrothermal system. No other source of large volumes of water supplying head to the system is evident.

Helena Hot Springs

Helena Hot Springs is located in the NE¼ of section 28, T10N, R4W of the Helena quadrangle. The Helena hydrothermal system discharges thermal water with a surface temperature of 63°C at a rate of 30 gallons per minute (Waring, 1965) from a quartz monzonite intrusive body (Figure 9) overlain by a 5 to 6 foot thick cover of Quaternary alluvium in the vicinity of the spring discharge. Evidence of shearing or faulting of the quartz monzonite is not present. The hydrothermal waters probably circulate in a dominant set of vertical joints trending N66E. The hydrothermal reservoir appears to be confined to the open channels of the dominant joints and subordinate intersecting joints. A zone at least 100 feet wide of thin pegmatitic sheet veins averaging 4 mm wide and confined to the vertical dipping dominant joints cuts across the center of the intrusive body from east to west and includes the hot spring discharge in its center. No alteration of the intrusive quartz monzonite by hydrothermal activity or pegmatitic vein emplacement is evident. The only sources of recharge of the hydrothermal system implied from the lithology and structure of the surrounding units are surface precipitation and runoff on the surface of the intrusive body, and shallow ground water.

Ten Mile Creek flows along the axis of the pegmatite zone as it crosses the intrusive body and may contribute significant amounts of recharge water. The quartz monzonite is intruded into Precambrian siltstones, argillites, quartzites and siliceous dolomites of the Spokane, Empire, and Helena Dolomite Formations, none of which can be ex-



Geology of the Helena Hot Springs Area

Geology from Adolph Knopf (1963)

Explanation

- Qal — Quaternary Alluvium
- Qg — Quaternary Gravel and Moraine
- Kba — Cretaceous Biotite Adamellite Intrusive
- €h — Cambrian Hasmark Dolomite (marble)
- €p — Cambrian Park Argillite
- €m — Cambrian Meagher Limestone
- €w — Cambrian Wolsey Shale
- €f — Cambrian Flathead Sandstone
- p€m — Precambrian Marsh Fm. (argillites and quartzites)
- p€h — Precambrian Helena Dolomite (siliceous)
- p€e — Precambrian Empire and Spokane Fms. (argillites)
- Geologic Contact
- 20 — Strike and Dip
- U / D — Fault
- Pegmatitic Zone

FIGURE 9

0 1/2 1 Mile

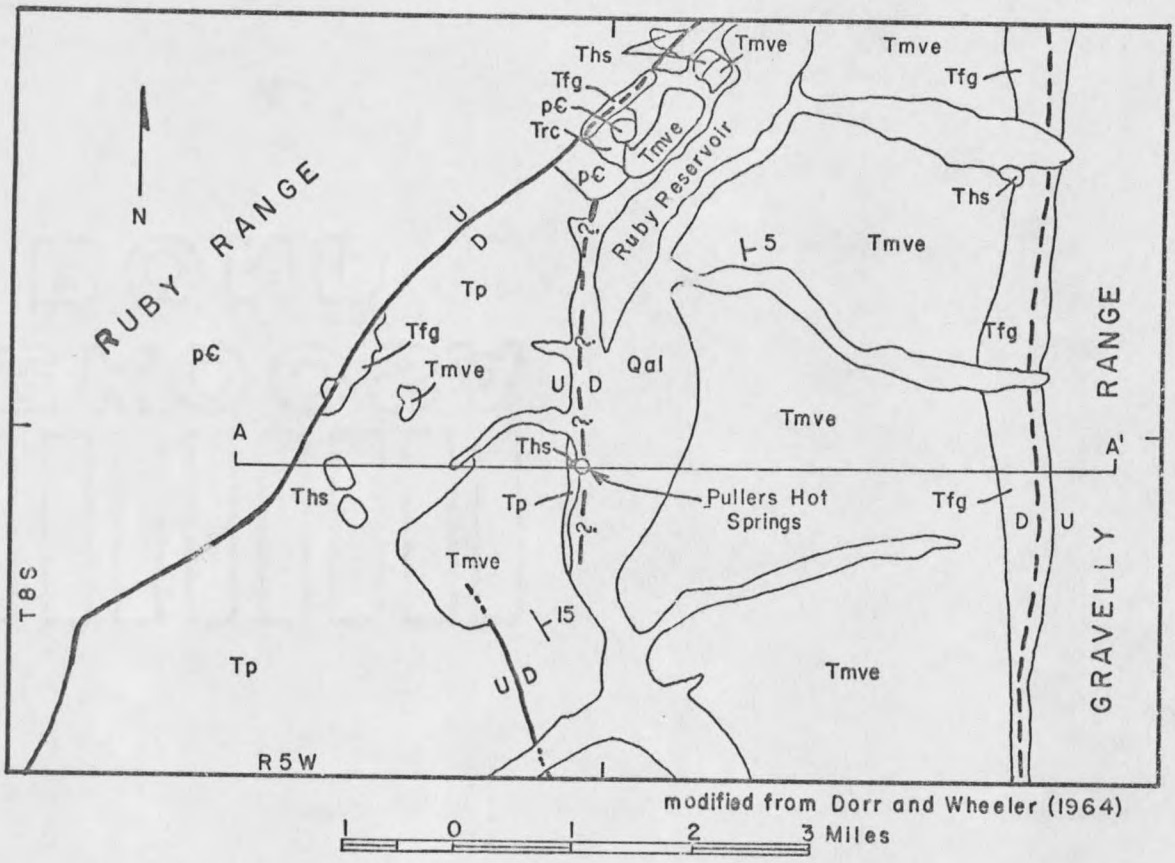
pected to contribute significant volumes of water to the hydrothermal system.

The quartz monzonite intrusive body consists of a light-gray, fine to medium-grained, seriate to hypidiomorphic-granular, biotite quartz monzonite which Knopf (1963) termed biotite adamellite to emphasize the nearly 1:1 ratio of plagioclase to K-feldspar in the rock. Other plutons mapped by Knopf (1963) as biotite adamellite intrude Knof's Clancy Granodiorite which Smedes (1966) states is coextensive with the Butte Quartz Monzonite. Thus, the Helena Hot Springs pluton appears to be a late stage or post batholith satellite pluton of the Boulder batholith. A K-Ar age date of 74 m.y. was obtained on a contemporaneous pluton intruding the Butte Quartz Monzonite (Tilling, Klepper, and Obradovich, 1968).

Puller Hot Springs

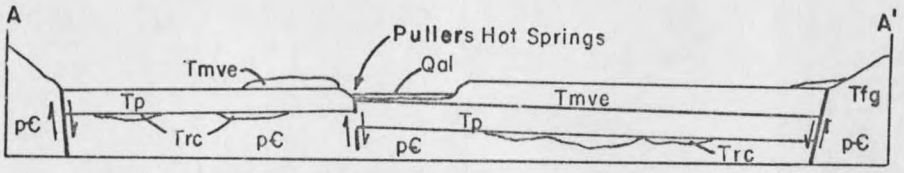
Puller Hot Springs is located in the NE$\frac{1}{4}$ of section 1, T8S, R5W of the Metzel Ranch quadrangle. The spring water issues from Quaternary alluvium with a surface temperature of 43°C and at a rate of about 150 gallons per minute (Waring, 1965). The hot spring is not depositing mineral deposits at present, however, nearby travertine deposits suggest that it deposited calcite some time in the past.

Becker (1961) and Dorr and Wheeler (1964) consider the Ruby River Valley to be a major graben block (Figure 10) bounded by north-south faults. The Precambrian metamorphic basement rocks underlying the valley consist of granitic gneiss and are overlain by Tertiary and Quaternary valley sediments. The valley sediments consist of a local Paleocene red conglomerate, Eocene to Oligocene lacustrine



modified from Dorr and Wheeler (1964)

General Geology of Pullers Hot Spring Area, Ruby River Basin



Generalized Cross-Section A-A'

Explanation

Qal — Alluvium

Ths — Hot Springs Deposits

Tfg — Fault Line Gravel

Tmve — Madison Valley Equivalent

Tp — Passamari fm.

Trc — "Red Conglomerate"

pC — Precambrian Gneiss and Schist

U/D — Fault

— — — Concealed Fault

—?—?— Implied Fault

15 — Strike and Dip

Geologic Contact

FIGURE 10

shales of the Passamari Formation, Miocene to Pliocene fluviatile conglomerates and tuffaceous sandstones of the Madison Valley Equivalent, and thin Quaternary alluvium (Dorr and Wheeler, 1964).

The Tertiary sediments have poor aquifer characteristics and the thermal waters are probably discharging from a hydrothermal reservoir circulating primarily in fractured metamorphic rocks of the crystalline basement. The relatively impermeable Passamari Formation acts as a confining stratum for such a system. An analysis of the minus 2 micron size fraction of various horizons in the lower member of the Passamari Formation indicates that the dominant clay mineral of the shales is a montmorillonite mineral. The minus 2 micron size fraction comprises at least 50 percent of the total shale volume in every sample examined and usually comprises 90 to 95 percent of the total volume of the shales of the lower member of the Passamari.

The system is recharged from shallow ground water flowing along valley marginal faults and local intervalley faults in the Tertiary sediments. Ground water "leaking" slowly downward through the Passamari Formation over a wide area in the valley could also contribute large volumes of water. The hot spring discharge system probably exploits a fault cutting through the basement gneiss and the Tertiary valley fill to gain access to the surface (Figure 10).

Hunters Hot Springs

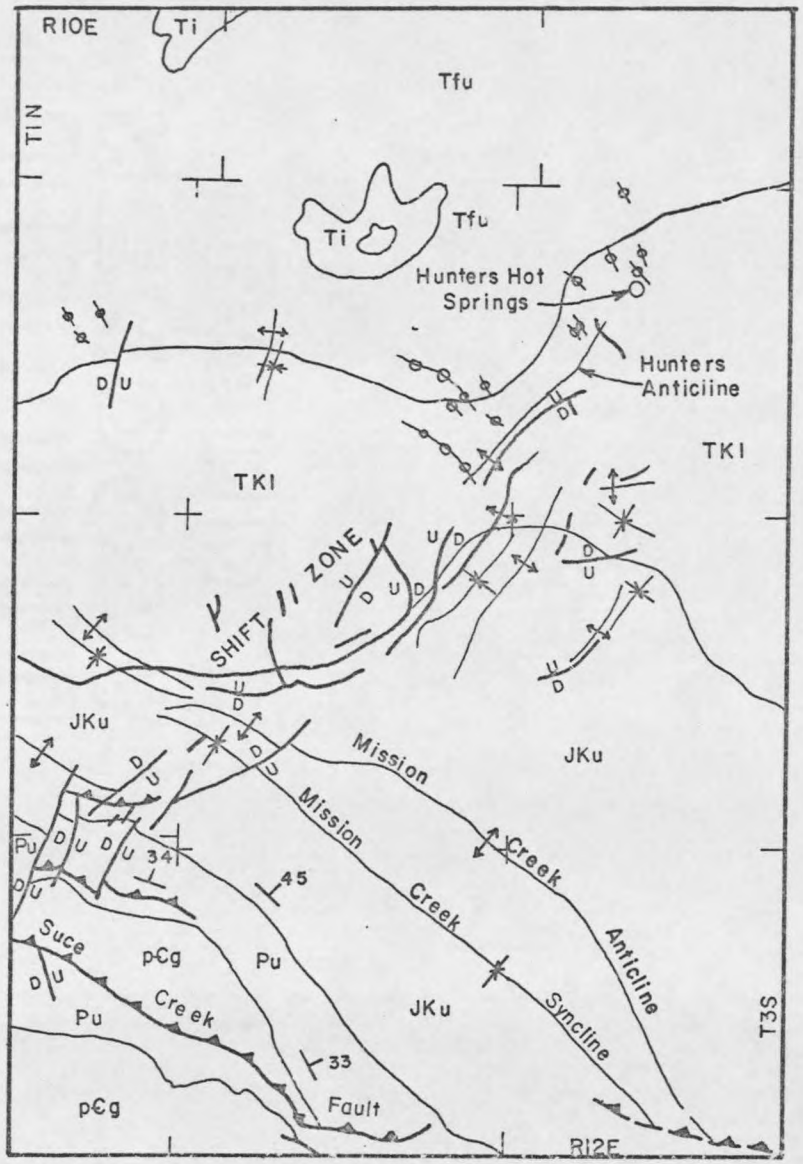
Hunters Hot Springs is located in the SW$\frac{1}{4}$ of section 9, T1S, R12E of the Hunters Hot Springs quadrangle. Thermal

waters with a maximum discharge temperature of 61°C are flowing from 9 main springs and at least 10 smaller springs with an estimated total discharge of 1500 gallons per minute (Waring, 1965). The thermal waters issue from sediments of the Late Cretaceous Livingston Formation; however, the low hydraulic conductivity of this poorly sorted andesitic sandstone makes it a doubtful aquifer. The hydrothermal reservoir is probably contained in one or more of several major aquifers present beneath the upper Cretaceous section.

Figure 11 depicts the general surface geology and structure of the Hunters area. Estimated depths to various formation contacts derived from oil and gas well data for the area (Hadley, 1972) are as follows:

Formation	Depth (Feet)
Base of Livingston Fm.	4000
Top Boulder River SS	4600
Base of Colorado Gp.	5400
Top of Lakota	5700
Top of Swift	6000
Top of Quadrant	6450
Top of Madison	6800

The geothermal gradient shown on the AAPG Geothermal Gradient Map (Map no. 21, Montana, 1973) for the Hunters area is 0.9°C/100 feet. Since the mean annual temperature is about 7°C, water rising under head from the Lakota would have an aquifer temperature of 58°C and water rising under head from the Madison would have an aquifer temperature of 68°C. Movement of water up the flank of the Hunters anticline from deeper areas in the basin structure may result in higher aquifer temperatures. Thus, the temperature of the Hunters Hot Springs discharge may be explained as the



REGIONAL GEOLOGY
HUNTERS HOT SPRINGS AREA

EXPLANATION

Ti	Tertiary Intrusives
Tfu	Tertiary Fort Union Fm.
TKl	Late Cretaceous Livingston Fm.
JKu	Jurassic-Cretaceous Undifferentiated
Pu	Paleozoic Undifferentiated
pCg	Precambrian Gneiss, Schist, and Granite

Anticlinal Axis

Synclinal Axis

U / D Fault

Thrust Fault

Geologic Contact

Calcite Dike

Scale
0 — 5 Miles

FIGURE II

result of deep ground water circulation affected by the local geothermal gradient along a confined aquifer in the Crazy Mountains Basin.

Garrett (1972) subdivides the Crazy Mountains Basin into five major structural blocks bounded by northeast-trending basement rock lineaments. One of these zones, designated the "Shift Zone" (Figure 11), is projected under the Hunters Hot Springs area. The Shift Zone is expressed as a dip-slip fault system terminating against the Beartooth Range to the south and as en echelon folding to the north. Garrett (1972) states that seismic surveys of the surface folds do not detect folding of Mesozoic and Paleozoic reflecting horizons and interprets this to mean that the en echelon folds at the surface are an expression of right-lateral movement along the Shift Zone during Laramide time.

Widespread northwest-trending calcite veins are present in a zone extending from the Hunters Hot Springs area northwest to the Clyde Park area. The calcite veins occupy steeply dipping normal faults and are up to 20 feet wide and several thousand feet long. Many veins are banded parallel to their walls and individual bands exhibit comb structure. The bands and narrow slip surfaces of granulated calcite imply repeated movement on the faults followed by subsequent calcite deposition. The usual presence of small amounts of stilbite in the veins, the continuation of the veins below the present water table, and the lack of alteration or replacement of the wall rock suggests a low-temperature hydrothermal origin for the veins. Stoll and Armstrong (1958) attribute the veins to ancient hot springs (similar to Hunters Hot Springs) ge-

ancient hot springs (similar to Hunters Hot Springs) genetically related to local igneous activity in the basin.

The low-temperature hydrothermal nature of the veins and the presence of calcite deposits in other areas of igneous activity evidently prompted Stoll and Armstrong (1958) to hypothesize a relation between the origin of the calcite veins and the andesites and other intermediate igneous rocks in the area. This hypothesis does not account for an adequate source of Ca needed for the veins and ignores the presence of carbonate strata underlying the area as a source of Ca. The relation of the northwest-trending vein structures to the Shift Zone of Garrett (1972) suggests that the veins represent fillings in extensional features similar to gash veins which formed due to tensional forces generated by recurring movement along the Shift Zone. Normal faults (dip-slip structures) resulting from tensional forces may have provided channels for deep ground water to ascend from carbonate aquifers in the basin. The deep ground water would have been hydrothermal in nature as previously shown.

Solution of calcite at depth from carbonate rock aquifers and deposition of the dissoved calcite as veins by the ascending waters would satisfactorily explain the origin of the veins. This theory accounts for both the temperature of the solutions and the source of the large volumes of calcite. Eventually, self-sealing of the fault channels by calcite stopped the discharge from the carbonate aquifers such as the Madison Formation. The low calcium content water currently issuing from Hunters Hot Springs is not in near proximity to any calcite veins and

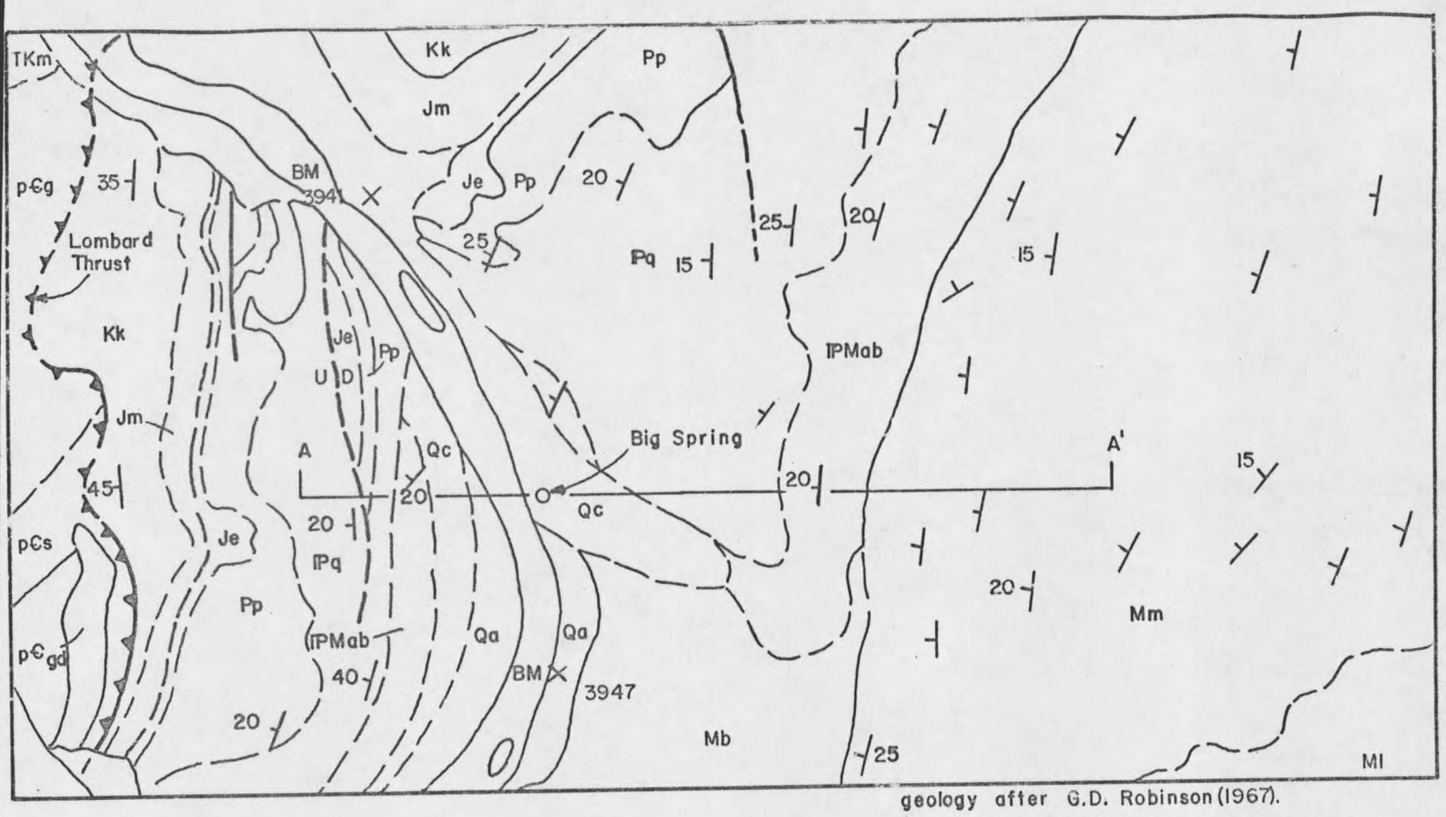
the hydrothermal system is probably not related to the veins.

Big Spring

Big Spring is located on the east bank of the Missouri River in the SE¼ of section 6, T4N, R3E of the Toston quadrangle. The surface discharge temperature is 15.5°C and the rate of discharge stated in Waring (1965) is 29,000 gallons per minute. This spring is classified as a thermal spring because its discharge temperature is more than 5°C hotter than the mean annual temperature of 7.0°C for this area.

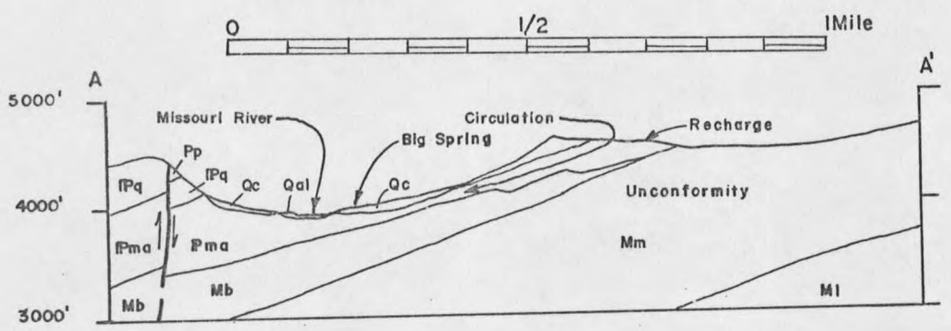
The spring discharges from the upper carbonate member of the Mississippian age Amsden Formation where it is overlain by a local deposit of colluvium (Figure 12). Robinson (1963) describes the Amsden Formation in the area south of the Toston quadrangle as consisting of a lower 200 feet of poorly sorted red mudstones and sandstones becoming better sorted upsection and an upper 100 feet of interbedded dolomite, limestone, and red sandstone. The section at Big Springs was not measured but Robinson (1967) has mapped a thickness of approximately 450 feet for the Amsden in this area (including 100 feet of the Big Snowy Group) which appears to be a continuation of the thickness trends in the Three Forks quadrangle to the south. The upper carbonate member of the formation is the aquifer which is discharging thermal water at Big Spring.

An east-west oriented cross section (Figure 12) at Big Spring depicts the structural details of the Big Spring hydrothermal system. The reservoir consists of the Amsden aquifer bounded above by the quartzitic and calcite-ce-



geology after G.D. Robinson (1967).

GEOLOGY of the BIG SPRING AREA, TOSTON



Cross-Section A-A': Hydrothermal circulation system.

Explanation

- Qal — Quaternary Alluvium
- Qc — Quaternary Colluvium
- TKm — Tertiary Quartz Monzonite Intrusive
- Kk — Cretaceous Kootenai Fm.
- Jm — Jurassic Morrison Fm.
- Je — Jurassic Ellis Group
- Pp — Permian Phosphoria Fm.
- Pq — Pennsylvanian Quadrant Fm.
- IPmab — Penns.-Miss. Amsden Fm (IPma) & Big Snowy Gp. (Mb)
- Mm — Mississippian Mission Canyon Limestone
- MI — Mississippian Lodgepole Limestone
- pCgd — Precambrian Gabbro and Diabase Sill
- pCs — Precambrian Belt Group-Spokane Shale
- pCg — Precambrian Belt Group-Greyson Shale

Geologic Contact

U / D Steep Fault

Thrust Fault

21 Strike and Dip

FIGURE 12

mented sandstone of the Quadrant Formation and bounded below by the poorly sorted clastic material in the lower member of the Amsden and in the shales of the Big Snowy Group. The reservoir is the west-dipping flank of a north-trending anticline, the axis of which is about 1.5 miles east of the spring. Surface water and possibly ground water under head rising along faults from the deeper Madison Limestone recharge the Amsden to the north of Big Spring. Water moves south through solution conduits in the essentially unconfined, cavernous limestone aquifer until it discharges at the level of the Missouri River where the river channel cuts the base of the Amsden Formation (Figure 12). The aquifer is considered to be unconfined to the extent that the strata bounding the Amsden in this particular structure do not produce a confining static pressure in the aquifer due to the large unconfined exposures of the dipping aquifer where it transects the surface (Figure 12).

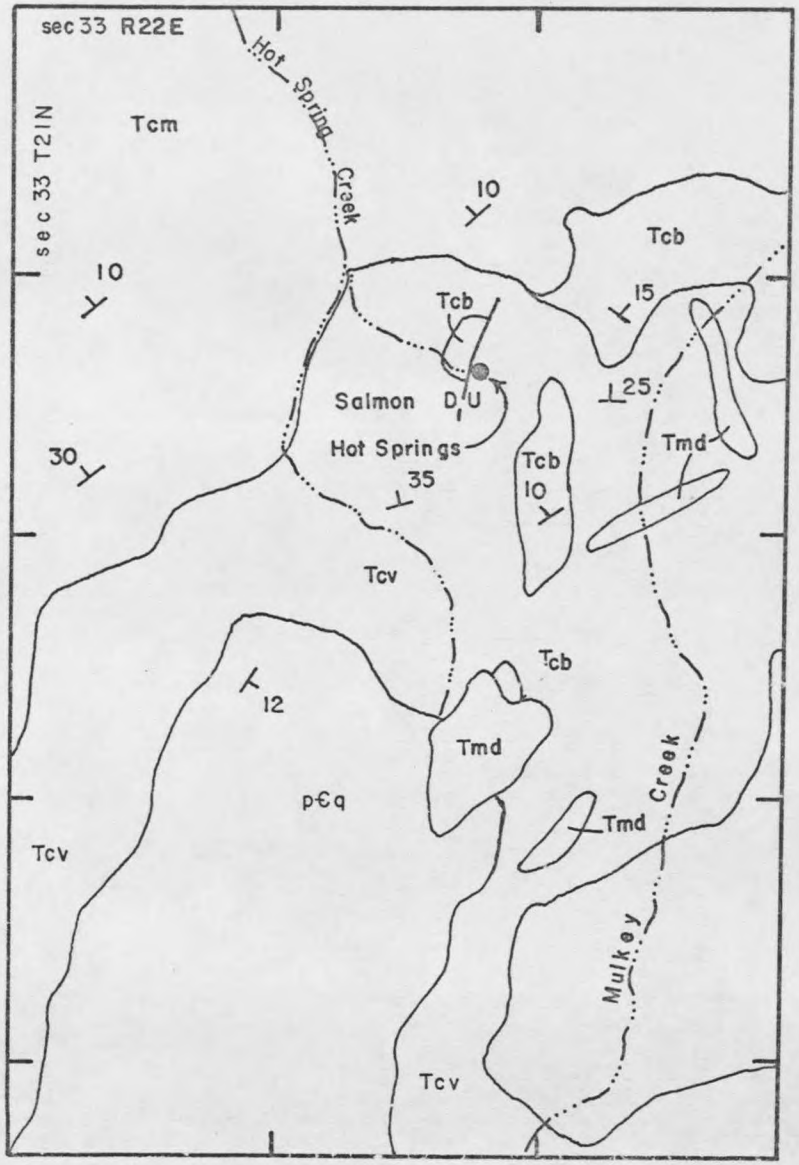
The AAPG Geothermal Gradient Map (Map no. 21, Montana, 1973) shows that the gradient in this region is about 0.85°C/100 feet which coincides well with values published by Roy, Blackwell, and Decker (1972). Assuming a mean annual temperature of 7.8°C for this area, (Robinson, 1963), ground water circulation to a depth of approximately 900 feet along the regional geothermal gradient would be required to heat ground water to 15.5°C in the Amsden aquifer. The difference between the Big Spring discharge elevation and the mean elevation of the recharge surface of the Amsden is about 900 feet. Thus, the potential exists for ground water circulation sufficiently deep in the

Amsden to heat water to 15.5°C along the 0.85°C/100 feet geothermal gradient of the region. Water does not have to circulate deeper than the discharge elevation in this system to reach the discharge temperature.

Salmon Hot Springs

Salmon Hot Springs is located in the NE¼ of section 3, T20N, R22E of the Salmon quadrangle, Idaho. The spring discharges thermal water with a discharge temperature of 44.5°C at a rate of 145 gallons per minute (Young and Mitchell, 1973) from a fault in the Oligocene Challis volcanics. The hydrothermal reservoir appears to consist of the fractured volcanic rocks in and adjacent to the fault and is probably an unconfined reservoir. Shallow ground water from precipitation and runoff circulates in joints and structural fractures in the stratified volcanics to recharge the hydrothermal system. The major source of recharge water is probably the topographically higher Challis volcanic surface to the south. Younger Miocene sediments of the Carmen Formation overlie the Challis volcanics to the north but have poor aquifer characteristics and are well drained by the major valleys of the area and probably contribute little water to the hydrothermal system.

The Salmon Hot Springs fault brings a basalt into contact with older rhyolitic(?) volcanics. Both rock units are members of the Challis volcanics. The rhyolitic(?) volcanics appear to comprise the wall rocks of the hydrothermal system. The base of the basalt is exposed slightly below the discharge elevation of the hot springs. This indicates that the basalt unit is located largely above the hydrothermal system and does not react appreciably with the thermal waters.



Geology of the Salmon Hot Springs Area

Geology from Alfered Anderson (1956)

Explanation

- Tcm — Miocene Carmen Fm. (shales, sandstones, bentonite)
- Tmd — Miocene intrusive quartz latite porphyry
- Tcb — Oligocene Challis Volcanics basaltic member
- Tcv — Oligocene Challis Volcanics rhyolitic member
- p€q — Precambrian quartzite
- Geologic Contact
- Strike and dip
- U/D — Fault

0 1/2 1 Mile

FIGURE 13

HYDROGEOCHEMICAL INTERPRETATIONS

Dilution Effects

Estimation of subsurface reservoir temperatures from thermal water chemistry at the hot spring discharge is based on the tacit assumption that the thermal discharge waters have not been diluted by cold surface and shallow ground water. It is necessary to establish the validity of this assumption for any hydrothermal system before evaluating hydrogeochemical data from its discharge water. An evaluation of the hydrologic aspects of the structure and lithology of the hydrothermal reservoir and discharge system will provide critical but not conclusive information regarding potential cold water dilution. A hydrogeologic evaluation of potential cold water dilution of a hydrothermal system can be conclusive, or at least much more useful, when combined with specific hydrogeochemical data for both the thermal water and the cold ground water.

The single most useful criterion for detecting cold water dilution of thermal water is Mg concentration. Thermal waters generally contain Mg concentrations of less than several parts per million whereas cold ground waters typically contain at least two to three times more (see section on Soluble Mineral Equilibria). Thus, in a qualitative sense, low Mg or low Mg/Ca ratios represent thermal water. Arnorsson (1970) provides data that indicates this relation extends down to temperatures of 100°C and possibly lower. Data from Montana hot springs suggests this relation extends down to a temperature of at least 60°C.

The most useful application of Mg and Mg/Ca ratios in detecting cold water dilution is where the average Mg

and Ca concentrations of the local cold ground waters are known. When such data is unavailable, evaluation of possible dilution based on order of magnitude values of Mg and Ca concentrations typical of cold ground water may be satisfactory. An exception to the application of this general method is thermal brines in which the concentrations of all dissolved constituents reach high absolute proportions. Cold water dilution of thermal brines might be detected by use of Mg/Ca ratios if the dilution is significant. Some thermal waters contain low Ca concentration due to lack of dissolved CO_2 and have relatively high Mg/Ca ratios. Absolute Mg concentration is more useful in detecting cold water dilution of this type of thermal water. The concentration of Mg is used in conjunction with hydrogeologic evaluation as an indicator of possible cold ground water dilution of the thermal water for each of the 7 hot spring areas discussed in this paper. Two assumptions are made. Low Mg content (less than 5 ppm) is assumed to indicate undiluted thermal waters. High Mg concentration (greater than 5 ppm) is assumed to indicate either thermal water diluted with cold surface water or water that is not much hotter at depth than at the surface.

Other criteria for detecting cold water dilution of thermal waters include differences in the surface temperature and cation concentrations in several adjacent hot springs. Such variations can result from factors other than cold water dilution, even between springs in near proximity. These criteria are only useful to supplement conclusions drawn from Mg and dissolved silica data. High

volume discharge hot springs are often regarded as discharging undiluted thermal water. The erroneous rationale of this assumption is that the head in a high volume spring exceeds the head of cold ground waters with the potential to mix with the thermal water. This may be true in some cases, however, the head in a high volume hot spring may also be due to the head in a cold water aquifer which is contributing significant amounts of water to the hydrothermal system. Thus, the volume of water discharged by a thermal spring does not indicate the extent of cold water dilution.

Cation concentrations and other pertinent data for thermal waters sampled in this study are shown in Table III. Evaluation of the geohydrologic conditions at Alhambra and Boulder Hot Springs indicates little potential for cold ground water dilution, and the low Mg contents of less than 1.0 ppm and 0.73 ppm, respectively support this conclusion. Samples 1, 2, and Tunnel from Boulder Hot Springs have been concentrated by evaporation (Table III).

The potential for dilution of the thermal discharge water by cold ground water in the Quaternary alluvium exists at Helena Hot Springs. However, the Quaternary alluvial sediments contain significant amounts of fine material and do not appear to be water bearing near the hot spring. Ground water is not seeping into the hot spring casement. The low Mg content (0.73 ppm) in the thermal water discharge supports the conclusion that ground water is not causing dilution.

Pullers Hot Spring discharges through an unknown thickness of Quaternary alluvial gravels at the level of

the Ruby River. At the time the spring waters were sampled, irrigation of hay meadows near the spring had raised the local ground water table in the alluvium to near ground surface. The potential for cold ground water dilution of the thermal waters is high at Pullers Hot Springs, and the relatively high Mg content (18.7 ppm) indicates that significant mixing of shallow ground water and thermal water is occuring in the hot spring discharge system.

Near surface dilution of the thermal water discharges at Hunters Hot Springs does not appear likely. The low Mg content of the thermal water discharge (3.6 ppm Ca plus Mg) indicates that the discharge waters are dominantly thermal in nature. This conclusion is supported by the high dissolved silica content relative to the surface discharge temperature. Several potential aquifers of significant yield capacity are present under the Hunters area, and water from one or more of them could dilute the hot ascending thermal water with lower temperature thermal water of comparable low Mg content.

The potential for shallow ground water dilution of Big Spring thermal waters is low due to lack of any source of recharge water for the thin colluvial deposit at the spring and the small storage capacity of the colluvium. The high Mg content (20.9 ppm) indicates that the warm waters discharging at the spring never attain temperatures much over the surface discharge water temperature. This interpretation is supported by a low dissolved silica content in the spring discharge water approximately in equilibrium with quartz at the discharge temperature and by the low chloride content in the discharge water as well as

by the hydrogeologic interpretation of the hydrothermal system (Figure 12).

Examination of the surface geology and hydrology does not reveal a source of significant shallow ground water dilution of the thermal waters at Salmon Hot Springs. However, the relatively high Mg content (11.0 ppm) in the thermal water implies cold water dilution. The relatively limited areal extent of the Salmon hydrothermal system suggests that marginal mixing of cold recharge water and ascending thermal water extends to the central core of the system or at least to the part of the hydrothermal system feeding the hot spring discharge.

Dissolved Silica Interpretation

Estimated reservoir temperatures based on dissolved silica content in the discharge waters of the springs discussed in this report are determined from the curve for conductive cooling of thermal waters (curve B, Figure 4). The curves for dissolved silica content in discharge water versus reservoir temperatures (curves A and B, Figure 4) are the same for reservoir temperatures below 100°C regardless of whether cooling of the ascending discharge water is due to steam loss or to conductive cooling. The congruity of these curves below 100°C is due to the fact that water does not boil below 100°C (at sea level). No steam can form without boiling. Thus, cooling of thermal water ascending from a reservoir with a base temperature of 100°C or less must take place by conductive transfer of heat to the wall rocks (assuming the absence of cold water mixing).

In practice, curves A and B are similar over an even

wider range of temperature. This is because hydrostatic pressure created by the weight of the water in the system causes the boiling temperature of the water to increase with depth. For example, in a hydrothermal system discharging water from a reservoir with a base temperature of 120°C through a hot spring with a surface elevation of 4000 feet above sea level, hydrostatic pressure in the hydrothermal system would prohibit boiling below a depth of approximately 60 feet below the discharge surface of the hot spring. Conductive cooling of the ascending water could cool it to a temperature below 120°C before it rises to within 60 feet of the surface, and boiling would never occur. This appears to be the cooling process in effect for the Montana thermal waters observed in this study.

The maximum reservoir temperature estimated from dissolved silica for this study is 111°C for Boulder Hot Springs. None of the hot springs sampled were observed to be boiling at the discharge elevation, and steam discharges were not present at any of the discharge areas. This implies that the thermal gradient in the hydrothermal systems sampled does not increase rapidly enough with depth to increase the water temperature to the boiling point at the hydrostatic pressure at any given depth in the system. This leads to the conclusion that cooling of thermal water ascending in the observed Montana hydrothermal systems is primarily due to transfer of heat from the thermal water to the cooler wall rocks by condution.

Implicit in the use of the dissolved silica hydrogeothermometer are the assumptions that silica is neither be-

TABLE III

Hot Spring	Surf Temp (°C)	SiO_2 Temp (°C)	NaKCa Temp (°C)	Na (ppm)	K (ppm)	Ca (ppm)	Mg (ppm)	Cl (ppm)	SiO_2 (ppm)	Cat.	Flow (gpm)	pH
Alhambra												
Main	54	103	162	268	15.0	26.0	?	20.2	53.7	4	500+	7.5
North	50	88	164	148	10.0	20.8	3.3	12.6	36.6	4	Seep	7.0
Boulder												
Main	75	111	81	102	2.5	6.0	0.7	18.1	63.8	4	1000+	8.3
#1	59	137	75	82	3.1	10.0	---	22.1	102.5	4	2	7.0
#2	64	135	74	74	3.2	10.0	---	17.3	97.0	4	5	7.0
Tunnel	42	135	76	84	3.3	10.0	---	21.7	97.0	4	2	7.0
Helena	63	108	92	148	4.7	12.0	0.7	35.0	59.5	4	30	7.0
Pullers	43	60	173	246	19.7	57.6	18.7	90.8	19.6	2	150	7.0
Hunters	60	104	41	80	0.6	3.6*	---	14.4	49.8	1	1500	7.6
Big Spring	15.5	15.5	18	14	2.0	44.0	20.9	3.8	15.9	4	29000	6.0
Salmon	45	79	204	189	25.0	23.2	11.0	50.0	30.5	4	145	7.0

*Combined Ca and Mg value based on Ca atomic weight.
?Below limit of detection (1.0ppm lower limit).

Hot Spring	log K*	Na/K	$Ca^{\frac{1}{2}}/Na$	log $Ca^{\frac{1}{2}}/Na$	log $Ca^{\frac{1}{2}}/K$
Alhambra	1.60	30.37	2.19	0.339	1.822
Boulder	2.43	69.36	2.76	0.440	2.281
Helena	2.30	53.53	2.69	0.429	2.158
Pullers	1.51	21.26	3.54	0.548	1.876
Hunters	2.97	245.73	2.74	0.438	2.828
Big Spring	3.39	11.90	54.43	1.735	2.811
Salmon	1.26	12.85	2.93	0.466	1.575

ing precipitated nor dissolved in the hydrothermal discharge system and that dissolved silica is in equilibrium with quartz rather than amorphous silica.

The absence of silica mineral deposits in even the low volume discharges of the Montana hot springs indicates that silica is not being precipitated in the discharge systems. The water depositing silica on the walls of the tunnel at Boulder Hot Springs is seeping down a wall in a thin sheet where silica precipitation is due to evaporation of the water. No silica crusts are evident below the level of standing water on the tunnel wall. The high discharge rates of the hot springs studied discourages silica precipitation. Rapid movement of water from the reservoir to the surface tends to discharge water from the system before significant silica precipitation can occur, even under highly supersaturated conditions (Mahon, 1966). Furthermore, White, Muffler, and Truesdell (1971) state that silica precipitation is not probable from thermal waters originating in reservoirs with base temperatures of 150°C or less.

Reservoir temperatures based on dissolved silica concentration in the discharges of Alhambra, Boulder, and Helena Hot Springs are probably representative of actual reservoir temperatures at depth. Dilution of thermal water dissolved silica content by low silica content cold ground water is not a possible source of error for these three not springs. The discharge waters of Alhambra, Boulder, and Helena Hot Springs are undersaturated with respect to amorphous silica (Table III and Figure 4) and could theoretically be dissolving additional silica

from opal deposits in the discharge system. This probably is not the case. The solubility of amorphous silica in water is such that the present discharge waters of these three hot springs are greatly undersaturated with respect to amorphous silica both at estimated reservoir temperatures and at surface discharge temperatures. This undersaturation would result in rapid dissolving of any amorphous silica minerals present in the hydrothermal system. Furthermore, glass and opal convert to crystalline phases fairly rapidly at higher temperatures (Fournier and Rowe, 1966). Thus, the control of dissolved silica in the thermal water by amorphous silica minerals is not likely in these three hot springs.

The reservoir temperature of 60°C based on dissolved silica concentration for Pullers Hot Spring is probably due to mixing of cold water with the thermal water. Cold water mixing indicated by the high Mg content suggests this. The magnitude of the dilution effects on calculated reservoir temperature is not known but can be estimated if the Mg and dissolved silica concentrations of the local ground water are known.

The limited availability of amorphous silica in the alluvial sediments carrying the ground water at Pullers Hot Springs suggests that the equilibrium of dissolved silica in the local ground water is primarily with respect to quartz. Assuming a mean annual temperature of 8°C for this area, dissolved silica concentration in the local ground water should be less than 5 ppm. Therefore, mixing of cold ground water and thermal water will result in lower dissolved silica content in the hot spring discharge.

Reservoir temperatures estimated from this dissolved silica content will be too low.

If the local ground water at Pullers Hot Springs is assumed to have a Mg concentration of 35 ppm due to its association with basaltic volcanic debris and with Ca and Mg saturated clays of the Passamari Formation, then the concentration of 18.7 ppm Mg in the thermal water discharge may represent approximately 1:1 mixing of cold water and thermal water. Assuming this ratio, then the dissolved silica content of the undiluted thermal water would be approximately 35 ppm (20 ppm diluted) and the approximate calculated reservoir temperature would be 84°C.

The preceding is only an example and is not intended to represent actual conditions at Pullers Hot Springs where a suitable sample of the local ground water was not obtained for Mg and dissolved silica analysis. However, this example does describe one way in which a correction for dilution might be made in order to derive fairly accurate calculated reservoir temperatures. An accurate correction requires a knowledge of both the dissolved silica concentration and the Mg concentration in the local ground water.

Actually a Mg concentration of 35 ppm is probably too high for ground water in alluvium similar to the Ruby River alluvium. If a lower figure is used, more dilution of the thermal water is required to increase its Mg content to the measured value of 18.7 ppm. Greater dilution results in an increase in the values for undiluted dissolved silica content. Thus, as lower Mg concentrations

are found in the local ground water, higher corrected dissolved silica contents will be calculated for the undiluted thermal water and higher calculated reservoir temperatures will result.

The basic assumptions made in application of the silica hydrogeothermometer appear to be valid at Hunters Hot Springs. The calculated reservoir temperature of 104°C is probably a minimum. This is because of the high potential for dilution of the higher temperature water by lower temperature thermal waters discharging from shallower aquifers.

The low dissolved silica content in the discharge water at Big Spring is approximately in equilibrium with respect to quartz at the discharge temperature. The hydrogeologic aspects of this spring suggest it is discharging at the lowest point of elevation in the circulation system contained in the low-temperature aquifer. The estimated reservoir temperature is in good agreement with this concept and the other dissolved solids concentrations, including Cl, are typical of normal low-temperature ground water in this area.

Microscopic examination of the hydrothermally altered volcanic rocks at Salmon Hot Springs reveals no volcanic glass remaining in an amorphous state. The lack of amorphous silica minerals in the volcanic rocks and the fact that the thermal discharge waters of the spring are highly undersaturated in dissolved silica with respect to amorphous silica indicates that the amorphous silica minerals have been totally dissolved by hydrothermal alteration or have altered to crystalline phases. Thus, the dissolved

silica concentration in the thermal discharge waters is in equilibrium with respect to quartz.

The dissolved silica concentration in the discharge water at Salmon Hot Springs is probably diluted by low-silica content recharge waters as implied by Mg concentrations in the discharge water. If the dissolved silica and Mg concentrations of the cold recharge water were known, a dilution correction for the estimated reservoir temperature could be calculated using the method described for Pullers Hot Springs.

Na-K-Ca Temperature Interpretation

The accuracy of the Na-K-Ca hydrogeothermometer would best be determined by comparing Na-K-Ca calculated reservoir temperatures with measured reservoir temperatures. Reservoir temperatures in Montana hydrothermal systems have not been measured; however, the dissolved silica calculated reservoir temperatures provide a reliable means of comparison. The dissolved silica calculated reservoir temperatures for Pullers and Salmon Hot Springs are probably low due to cold water dilution but are still useful for comparison.

Comparison of the Na-K-Ca and dissolved silica temperatures shown on Table III indicates that only two pairs of calculated reservoir temperatures agree within the $\pm$ 20 percent accuracy limits. These are the temperatures at Helena Hot Springs and Big Spring. The Na-K-Ca calculated reservoir temperatures for other hot springs are significantly higher or lower than corresponding dissolved silica calculated temperatures, even after correction for dilution effects present at Pullers and Salmon Hot Springs.

The Na-K-Ca calculated temperatures of 162 and 204°C at Alhambra and Salmon Hot Springs are theoretically compatible with unconfined hydrothermal systems. Water at 162 and 204°C would boil at approximately 220 and 650 feet below the surface, respectively, for unconfined hydrothermal systems at the elevations of Alhambra and Salmon Hot Springs. Conductive cooling of rising hot water with an initial reservoir temperature of 200°C could lower water temperatures below the boiling point throughout the system. Thus, either the dissolved silica or Na-K-Ca calculated reservoir temperatures are theoretically reliable for Montana hydrothermal systems. The 41°C Na-K-Ca calculated reservoir temperature for Hunters Hot Springs is 19°C less than the maximum measured discharge temperature and is highly improbable.

The disagreement between Na-K-Ca and dissolved silica calculated temperatures suggests significant differences between the net water-rock reactions in Montana hydrothermal systems and the net reactions which impose the limits of applicability of the representative empirical curve on Figure 5. If K concentration is decreased relative to fixed Na and Ca concentrations, lower Na-K-Ca calculated temperatures result. If K concentration is increased relative to fixed Na and Ca concentration, higher Na-K-Ca calculated temperatures result. Extensive kaolinitic alteration present in the wall rocks at Alhambra Hot Springs suggests that K concentrations in the discharge waters may be unusually high relative to corresponding Na and Ca concentrations at the same temperature. Kaolinization contributes K to hydrothermal waters. Similarly, extensive

sericitic (K-mica) alteration present in the wall rocks at Boulder Hot Springs suggests that fixing of K in K-mica may be causing unusually low K concentration relative to Na and Ca concentrations at the some temperature. As shown in the following section on Water-Rock Reactions, significant anomalies in the relative K concentrations are in fact controlling Na-K-Ca calculated temperatures for these hot springs. This association appears to apply to other Montana hydrothermal systems and indicates that the net reactions in the systems are significantly different than those represented by the empirical curve on Figure 5.

The Na-K-Ca calculated reservoir temperature of 162°C at Alhambra Hot Springs is much higher than the dissolved silica calculated temperature of 103°C due to the relatively high K concentration in the thermal water. The relatively high K concentration is the result of kaolinization of K-feldspars in the wall rocks. The Na-K-Ca calculated temperature is probably substantially higher than actual reservoir temperatures for reasons that will be discussed further.

Dissolved solids concentrations in samples 1, 2, and the tunnel sample at Boulder Hot Springs have been increased by evaporation. The calculated reservoir temperatures are based on the sample collected at the main spring. The Na-K-Ca calculated reservoir temperature at Boulder Hot Springs is substantially lower than the dissolved silica calculated temperature. This is the result of a low concentration of K in the thermal water caused by fixation of K in secondary K-mica. This Na-K-Ca temperature is probably somewhat lower than the actual reser-

voir temperature.

The Na-K-Ca calculated reservoir temperature of 92°C at Helena Hot Springs agrees with the dissolved silica calculated temperature within the limits of error of the empirical curve and is probably a slightly low representation of actual reservoir temperatures. The K concentration in the thermal water discharge is within the range of K concentration normally anticipated in cold ground water in granitic rocks similar to the Helena Hot Springs pluton. Thin section examination of the quartz monzonite wall rocks near the hot spring shows slight sericitic (K-mica) alteration of a degree typical in normal surface weathering. Wall rock samples were not obtained from the actual hydrothermal system. The slightly low Na-K-Ca calculated temperature indicates that mild K-mica alteration of the feldspars in the wall rocks is occurring in this system.

The relatively high Na-K-Ca calculated reservoir temperature of 173°C for Pullers Hot Spring is probably caused by kaolinitic alteration of granitic metamorphic wall rock in the hydrothermal reservoir. This is implied by the relatively high K concentration in the thermal water. Dilution of the Ca concentration in the thermal waters by cold ground waters might also be a factor, however, the Ca concentration of the local ground water must be measured in order to make this determination. Continued reaction of the thermal waters with the montmorillonite clays of the confining Passamari Formation probably does not affect the Na-K-Ca ratios of the discharge waters. If cation exchange with the montmorillonite were occurring, K would

selectively replace Na and Ca in the exchange sites. This would result in relatively low K concentrations and high Na and Ca concentrations in the thermal water while cation exchange was taking place. The present high K content of the thermal waters indicates that any cation exchange sites available for reaction in the rather impermeable shales in the discharge system are saturated with K and significant cation exchange is no longer taking place.

The extremely low Na-K-Ca calculated reservoir temperature of 41°C for Hunters Hot Springs is probably due to continued reaction of the ascending thermal water with the wall rocks. Two types of water-rock reactions might cause error in the calculation. The Ca concentration of the hot spring discharge water is very low. Assimilation of Ca by extremely low Ca content ascending thermal water would cause calculated reservoir temperatures to be low. This effect is not significant at Hunters Hot Springs because of the low absolute concentration of Ca relative the absolute concentration of Na in the discharge waters. Continued reaction of the thermal waters rising through the thick andesitic sandstones of the Livingston Formation probably is the cause of the extremely low K concentration in the thermal waters. Alteration of NaCa-feldspars to K-mica in the clastic volcanic grains contained in the approximately 4000 foot thick Livingston section could fix appreciable K from the thermal water. This would cause extremely high Na/K ratios and low calculated temperatures.

The low chloride, Na, and K concentrations and the relatively high Ca concentration in the discharge water of Big Spring are characteristic of cold ground waters in

limestone aquifers in temperate climates. Although the waters have been heated slightly above the mean annual temperature for the area by deep circulation, they are essentially cold ground waters chemically. The empirical curve of Fournier and Truesdell (1973) is compiled in part from cold ground waters. Thus, agreement of the low Na-K-Ca calculated reservoir temperature for Big Spring with the dissolved silica calculated temperature is not by chance and is an accurate approximation of the true reservoir temperature.

The relatively high Na-K-Ca calculated reservoir temperature of 204°C for Salmon Hot Springs is apparently the result of high K concentrations caused by release of K to the thermal water during kaolinization of rhyolitic wall rocks in the system. This temperature is probably nearly twice as hot as the actual reservoir temperature. Possible effects from ground water dilution of the thermal water Ca concentration are probably obscured by the greater effects of K concentration.

Water-Rock Reactions

The nature of the correlation of Na-K-Ca calculated reservoir temperatures with K concentrations is explained in the following discussion. Evidence indicating control of K concentration in the thermal waters by sericitic and kaolinitic alteration reactions is presented. The net reactions are discussed in relation to the empirical Na-K-Ca temperature.

Reservoir temperatures calculated from Na-K-Ca ratios can be related directly to K concentrations in the thermal waters. Davis and DeWiest (1970) state that the average

K concentration in cold ground water ranges from 1.0 to 5.0 ppm. Feth, Roberson, and Polzer (1964) show an average K concentration of 1.1 ppm for cold ground water in granitic rocks. It is readily apparent that Montana hydrothermal systems in which the Na-K-Ca calculated reservoir temperature is high relative to the dissolved silica calculated reservoir temperature contain K concentrations two to three times higher than the upper value of 5.0 ppm assumed for the recharge waters. Similarly, Montana hydrothermal systems in which the Na-K-Ca calculated reservoir temperatures are relatively low contain K concentrations of one-half or less of the maximum value of 5.0 ppm K assumed for the recharge waters. Thus, the Na-K-Ca calculated reservoir temperatures appear to be directly related to K concentration in the thermal water.

Individual hydrothermal systems with similar temperatures do not have similar Ca concentrations. The Ca concentration in water is controlled by calcite solubility. Calcite solubility in water may increase or decrease as the partial pressure of CO_2 is increased. Below a certain CO_2 concentration, pH is controlled or buffered by silicate hydrolysis reactions. In such a system, an increase in CO_2 concentration increases the rate of hydrolysis. This causes Ca concentration to decrease due to competitive silicate reactions, and calcite solubility decreases accordingly. When CO_2 partial pressure increases to a certain level, silicate reactions are no longer sufficiently rapid to buffer the pH. The solubility of calcite begins to increase in response to increases in CO_2 partial pressure and Ca concentration increases

accordingly. Thus, Ca concentration is affected by temperature, the partial pressure of CO_2, pH, and salinity of the solution. All of these factors may vary widely from one hydrothermal system to another depending on wall rock composition and flow conditions.

Calcium enters into competitive silicate reactions with Na and K. The amount of Ca in solution influences the amounts of Na and K in solution. Montana thermal waters contain much less K than Na. Thus, concentrations of K should vary more than concentrations of Na in response to changes of Ca in the thermal water. This relation is shown by Fournier and Truesdell (1973) for natural cold and thermal waters.

As shown on Figure 14, Na concentrations in Montana thermal waters are more responsive than K concentrations to changes in Ca concentration. The poor correlation of K concentration with Ca concentration indicates that some factor other than response to changes in Ca and Na concentrations is influencing the equilibrium of K in solution in the thermal waters. Concentrations of Na and K in solution represent an aqueous mineral phase in equilibrium with a solid mineral phase in the wall rocks. This suggests that K concentrations in Montana thermal waters may be in equilibrium with a solid mineral phase which reacts only with K and not with Na or Ca. This would allow K concentration to equilibrate independently of other competitive cations.

Thin section examination of quartz monzonite wall rock currently being altered by low K concentration thermal waters at Boulder Hot Springs suggest that the mineral

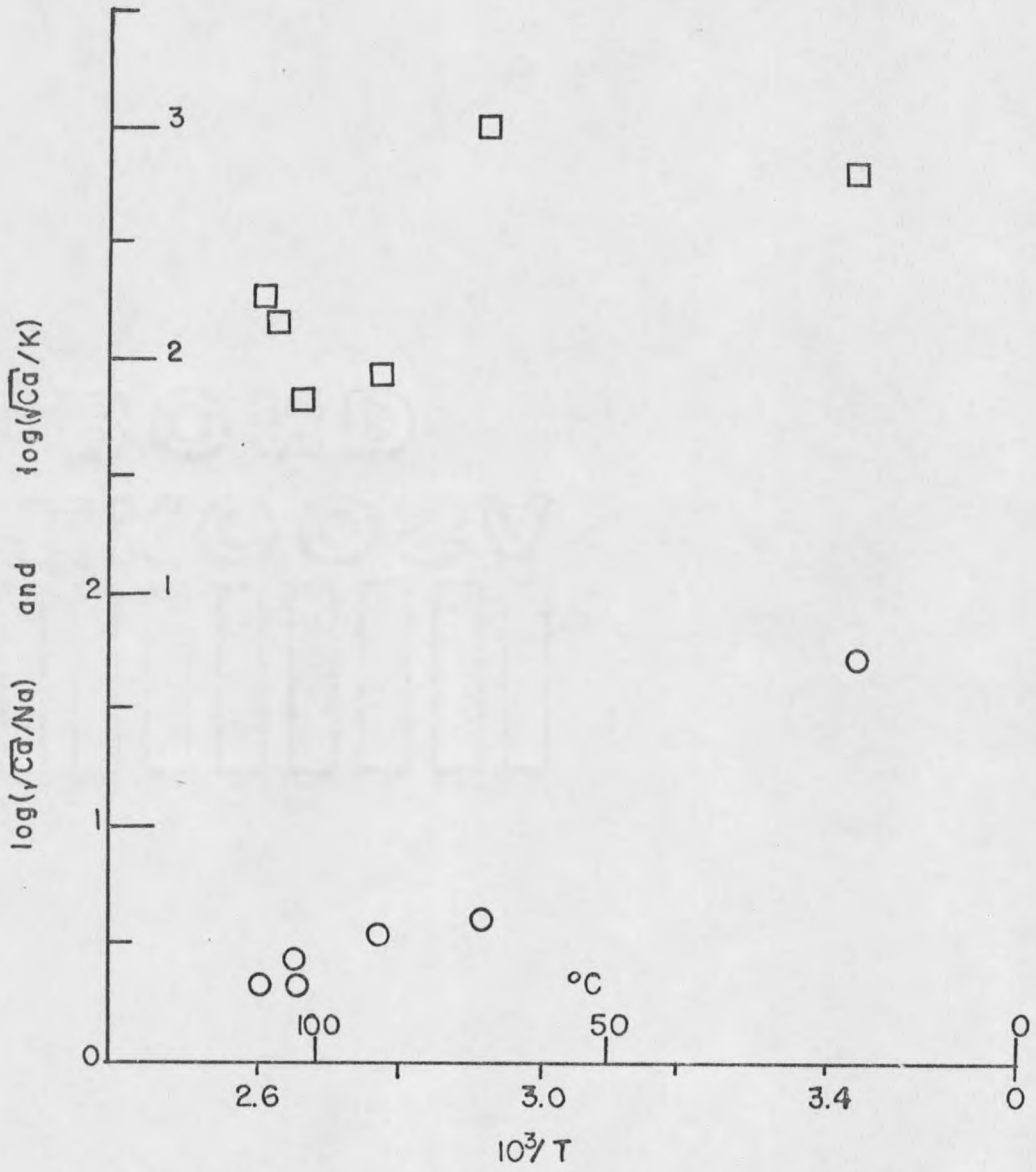


Fig. 14. Log (√Ca/ Na) and log(√Ca/K) vs Reciprical of Temperature.
○ log(√Ca/Na) vs $10^3/T$ □ log(√Ca/K) vs $10^3/T$

phase controlling low aqueous K concentrations is K-mica in the form of Muscovite (sericite in microcrystalline sizes). Thin section examination and X-ray diffraction analysis of wall rocks altered by high K concentration thermal waters at Alhambra Hot Springs suggest that the mineral phase controlling high aqueous K concentrations is kaolinite.

K-mica is present in the Boulder hydrothermal system as an alteration mineral which replaces plagioclase and K-feldspar in the wall rocks. It is noteworthy that the K-mica (sericite) is growing at the expense of the feldspars and not due to addition of material to the system. The equations below express the general reactions occurring during hydrothermal sericitization of feldspars (Feth, Roberson, and Polzer, 1964). Plagioclase feldspar is represented by albite for simplicity.

$$\underset{\text{orthoclase}}{3KAlSi_3O_8(s)} + 2H^+(aq) + 12H_2O(liq)$$

$$\rightarrow \underset{\text{K-mica}}{KAl_3Si_3O_{10}(OH)_2(s)} + 6H_4SiO_4(aq) + 2K^+(aq) \qquad (1)$$

$$\underset{\text{albite}}{6NaAlSi_3O_8(s)} + 4H^+(aq) + 2K^+(aq)$$

$$\rightarrow \underset{\text{K-mica}}{2KAl_3Si_3O_{10}(OH)_2(s)} + 12H_4SiO_4(aq) + 6Na^+(aq) \qquad (2)$$

Solid mineral phases, aqueous species, and liquids are denoted by subtended (s), (aq), and (liq) respectively. The silicic acid shown in the equations equilibrates with the solid quartz phase in the system.

Equations (1) and (2) show that sericitization of K-feldspar releases K cations into the thermal solution whereas sericitization of plagioclase fixes K cations and releases Na and Ca into the thermal solution. Thus, sericitization of wall rocks in a hydrothermal system can result in either low or high K concentrations in solution. The ratio of K-feldspar to plagioclase (feldspar ratio) in the unaltered wall rocks and the degree of alteration (sericitization) of the feldspars determines the bulk chemical reactions occurring between the thermal water and the wall rocks.

For example, Table I indicates a modal feldspar ratio for the Boulder Hot Springs wall rocks of about 1:1. Equations (1) and (2) show that sericitization of 3 moles K-feldspar will release sufficient K into the thermal solution to react with 6 moles of plagioclase. Additional K initially present in the recharge waters contributes to further sericitization of the plagioclase. Thus, contemporaneous sericitization of equal amounts of K-feldspar and plagioclase will alter all of the plagioclase when at least one-half of the K-feldspar remains unsericitized. Contemporaneous sericitization of K-feldspar and plagioclase is probably the cause of the present low K concentration in the Boulder Hot Springs discharge.

Alteration of primary feldspars to kaolinite appears to be the reaction causing high K concentrations in Montana thermal waters. Kaolinite is present as the alteration mineral in the wall rocks at Alhambra Hot Springs where it totally replaces the feldspar minerals. Kaolinization involves leaching of K, Na, and Ca from the feld-

spars as is shown by the following equations (Feth, Roberson, and Polzer, 1964).

$$2KAlSi_3O_8(s) + 2H^+(aq) + 9H_2O(liq) \rightarrow H_4Al_2Si_2O_9(s) + 4H_4SiO_4(aq) + 2K^+(aq) \quad (3)$$

orthoclase → kaolinite

$$2NaAlSi_3O_8(s) + 2H^+(aq) + 9H_2O(liq) \rightarrow H_4Al_2Si_2O_9(s) + 4H_2SiO_4(aq) + 2Na^+(aq) \quad (4)$$

albite → kaolinite

$$2KAl_3Si_3O_{10}(OH)_2(s) + 2H^+(aq) + 3H_2O(liq) \rightarrow 3H_4Al_2Si_2O_9(s) + 2K^+(aq) \quad (5)$$

K-mica → kaolinite

It is not known if reaction (5) is an intermediate step in kaolinitic alteration of the feldspars or if reactions (3) and (4) go directly to completion without formation of a K-mica phase. The presence of kaolinite suggests that it is the stable phase rather than sericite in the Alhambra hydrothermal system and that sericite should not form. The Boulder and Alhambra hydrothermal systems circulate in structures probably having ages of the same order of magnitude. The wall rock alteration should have advanced to similar degrees in both systems. This again suggests that K-mica and kaolinite are different stable mineral phases. However, the fault-related shearing and fracturing of the Alhambra wall rocks may have made them more subject to alteration. Thus, hydrothermal alteration of comparable age at Boulder and Alhambra may have advan-

ced further at Alhambra and passed through a K-mica phase to attain a stable kaolinite phase.

Other evidence suggests that K-mica and kaolinite are unique mineral phases with no mutual stability fields or transitional phases. Becraft, Pinckney, and Rosenblum (1963) describe typical alteration zoning outward from quartz and chalcedony veins in the Boulder batholith as consisting of a sericite zone adjacent the vein. Outward is an argillic zone and a chlorite zone, respectively. The sericite zone is usually absent adjacent to low-temperature chalcedony veins but is usually present adjacent to the mesothermal(?) quartz veins. Zone contacts are gradational over a distance of a fraction of an inch to several inches. Sigvaldason (1962) and White and Sigvaldason (1962) show that kaolinite and other clay minerals are limited to the upper, low-temperature zones of deep drill holes in both high temperature hydrothermal systems (250°C base temperature) and epithermal ore deposits. Thus, kaolinite appears to be a unique mineral phase. The stability fields of the two minerals both extend into the range from 150°C down to cold ground water temperatures of 6 to 8°C; however, other factors such as pH affect the mineral phase stability.

Evaluation of Net Reactions

The selective stability and formation of either K-mica or kaolinite individually has significant impact on the Na-K-Ca calculated temperatures. This is not simply because of the mathematical impact of the absolute K values on the Na/K ratios in the equation for $\log K^*$. The net reactions for formation of these minerals differ signifi-

cantly from the net reactions represented by the empirical $\log K^*$ values. Fournier and Truesdell (1973) show that reactions involving only aqueous Na, K, and Ca are limited to the following three configurations:

$$(x + 2y)K + \text{solid} = xNa + yCa + \text{solid} \quad (6)$$
$$(2y - x)K + Na + \text{solid} = yCa + \text{solid} \quad (7)$$
$$(x - 2y)K + yCa + \text{solid} = xNa + \text{solid} \quad (8)$$

Fournier and Truesdell (1973) write equations (6), (7), and (8) in terms of a single K ion participating in the net reactions so that the approximate equilibrium constant, K^*, for all possible reactions can be written in the general form,

$$\log K^* = \log \frac{Na}{K} + b \log(Ca^{\frac{1}{2}}/Na), \quad (9)$$

which is used in formulating the empirical curve on Figure 5.

The reaction controlling aqueous K concentration in the thermal water during sericitization of plagioclase is as follows:

$$\underset{\text{andesine}}{3Na_{0.66}Ca_{0.33}AlSi_3O_8(s)} + 2H^+(aq) + K^+ + 12H_2O(liq) \quad (10)$$
$$\rightarrow \underset{\text{K-mica}}{KAl_3Si_3O_{10}(OH)_2(s)} + 6H_4SiO_4(aq) + 2Na^+(aq) + Ca^+(aq)$$

Reaction (10) fits the general configuration of equation (6) for a reaction involving aqueous Na, K, and Ca. Fournier and Truesdell (1973) show that for any reaction with the configuration of equation (6), where one unit K is fixed in the solid and corresponding amounts of Na and Ca are released, the value of b in equation (9) is between 0 and 1.

The $\log K^*$ values shown on Table III indicate that in each case of relatively low K concentration, a value for b of 1.333 was used to correspond with that portion of the empirical curve (Figure 5) for temperatures below 100°C. Clearly, the empirical curve does not describe temperature-dependent Na-K-Ca equilibrium where K-mica is forming at the expense of plagioclase. A value of b between 0 and 1 is required to bring the general equation (9) into agreement with the stoichiometry of the net reaction shown by equation (10). Application of an empirical value of b = 0.8 in equation (9) results in Na-K-Ca calculated reservoir temperatures of 120°C for both Boulder and Helena Hot Springs. These values are in agreement with the dissolved silica calculated temperatures of 111 and 108°C, respectively, within the ± 20 percent accuracy limitations.

The reactions controlling aqueous K concentration in the thermal water during kaolinization of the feldspars are expressed by equations (3) and (4). If equation (4) is written for andesine instead of albite, then equations (3) and (4) have the following general configurations, respectively:

$$(x)H^+ + \text{solid} = xK + \text{solid} \qquad (11)$$

$$(x + 2y)H^+ + \text{solid} = xNa + yCa + \text{solid} \qquad (12)$$

Equations (3) and (4) essentially denote leaching of Na, K, and Ca where these elements do not equilibrate with a solid phase. As will be shown, the Ca concentration for equations (3) and (4) is in carbonate equilibrium. Thus, equations (3) and (4) denote reactions essentially involving only Na- and K-bearing minerals. Equation (9) sim-

plifies to $\log K^* = \log(Na/K)$ and the Na and K concentrations are established by the composition of the unaltered wall rocks. Use of Na and K to estimate reservoir temperatures under these conditions requires knowledge of the wall rock composition.

Mineral Stability

Thermal water discharge chemistry may be used to determine the stable mineral phase, kaolinite or K-mica, in equilibrium with K in the thermal water. Garrels and Christ (1965) have calculated stability relations for the expected compatible phases in the system K_2O-Al_2O_3-SiO_2-H_2O at 25°C and 1 atmosphere (Figure 15). The stability diagram was constructed using the equilibrium constant for each particular reaction calculated from the free energy of formation of the constituents involved in the reaction. For example, given the reaction

$$aA + bB = cC + dD$$

then $\Delta G^\circ_R = c\Delta G^\circ_{fC} + d\Delta G^\circ_{fD} - a\Delta G^\circ_{fA} - b\Delta G^\circ_{fB}$

where ΔG°_R = standard free energy of the reaction

and $\Delta G^\circ_{fA}, \Delta G^\circ_{fB}, \Delta G^\circ_{fC}, \Delta G^\circ_{fD}$ = standard free energy of formation of the reactants and products.

Also $\Delta G^\circ_R = -RT \log K_{eq}$

where R = gas constant

T = absolute temperature

K_{eq} = equilibrium constant of the reaction

and $K_{eq} = (a_C \cdot a_D)/(a_A \cdot a_B)$

where a_C, a_D, a_A, a_B = activities of products and reactents.

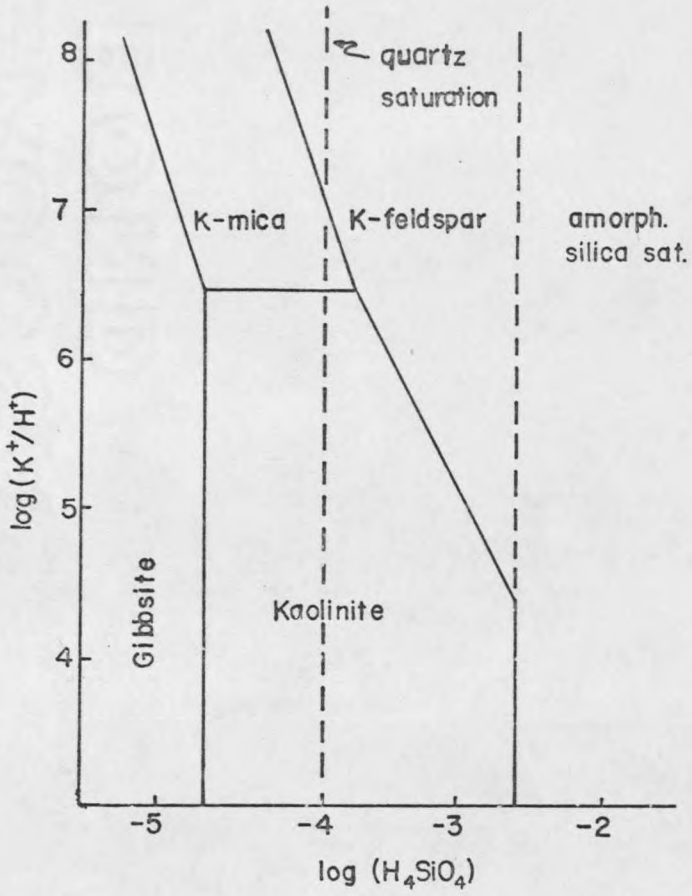


Fig. 15. Stability relations of the phases in the system $K_2O-Al_2O_3-SiO_2-H_2O$ at 25°C (298.15°K). After Garrels and Christ (1965).

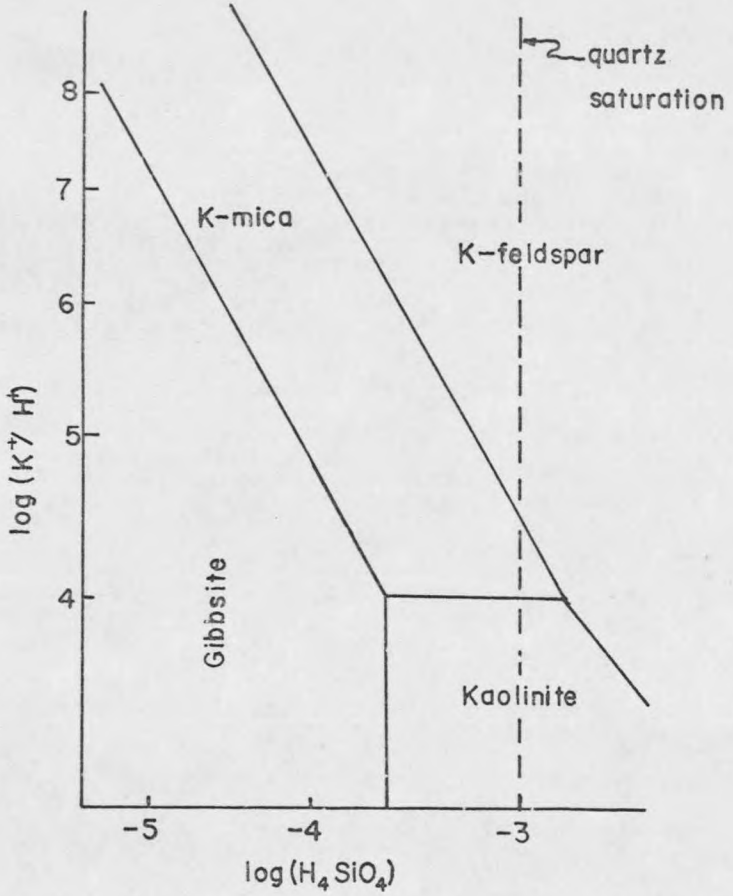


Fig. 16. Stability relations of the phases in the system $K_2O-Al_2O_3-SiO_2-H_2O$ at 127°C (400°K). Constructed from equilibria constants.

The same assumptions are made here as in deriving the general equilibrium constant of equation (9); i.e., that the activity of any solid is unity and that the molality of soluble constituents equals activity. As indicated on Figure 15, the free energies of formation used to calculate stability relations are based on a temperature of $25^{\circ}C$.

Stability relations for the above system can be calculated for temperatures above $25^{\circ}C$ when adequate thermochemical information is available to calculate standard free energies for the reactions at the elevated temperatures using the equation

$$\Delta G^{\circ}_{R} = \Delta H^{\circ}_{298.15} - T\Delta S^{\circ}$$

where $\Delta H^{\circ}_{298.15}$ = change in specific heat capacity at $298.15^{\circ}K$

ΔT = absolute temperature

and S° = change in entropy per degree.

Reactions for the various mineral compatibilities shown on Figure 15 involve only 3 variables: molal K, molal H, and molal H_4SiO_4 where molality represents activity (Garrels and Christ, 1965). Furthermore, the ratio of molal K to molal H is always unity. Thus, the mineral relations can be described using the ratio of molal K to molal H as one axis and the activity (molality) of H_4SiO_4 as the other. Appendix III provides a sample calculation for the stability relations of K-feldspar and K-mica at $400^{\circ}K$, depicting the above relations.

Figure 16 shows stability relations for the system K_2O-Al_2O_3-SiO_2-H_2O recalculated for a temperature of ap-

proximately 127°C (400°K) at 1 atmosphere based in part on thermochemical data from Robie and Walbaum (1968) and Huang and Kiang (1973). Unfortunately, complete free-energy data have not been published (to this author's knowledge) for kaolinite. Although the general geometry of Figure 16 is reliable, dictated by the equilibrium constants, the actual numbers on the axis are estimated. The most important feature of Figure 16 is the stability field boundary between K-mica and kaolinite. The increase in temperature from Figure 15 to Figure 16 has resulted in the K-mica phase extending into an area with lower $\log(K^+/H^+)$ ratios, indicating that K-mica is stable at higher pH for higher temperatures. As temperature increases, kaolinite will cease to be a stable phase in the system at some temperature level. Thus, in hotter hydrothermal systems (hotter than 150 or 175°C) kaolinite may be confined to the discharge system.

The vertical axis of Figure 16, labeled log (K/H) where K and H are molal values, could be written as logK - logH. Since -logH = pH, the axis can be defined as logK + pH where K concentration and pH are measured in the discharge water. The other axis of Figure 16, $\log H_4SiO_4$, is simply the logarithm of the molal dissolved silica content written as silicic acid. Dissolved silica is measured in the discharge water.

Points plotted on Figure 16 from measured pH values, K concentrations, and dissolved silica concentrations should fall into the stability field of the mineral phase controlling K concentration in the thermal waters (assuming accurate free-energy data for kaolinite is used).

However, a plot of values from Alhambra and Boulder Hot Springs on Figure 16 demonstrates that as the absolute concentration of K increases, the plotted stability point moves from the kaolinite stability field into the K-mica stability field. This is just the opposite relation as that indicated by field observations and by the net reactions. Increasingly higher K concentrations should plot further into the kaolinite stability field, not into the K-mica stability field when plotted as log(K/H) vs log(H_4SiO_4).

This example demonstrates the significance and magnitude of the changes in pH occurring between the hydrothermal reservoir and the discharge hot spring. Data from high K concentration discharge waters, such as Alhambra, plot well within the kaolinite stability field on Figure 16 if low pH values are assumed for the reservoir. Data from low K concentration discharge waters, such as Boulder, plot within the K-mica stability field at higher assumed pH values and at neutral to alkaline pH values as measured in the surface discharge. This is consistant with various investigators' observations that kaolinite tends to form as an alteration product in gassy, acidic springs (Ellis, 1970). Kaolinite is a common alteration product of vapor-dominated systems which produce acid-sulfate discharges (White, Muffler, and Truesdell, 1971).

Thermal water pH changes several orders of magnitude between the reservoir and the discharge in some hydrothermal systems as shown. This means that pH measurements of discharge waters are meaningless in terms of reservoir conditions. Thus, stable mineral phases controlling K

concentrations connot be determined reliably from surface discharge chemistry and phase stability diagrams. However, the pH dependent solubility of calcite is reflected in Ca concentrations in the thermal water and is a qualitative indicator of pH conditions in the hydrothermal reservoir using the criteria presented below.

The net reactions previously discussed and phase stability relations shown on Figure 16 demonstrate that both K-mica and kaolinite form by silicate hydrolysis reactions. In the case of kaolinite, hydrolysis is sufficiently active to prevent fixing of K in exchange for Na and Ca. That is, acid conditions are too strong to be significantly buffered by silicate hydrolysis whereas K-mica formation suggests control or strong buffering of pH by silicate hydrolysis. Thus, Ca concentrations in the kaolinite stability field should be in carbonate equilibrium and should be relatively high. The Ca concentrations in the K-mica stability field should be in equilibrium with silicates and should be relatively low.

Based on the foregoing criteria, Ca concentration can be used in conjunction with K concentration as a supplemental semiquantitative means of determining the stable mineral phase inequilibrium with or controlling K concentration in the thermal water. This method is practical because reservoir pH conditions do not have to be determined as is necessary to use stability phase diagrams. In very general terms, K concentrations of 5.0 ppm or less and Ca concentrations of 10.0 ppm or less are indicative of K-mica stability; K concentrations greater than 5.0 ppm and Ca concentrations of 15.0 to 25.0 ppm are indicative

of kaolinite stability; K concentrations of 5.0 ppm or less and Ca concentrations 10.0 to 15.0 ppm are indicative of the range of applicability of the empirical curve on Figure 5; and Ca concentrations of 30.0 ppm or greater with any of the above K concentrations is indicative of ground water dilution, low-temperature deep circulating ground water, or a carbonate reservoir rock. These relations are based on the limited data collected for this study and are quite tentitive. However, dominant feldspar alteration reactions in the temperature range of 100 to 150°C can be determined from these relations with fair success.

Conclusions

Calculated reservoir temperatures based on dissolved silica concentrations in thermal discharge waters are the most reliable estimate of reservoir temperatures. Precipitation of silica or assimilation of silica by ascending thermal waters does not appear to be occurring in the Montana hydrothermal systems studied. Equilibrium of dissolved silica with amorphous silica in the form of volcanic glass or opal in the wall rocks may prove to be a problem in some areas with extensive glassy volcanic rock strata such as stratified volcanics containig welded tuff or obsidian.

Cold water dilution of thermal water is the major source of error in applying the dissolved silica hydrogeothermometer. The Cl concentration may help indicate the presence of cold water dilution, however, Mg concentration above 5.0 ppm is usually diagnostic of cold water dilution. Comparison of thermal water and cold ground water

Mg content may provide a means of estimating the approximate volume of cold water dilution.

The Na-K-Ca hydrogeothermometer is less reliable than the dissolved silica hydrogeothermometer in the temperature range below 150°C. However, the Na-K-Ca method may have important uses in areas where the dissolved silica method fails due to assimilation of amorphous silica by the discharge waters. The absolute K and Ca concentrations in the discharge waters can be used to determine which mineral phase is stable in the hydrothermal system. If K-mica is stable, the empirical curve of Fournier and Truesdell (1973) can be used to estimate reservoir temperature if an empirical value of b between 0 and 1 is established for the equation for $\log K^*$. If kaolinite is the stable mineral phase, the Na-K-Ca method cannot be used to estimate reservoir temperature due to the present lack of knowledge about low-temperature (less than 200°C) mineral stability and water-rock reaction equilibrium.

Further research should include a literature review and written communication with appropriate researchers to obtain sufficient thermochemical data to calculate theoretical stability relations for kaolinite in the temperature range of 100 to 200°C. The information currently required is the change in specific heat capacity (ΔH°_T) with temperature and the change in entropy (ΔS°) for kaolinite. Calculation of the stability field of kaolinite at various temperatures would be useful in evaluating future hydrogeothermometry data.

Additional research should include compilation of all discharge chemistry data that satisfy the requirements for

K-mica stability in the reservoir for temperatures below 200°C as indicated by undiluted dissolved silica concentrations. These data should be used to construct a new empirical curve similar to that of Fournier and Truesdell (1973) in order to establish a constant (b), between 0 and 1, that best represents the stoichiometry of the K-mica reactions. Accurate Na-K-Ca calculated reservoir temperatures for low-temperature reservoirs where K is in equilibrium with K-mica cannot be derived without such a curve.

BASE TEMPERATURES

Range

Base temperatures (calculated reservoir temperatures) indicated by dissolved silica geothermometry for Montana hydrothermal systems cluster into two categories. The lower temperature category includes base temperatures only 8 to 10°C hotter than the local mean annual temperature. Base temperatures in the second category range between near 100°C to as high as 120°C. Few calculated base temperatures lie between these distinct categories. Base temperatures of 60 and 79°C indicated for Pullers and Salmon Hot Springs are derived from diluted dissolved silica concentrations and probably represent base temperatures closer to 100°C before cold water dilution.

Typically, hydrothermal systems with base temperatures in the 15 to 20°C range (relatively low-temperature category) discharge water with low Cl content and high Mg content characteristic of normal cold ground waters. Big Spring typifies the geohydrology of this type of system. Water circulates through a relatively shallow confined aquifer on an anticlinal flank, a faulted zone, or across a synclinal structure. Differential head is imposed by an elevation difference between the recharge and discharge areas in the structure.

The single most striking feature of the relatively high-temperature category of base temperatures is their tendency to group in a narrow temperature range between 100 and 120°C. Hydrothermal systems with base temperatures in the 100 to 120°C range typically circulate in fault zones or fracture zones in brittle, competent rocks.

Alhambra and Boulder Hot Springs typify such systems. Water from a few higher-temperature category systems circulates in deep confined aquifers along major regional structures. These systems are hydrologically similar to the low-temperature group but water circulates to greater depths. Hunters Hot Springs is an example.

Control

McNitt (1965) and many others note the fact that all geothermal areas of current economic importance throughout the world are located in regions of Cenozoic volcanism. This relation suggests that the source of heat for these areas is related to the processes of volcanism and magmatic intrusion. Various investigators working in Montana and other areas have extended this association to imply that heat is still dissipating from cooling igneous bodies of Cretaceous and Early to Middle Tertiary age, and that this heat is still effective in modern hydrothermal systems.

Balster and Groff (1972), referring to the thermal springs of the Upper Yellowstone Valley, state that, "Late Tertiary intrusive bodies in the Beartooth Mountains area are the probable source of thermal energy, but Tertiary volcanic activity in the Crazy Mountains basin may also be a source." These authors further propose several other intrusions of Tertiary age as heat sources for various thermal springs and in reference to the thermal springs of the Idaho batholith of Cretaceous age they state, "Heat is still emanating from the cooling rocks." The writer believes this interpretation is unwarranted.

Blackwell (oral communication, 1973), in reference to

the Cretaceous Boulder batholith and its smaller satellite plutons, believes that relict heat flow from these plutons has long since dissipated. Heat flow measurements confirm this conclusion. Regarding the Eocene Lowland Creek volcanics, Blackwell and Robertson (1973) state, "The thermal consequences of these earlier igneous events have long since been dissipated, however, and make no contribution to the present heat flow."

Blackwell and Baag (1973) published heat flow values of 19.5 HFU (microcalories/cm^2sec) for a blind thermal anomaly at Marysville, Montana. This heat flow is more than sufficient to supply a high-temperature hydrothermal system; however, the thermal anomaly appears to be dry. Several models are discussed for the thermal anomaly. The model resulting in the oldest estimated age for the anomaly is an assumed spherical magma chamber model which is 4 km in radius and buried 1.5 km deep. Using equations derived by Rikitake (1959), Blackwell and Baag (1973) estimate the maximum age of the model at 60,000 years and estimate a range of ages for various magma chamber models between 10,000 to 60,000 years. Although these models are based on a number of assumptions, they do provide an estimate within an order of magnitude of the possible age of igneous heat sources.

The close relation of hydrothermal systems to areas of Cenozoic volcanism and intrusion is not fortuitous, although Tertiary igneous bodies are probably no longer contributing heat to hydrothermal systems in Montana and other parts of the world. Cenozoic igneous rocks are commonly emplaced along major structural features, particu-

larly fault zones. The same fault zones exploited by Cenozoic magmas provide permeable avenues for circulation of modern hydrothermal systems. Microseismic activity in the vicinity of modern hydrothermal systems suggests that faulting may be active or recurring in order to maintain permeability required for circulation. Areas of previous Tertiary volcanic and intrusive activity are the logical places in which to expect Quaternary intrusive activity, since the zones of weakness historically exploited by intrusive activity still exist. This is consistent with the association of current high-temperature geothermal areas with regions of Cenozoic igneous activity.

No surface manifestations of high-temperature geothermal activity exist in Montana outside of Yellowstone Park. Only a few outcrops of Pliocene or Pleistocene volcanics are known to exist in Montana. If individual bodies of cooling intrusive rocks are providing heat to modern Montana hot springs, the similarity of reservoir base temperatures throughout the state seems to be an unlikely coincidence. Hydrothermal systems deriving heat from various unrelated intrusive rock bodies would probably have significantly different base temperatures. This would result from differences in the size and depth of emplacement (and possibly age) of the different intrusive bodies. An alternate source of heat for Montana hydrothermal systems is the regional heat flow.

Geothermal Gradient

The heat flow values for the western United States shown on Figure 17, taken from Roy, Blackwell, and Decker (1972), are the sum of heat flow from the mantle and from decay of radioactive elements in the crust. Roy, Black-

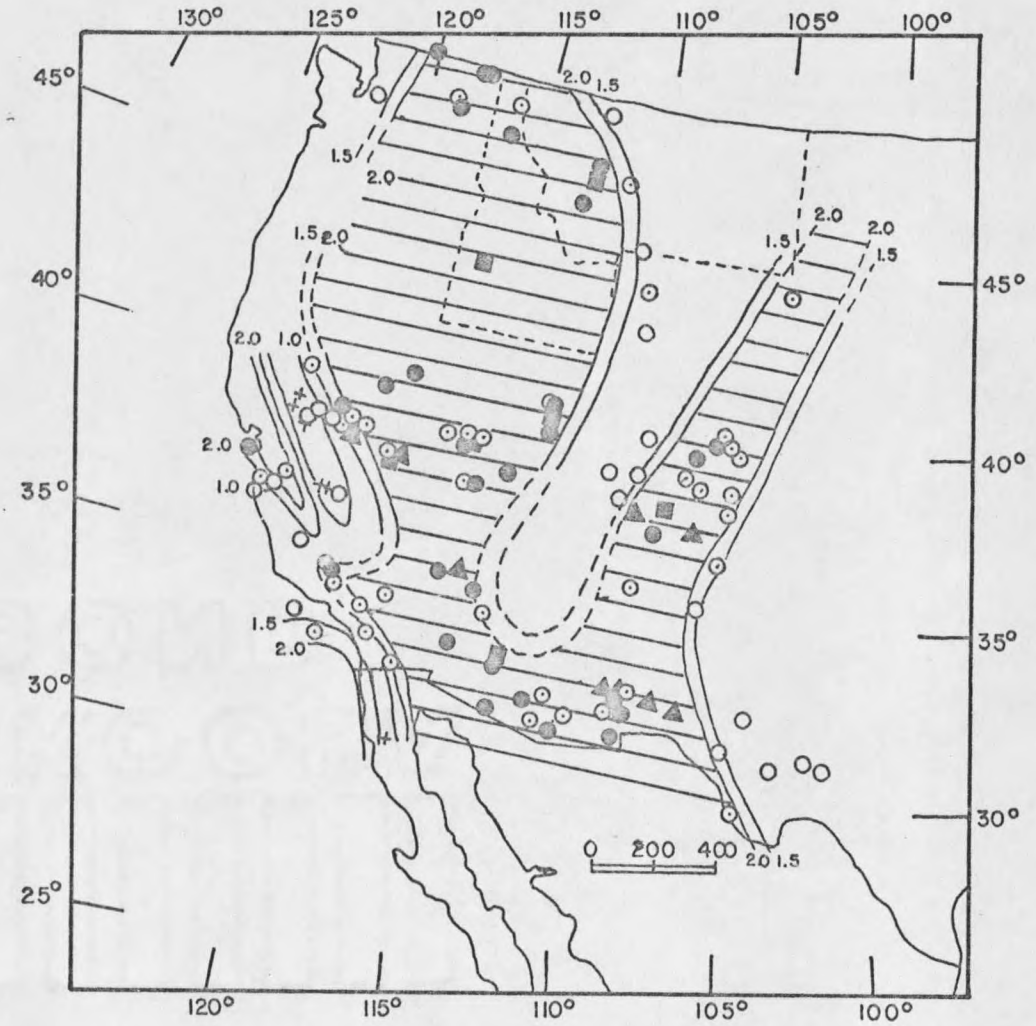


Fig. 17. Heat flow in the western United States, after Roy, Blackwell, and Decker (1972).

+ 0 to 0.99 HFU
○ 1.0 to 1.49 HFU
⊙ 1.50 to 1.99 HFU
● 2.0 to 2.49 HFU
▲ 2.5 to 2.99 HFU
■ Greater than 3.0 HFU

well, and Decker (1972) show that most of the heat flow in the western United States (1.4 HFU) comes from the mantle. The remaining 0.6 HFU comes from radiogenic heat production in the crust. Local variations in heat flow may result from local variations in the concentration of radioactive elements in the crust and this factor has to be compensated for in determining heat flow in an area.

Heat flow is the product of the geothermal gradient times the thermal conductivity of the rocks conducting the heat. Thus, the geothermal gradient may vary considerably from place to place within an area of constant heat flow due to variations in composition and thermal conductivity of the strata from one to another. Ground water may also transport a portion of the normal heat flow away laterally, thus masking the actual heat flow in an area. Geothermal gradient measurements from oil and gas drill holes and from other sources are not indicative of the true heat flow in an area unless the average thermal conductivity of the underlying strata is known and taken into account. Furthermore, flowing fluids introduce large errors into measurements of the geothermal gradient.

Blackwell and Robertson (1973) calculated an average value for radiogenic heat production in the crust of Montana based on the distribution of radioactive elements in the Boulder batholith. The calculated value for radiogenic heat production is about 0.6 HFU, and the average measured value of heat flow for the batholith is 1.98 HFU. Thus, the average value for heat flow from the mantle in this part of Montana is about 1.4 HFU.

The measured geothermal gradient of 31.9°C/km at

Butte, Montana (Robertson and Bossard, 1970) is the quotient of the heat flow value of 2.0 HFU divided by the thermal conductivity of the Butte Quartz Monzonite as measured in this area. The thermal conductivity of the Butte Quartz Monzonite can be assumed to approximate the thermal conductivity of the crystalline basement rocks in the crust under western Montana where a minimum thermal conductivity is 6.6×10^{-13} calcmsec$^{\circ}$C. In order for water circulating to depth in the Butte area to attain a reservoir temperature of 100°C, the water will have to circulate to a depth of 3 km where it will attain a temperature of 103.5°C, assuming a mean annual surface temperature of 8°C for the area.

Permeable fault zones attaining a depth of 3 km must extend well below the normal Paleozoic sediment thickness into crystalline basement rocks. The depth of the permeable portion of such faults where ground water can circulate is probably limited by earth pressures which force the permeable zone closed at a certain depth. This depth probably averages 3 km fairly consistently throughout western Montana due to the similarity of rock strength for fairly homogeneous basement rocks.

The effective geothermal gradient establishing the base temperature in the reservoir of a hydrothermal system circulating in such a fault zone is that of the rock units below the deepest level of water circulation. The geothermal gradient in the wall rocks above the level of heat transfer to the thermal waters determines the rate of loss of heat due to conduction of heat from the thermal fluid into the wall rocks. Thus, the geothermal reservoir in

such a system may be defined as the zone in which the thermal water is gaining heat from the wall rocks. The thermal water is probably losing heat to the wall rocks in the discharge system.

The radiogenic heat production in the Precambrian basement rocks can be assumed to be negligible (Sclater and Francheteau, 1970). Thus, the average minimum heat flow for western Montana is 1.4 HFU and the minimum assumed geothermal gradient is 30.0°C/km based on the Butte heat flow data (Table II). Local increases in radiogenic heat production or thermal conductivity of the Precambrian basement rocks will result in a higher geothermal gradient (higher temperatures per unit of depth). The similarity of calculated base temperatures for Montana hydrothermal systems (in the relatively high-temperature category) suggests that these hydrothermal systems result from circulation of ground water to depths of approximately 3 km along a geothermal gradient of about 30°C/km. This conclusion is supported by the close association of the relatively high-temperature category of hot springs with major faults, potentially deep fracture zones, and vertically deformed aquifers in deep regional structures.

SUMMARY

Montana hydrothermal systems consist of deep ground water circulating in permeable fault zones, fracture zones, and vertically deformed aquifers. Heat is transferred to the deep ground waters from the wall rocks by conduction. The major heat source is heat flow from the mantle. Base temperatures are determined by the regional heat flow, thermal conductivity of the crystalline basement rocks, and the depth of circulation of the thermal waters.

Thermal waters ascending from hydrothermal reservoirs in Montana hydrothermal systems cool by conductive transfer of heat from the waters to the wall rocks of the discharge system. Steam loss is not a significant mechanism of cooling in Montana hydrothermal systems. Discharge temperatures vary widely for different Montana hot springs; however, base temperatures fall into two groups. The low-temperature group of base temperatures averages 15 to 20°C and usually result from circulation in shallow structures on the flanks of uplifts. The high-temperature group of base temperatures averages 100 to 120°C and results from deep circulation in major faults or in deep regional structures.

Dissolved silica calculated base temperatures are the most reliable estimate of hydrothermal reservoir temperatures for the temperature range 15 to 150°C. Dilution of thermal waters by cold ground waters will cause base temperatures calculated from dissolved silica concentrations to be low. Cold water dilution is indicated by a Mg concentration greater than 3 to 5 ppm in the thermal discharge water. The approximate amount of

cold water dilution can be calculated and corrected for if the Mg and dissolved silica concentrations of the diluting cold waters are known. Assimilation of dissolved silica from amorphous silica in the wall rocks of Montana hydrothermal systems is not a source of error in the systems studied. However, amorphous silica assimilation could be a significant source of error in hydrothermal systems circulating in stratified volcanics containing obsidian or welded tuff units.

Net reactions controlling Na, K, and Ca concentrations in the temperature range 15 to 150°C may be considerably different from those net reactions assumed for the empirical curve for Na-K-Ca temperature relations. Net reactions in the temperature range 15 to 150°C may belong to three categories. In one category, the net reactions are those assumed for the empirical curve of Fournier and Truesdell (1973). Where the formation of the alteration mineral, K-mica, controls K concentrations, the stoichiometry of the net reations changes to that of reactions involving only Na and Ca minerals. The empirical curve of Fournier and Truesdell (1973) can be adjusted to these net reactions by using a stoichiometric contrast between 0 and 1. Where formation of the alteration mineral, kaolinite, controls K concentrations, the reactions change to those involving only Na and K minerals. Use of Na-K-Ca ratios to calculate reservoir temperatures where these net reactions are in effect requires knowledge of (1) the composition of the wall rocks in the system and (2) the low-temperature stability phase relations of the systems describing

the wall rock minerals.

Stability relations for phases in the system K_2O-Al_2O_3-SiO_2-H_2O at various temperatures can be calculated from thermochemical data. These stability relations can be used to semiquantitatively predict the relative amounts of Na, K, and Ca in solution in thermal discharge waters for a given stability relation. Based on these general relations, the Na, K, and Ca concentrations in thermal discharge waters can be used to determine the stable mineral phase in a hydrothermal system. This knowledge makes it possible to select the proper net reactions for the water/rock reactions in the system and thus choose the proper Na-K-Ca versus temperature relation for the hydrothermal system.

Further research should include construction of a new empirical curve from existing data for systems in which K-mica is the stable alteration mineral. This would determine the correct stoichiometric constant for these systems. Calculation of stability relations in the systems K_2O-Al_2O_3-SiO_2-H_2O at various temperatures would be helpful in predicting stable mineral phases from dissolved solids content in discharging waters. Additional research regarding the temperature dependency of Na and K leaching during kaolinization in the temperature range 15 to 150°C is required if Na-K-Ca temperatures are to be calculated for systems where kaolinite is the stable alteration mineral.

APPENDIX I

WATER ANALYSIS

Sodium and Potassium

The Na and K concentrations in the thermal water were determined by direct-intensity measurements of selected spectral lines in a Perkins-Elmer flame photometer. The principles and procedures of the flame photometer method are the same for both Na and K and will be discussed together.

The water sample is sprayed into a gas flame by a continous feed aspirator where excitation and spectral emission are reproducible. Spectral lines of wavelengths 589 mu and 768 mu for Na and K, respectively, are isolated by a slit arrangement. The light intensity of the spectral lines is measured directly by a phototube potentiometer. The intensity of light at these wave lengths is approximately proportional to the concentration of the element.

Calibration curves of intensity versus element concentration are constructed from known standards. In this study, Na standards of 0, 50, 100, and 200 ppm and a K standard of 0, 10, 25, and 50 ppm were used to construct calibration curves for the Na range of 0 to 200 ppm and the K ranges of 0 to 10 and 0 to 50 ppm. The Na and K concentrations in thermal water samples were determined by consulting the appropriate calibration curve. Standard solutions were prepared according to procedures set forth in Standard Methods for the Examination of Water and Wastewater published by the American Public Health Associations, Inc.

The presence of interfering substances was not a

problem in analysis of the thermal waters. Burner-clogging particulate matter was absent; however, some problems with aspirator clogging were encountered. The empirical reproducibility of this method is within ± 10 percent error with the instrument used. For direct reference to the calibration curve:

$$\text{ppm Na or K} = (\text{ppm Na or K in sample}) \times D$$

where D = dilution ratio = $\frac{\text{ml sample} + \text{ml distilled water}}{\text{ml sample}}$

Calcium and Magnesium

Calcium and Mg concentrations in the thermal water samples were determined using the EDTA (ethylenediaminetetraacetic acid) titrimetric method. Reproducibility within ± 5 percent was attained. In this method, EDTA added to the sample combines with Ca and Mg presennt. When all the available Ca and Mg in the sample reacts with the EDTA titrant, additional EDTA titrant reacts with an indicator to give a distinct end point. If pH is made sufficiently high, Mg precipitates as a hydroxide and the EDTA reacts only with Ca.

Total Ca and Mg concentrations are determined by buffering 20 or 25 ml of sample to pH 10 with ammonium chloride and titrating with 0.020 M EDTA to a blue end point using Eriochrome Blue and Black R indicator. The general calculation is as follows:

$$\frac{\text{ml EDTA (titration)}}{\text{ml sample}} \times 0.02 = \text{Molal Ca + Mg}$$

Calcium is determined by buffering 20 or 25 ml of sample to pH 10 with 1M NaOH and titrating with 0.020M

EDTA to a purple end point using Calmagite (ammonium purpurate) indicator. The general calculation is as follows:

$$\frac{\text{ml EDTA (titration)}}{\text{ml sample}} \times 0.02 = \text{molal Ca.}$$

Molality Ca x 10^5 = ppm $CaCO_3$;

0.4 x ppm $CaCO_3$ + ppm Ca.

Molal (ca + Mg) - molal (Ca) = molal Mg

and molal Mg x 24.3 = ppm Mg.

Chloride

Chloride concentrations in the thermal water samples were determined using a silver nitrate back-titration. Chloride in the water samples is reacted with an excess of $AgNO_3$ which is added in a known amount. The sample is then back-titrated with KSCN (potassium thiocyanide) which reacts with the excess Ag. When the excess Ag reacts completely with the KSCN, additional KSCN reacts with a suitable Fe indicator (any soluble Fe) to form a salmon pink soft end point. This method is easily reproducible within ± 10 percent accuracy. A sample procedure and calculation is shown below.

Example:

Assume 9.85 ml 0.01NKSN are required to precipitate the Ag in 1.0 ml 0.1N $AgNO_3$ in distilled water (Cl free). Assume also that 9.32 ml 0.01N KSCN is required to titrate a 15 ml sample with 1.0 ml 0.1N $AgNO_3$ to a salmon pink end point under acid conditions using Fe indicator (add HNO_3 to obtain acid conditions).

Then 9.85 - 9.32 = 0.53 KSCN not required to react with Ag. Therefore the silver used by Cl corresponds to

$(.53/9.85)(0.1)(10^{-3}) = 5.38 \times 10^{-6}$ equivalents of Ag/15 ml sample,

so $(1000/15)(5.38 \times 10^{-6}) = 3.58 \times 10^{-4}$ equivanents per liter Cl,

$(35.5)(3.58 \times 10^{-4}) = 1.26 \times 10^{-2}$ grams Cl,

so Cl = 12.6 ppm.

Dissolved Silica

Dissolved silica is detected by a modification of the Heteropoly Blue method for use in the field. Two types of silica are analysed for. Silica initially in a "molybdate-reactive" form in the thermal waters considered to be monosilicic "dissolved" silica. Silica initially in a "molybdate-unreactive" form is considered to be polysilicic of possibly colloidal silicate. Molybdate-unreactive silica is converted to a reactive form by addition of NaOH which reacts to dissolve all forms of silica present. The total silica content measured after treatment of the sample with NaOH is termed "total" silica. Dissolved silica values are used for estimating hydrothermal reservoir temperatures and the optional step to detect total silica content may be omitted.

Ammonium molybdate at approximately pH 1.2 reacts with monosilicic molecules and with phosphate to produce heteropoly acids. Oxalic acid destroys molybdophosphoric acid but not molybdosilicic acid. Yellow molybdosilicic acid is reduced to heteropoly blue by means of stannous chloride in glycerin. Heteropoly blue provides increased sensitivity and is measured with a

portable filter photometer in the wavelength range 600-815 mu.

Because this method has been modified for field use, it is set forth here in detail. Apparatus includes the following:

four 15 ml graduated polyethylene centrifuge tubes, with corks
four 15 ml polypropylene squeeze-dropper bottles
one dark glass bottle with eye dropper
one 1.0 ml pipette
two 500 ml polypropylene wash bottles
one portable filter photometer with curvette tubes
one saucepan with 4-tube testtube rack
one portable stove
one laboratory testtube rack
miscellaneous polypropylene bottles for reagents

The field analysis for dissolved and total silica is described below. The four centrifuge tubes containing the blank; dissolved silica; total silica; and standard silica solution will be referred to as tubes 1, 2, 3, and 4 respectively.

Procedure:

1. Pipette 1.0 ml water sample into tubes 2 and 3. Pipette 1 ml 250 ppm standard silica solution into tube 4.

2. Dilute tubes 1, 2, 3, and 4 up to 5 ml with silica-free water.

3. Add 1 drop 1N NaOH solution to tubes 1, 3, and 4 from a squeeze-dropper bottle and boil samples in saucepan for 5 minutes.

4. At end of 5 minutes add 1 drop 6N HCl, 1 drop 1N NaOH, and 2 drops 6N HCl to tube 2 in that order. This step is to adjust salinity in tube 2 to match salinity in the others because salinity affects color intensity.

5. Add 3 drops 6N HCl to tubes 1, 3, and 4 and 3 drops ammonium molybdate solution to all tubes. Wait 5 minutes to insure complete reaction.

6. Add 3 drops oxalic and solution to all tubes and wait 2 minutes to insure complete breakdown of any molybdophosphoric acid in the samples.

7. Add 1 drop stannous chloride solution to each sample and mix vigorously.

8. Transfer samples to curvette tubes and measure color intensity.

9. Calibrate colorimeter to 100 percent transmissibility using tube 1 to zero out any silica present in the stock reagents.

10. Measure transmissibility of tubes 2, 3, and 4 while checking calibration with tube 1 between measurements.

Calculations:

Absorbance = $\log(100/\%T) = 2 - \log\%T$

where %T = transmissibility measured with the colorimeter

and ppm silica in sample = $250 \times \frac{\text{absorbance sample}}{\text{absorbance standard}}$

This method consistently yields results within $\pm$ 10 percent error and usually within $\pm$ 5 percent error. The main source of error in inaccurate pipetting and dilutions. All polypropylene or polyethylene bottles and centrifuge tubes must be used to prevent silica assimilation.

APPENDIX II

PETROLOGY

Alhambra Hot Springs

The Butte Quartz Monzonite at Alhambra Hot Springs consists of a medium-grained, seriate, biotite quartz monzonite. Modal composition is 39.0 percent plagioclase; 26.6 percent of K-feldspar; 25.8 percent quartz; 8 percent biotite; and traces of magnetite, zircon, and other unidentified non-opaque accessory minerals. Blocky euhedral to subhedral plagioclase crystals are enclosed by smaller interstitual grains of anhedral K-feldspar and quartz. The palgioclase grains are mostly andesine, An_{40} to An_{45}, as determined from the extinction angles of Carlsbad-albite twins. Euhedral to subhedral biotite books are partially to completely chloritized. Other secondary minerals include hematite and limonite after magnetite and traces of poorly developed sericite in most feldspar grains. Hydrothermally altered samples of quartz monzonite were not collected.

Samples of hydrothermally altered alaskite consist of fine to coarse-grained, seriate, limonitic, kaolinitic, alaskite with a modal composition of 77.0 percent quartz, 19.4 percent secondary kaolinite after feldspars, 30 percent K-feldspar, and 0.6 percent secondary limonite after biotite. Prior to alteration, this rock was a granophysic mass of intergrown quartz enclosing slightly larger grains of feldspars. The remaining unaltered K-feldspar is microcline and is completely enclosed in quartz which protects it from hydrothermal alteration. The kaolinite mineral alteration product replacing the feldspars was identified by X-ray diffraction.

Boulder Hot Springs

The Butte Quartz Monzonite at Boulder Hot Springs is a dark greenish-gray, medium-grained, hypidiomorphic, porphyritic, biotite-hornblende quartz monzonite consisting of 33.6 percent K-feldspar; 30.8 percent plagioclase; 26.4 percent quartz; 4.4 percent biotite; 3.1 percent amphibole; 0.9 percent chlorite; and 0.8 percent opaque and non-opaque accessory minerals, predominately magnetite. The euhedral plagioclase phenocrysts are andesine, An_{40} to An_{45}, as determined from Carlsbad-albite, twin extinction angles. K-feldspar (orthoclase) forms blocky subhedral replacement phenocrysts. Quartz is anhedral and interstitual. Biotite shreds and irregular hornblende and actinolite masses are generally unaltered. Traces of sericite are present along cleavages of most of the feldspars.

The highly sericitized aplitic alaskite is a light gray, fine-grained, hypidiomorphic-granular, sericitized, quartz grantite (alaskite). Modal composition of the alaskite varies considerably but averages but averages 50 percent quartz and 50 percent orthoclase. Semiraidiating foils of sericite are developing in grain contacts, mostly at the expense of orthoclase. Many sericite foils are megascopic muscovite.

Hydrothermally altered quartz monzonite saturated with thermal waters, as at the tunnel (Figure 8) was not collected in time X-ray diffraction analysis. This altered rock is friable and megascopically consits of unaltered quartz grains, biotite grains, and a very pale green crumbly alteration product of the feldspars. The

pale green alteration mineral is thought to be sericite.

The dike-like hydrothermal veins filling the joints at Boulder Hot Springs consist of a central core of chalcedony sandwiched by calcite layers. The weathered surfaces of the calcite layers often exhibit a skeletal box-work consisting of thin silicate sheets from which enclosed calcite has been etched. Optical examination shows the silicate films of the box-work to be microcrystalline silica replacements of another mineral. Descriptions of the veins by Weed (1900) suggest that the veins also show that silica is replacing the primary calcite.

Helena Hot Springs

Samples of hydrothermally altered wall rock were not obtained at Helena Hot Springs and no extensive hydrothermal alteration is evident near the springs. The wall rocks consist of a light gray, fine to medium-grained, seriate to hypidiomorphic-granular, biotite quartz monzonite. The modal composition is 33.1 percent plagioclase, 25.5 percent K-feldspar, 24.8 percent quartz, 16.6 percent biotite, and trace amounts of magnetite and other unidentified accessory minerals. Traces of sericite are commonly present along cleavages and fractures of most of the feldspar grains.

Salmon Hot Springs

The dominant wall rocks of the Salmon Hot Springs hydrothermal system are a hard, dense, dark-colored, pink to lavender, volcanic breccia. Megascopically, the volcanic fragments average about 1.5 cm in size and contain a few biotite and quartz phenocrysts set in the finely

microcrystalline to glassy groundmass. In thin section, the megascopically observable quartz phenocrysts appear as quartzite fragments, probably plucked from the Precambrian Belt rocks in the volcanic vent. Smaller quartz phenocrysts about 0.2 mm in size are present in large numbers but are not distinguishable megascopically. The quartz phenocrysts are mostly confined within the volcanic rock fragments, however, a few cut across mutual contacts of adjacent rock fragments. The quartz phenocrysts and the quartzite fragments often exhibit embayed and crenulated margins and smaller quartz phenocrysts are often partially resorbed. The quartz phenocrysts exhibit uniform extinction.

In thin section, the volcanic rock fragments consist of clastic, fine-grained, microgranular intergrowths of quartz and K-feldspar(?) containing a few biotite shreds and quartz phenocrysts. The hematitic matrix cementing the volcanic rock fragments appears to be devitrified glass in some samples and altered microgranular rock in other samples. In some samples, the devitrified appearing matrix consists of shard-like aggregates of a mineral with high interference colors which may be a montmorillonite mineral.

Megascopically, the hydrothermally altered volcanic breccia appears bleached and is softened presumably due to the formation of clay alteration minerals. In thin section, the hydrothermally altered volcanic breccia is very similar in appearance to the unaltered rocks. The only obvious difference is the chloritization and hematization of the biotite shreds. This is not meant to imply

that they hydrothermally altered rocks are not significantly altered. The megascopically visible clayey alteration product is probably a kaolinite mineral with typically weak gray to white interference colors which cannot be resolved from the microgranular K-feldspar by the microscope used in this study.

APPENDIX III

MINERAL STABILITY CALCULATION

The stability phase relations for K-feldspar and K-mica may be calculated for any temperature using the method shown by Garrels and Christ (1965). The reaction for alteration of K-feldspar to K-mica shows that only three variables are involved: K, H, and H_4SiO_4. The ratio of K to H remains unity in the equilibrium constant. Thus, the mineral relations can be described in two-dimensions using the ratio of K to H as one axis, and the activity (molality) of H_4SiO_4 as the other axis. The reaction and its equilibrium constant are as follows:

$$3KAlSi_3O_8(s) + 2H^+(aq) + 12H_2O(liq)$$

K-feldspar

$$\text{---} \; KAl_3Si_3O_{10}(OH)_2(s) + 6H_4SiO_4(aq) + 2K^+(aq) \qquad (1)$$

K-mica

$$K_{eq} = (K^+)(H_4SiO_4)^3/(H^+) \qquad (2)$$

$$\log K_{eq} = -4.9 = \log(K^+)/(H^+) + 3\log(H_4SiO_4) \qquad (3)$$

The value -4.9 represents the sum of the free energy of formation of the constituents in reaction (1) at 25°C. The equilibrium constant, K_{eq}, may be recalculated for any temperature by summation of the free energy of formation of the reaction constituents at the specified temperature. Robie and Waldbaum (1968) show the free energies of formation at 400°K for the following constituents: K-feldspar, -874.504; K-mica, -1299.103; H_2O, -58.081; and H_4SiO_4, -200.197.

Thus, $3(-874.504) + 12(-58.081) = -1299.103 + 6(-200.197)$
and $-2623.512 - 696.272 + 1299.103 + 1201.182 = -820.234$

so $G^{\circ}_{400} = -820.234$ kcal/gram formula weight

and $G^{\circ}_{T} = -RT\log K_{eq}$

so $\log K_{eq} = G^{\circ}_{400}/-RT = *8.20/1.83 = -4.48.$

Now $-4.48 = \log(K^+/H^+) + 3\log(H_4SiO_4)$ at 400°K where H_4SiO_4 is the dissolved silica measured in the discharge water. Thus, $\log(K^+/H^+)$ can be solved for using any number of dissolved silica values and the line described by the resultant points plotted as $\log(K^+/H^+)$ vs $\log(H_4SiO_4)$ is the boundary between the K-mica and K-feldspar stability fields. Some points on the line for $\log K_{eq} = -4.48$ are as follows:

SiO_2 (ppm)	$\log(K^+/H^+)$
10	-8.37
20	-6.57
30	-6.04
40	-5.66
50	-5.37
60	-5.13
80	-4.76
100	-4.47

REFERENCES CITED

American Public Health Association, 1971, Standard methods for the examination of water and wastewater, 13th ed.

Arnorsson, S., 1970, Geochemical studies of thermal waters in the southern lowlands of Iceland: U.N. Symp. Devel. Util. Geotherm. Res., Pisa.

Balster, C.A., and Groff, S.L., 1972, Potential geothermal resources in Montana, in Geothermal Overviews of the Western U.S., Geothermal Resources Council, p. G-1 to G-9.

Becker, H.F., 1961 Oligocene plants from the upper Ruby River basin, southwestern Montana: Geol. Soc. America Mem. 82, 127 p.

Becraft, G.E., Pickney, D.M., and Rosenblum, Sam, 1963, Geology and mineral deposits of the Jefferson City quadrangle, Jefferson and Lewis and Clark counties, Montana: U.S. Geol. Survey Prof. Paper 428, 101 p.

Biehler, Shawn, and Bonani, W.E., 1969, A regional gravity study of the Boulder batholith, Montana: Geol. Soc. America Mem. 115, p. 401-422.

Blackwell, D.D., 1973, Oral communication regarding relict heat in Tertiary intrusives.

Blackwell, D.D., 1969, Heat-flow determinations in the northwestern United States: Jour. Geophys. Res., v. 74, p. 992-1007.

Blackwell, D.D., and Baag, C., 1973, Heat flow in a blind geothermal area near Marysville, Montana: Geophysics preprint.

Blackwell, D.D., and Robertson, E.C., 1973, Thermal studies of the Boulder batholith and vicinity, Montana: Soc. Econ. Geol., Butte Field Meeting Guidebook, p. D-1 to D-8.

Brown, G., Editor, 1961, The X-ray identification and crystal structures of clay minerals: Mineralog. Soc. London, Jarrold & Sons Ltd., Norwich, 544 p.

Browne, P.R.L., 1970, Hydrothermal alteration as an aid in investigating geothermal fields: U.N. Symp. Devel. Util. Geotherm. Res., Pisa.

Clarke, Frank Wigglesworth, and Others, 1886, Report of work done in the division of chemistry and physics, mainly during the fiscal year 1884-85: U.S. Geol. Survey Bull. 27, 80 p.

Dorr, J.A., and Wheeler, W.H., 1964, Cenozoic paleontology, stratigraphy, and reconnaissance geology of the upper Ruby River basin, southwestern Montana: University of Michigan Contr. Museum Paleont., v. XIII, no. 12, p. 297-339.

Ellis, A.J., 1970, Quantitative interpretation of chemical characteristics of hydrothermal systems: U.N. Symp. Devel. Util. Geotherm. Res., Pisa, v. 25.

Ellis, A.J., and Mahon, W.A.J., 1967, Natural hydrothermal systems and experimental hot-water/rock interactions (Part II): Geochim. et Cosmochim. Acta, v. 31, p. 519-538.

Ellis, A.J., and Mahon, W.A.J., 1964, Natural hydrothermal systems and experimental hot-water/rock interactions (Part I): Geochim. et Cosmochim. Acta, v. 28, p. 1323-1357.

Ellis, A.J., and McFadden, I.M., 1972, Partial molal volumes of ions in hydrothermal solutions: Geochim. et Cosmochim. Acta, v. 36, p. 413-426.

Facca, G., 1969, Geophysical investigations in the self-sealing geothermal fields: Bull. volcanol., v. 33, p. 119-121.

Facca, G., and Tonani, F., 1967, The self-sealing geothermal field: Bull. volcanol., v. 30, p. 271-273.

Feth, J.H., Roberson, C.E., and Polzer, W.L., 1964, Sources of mineral constituents in water from granitic rocks, Sierra Nevada, California and Nevada: U.S. Geol. Survey Water-Supply Paper 1535-I.

Fournier, R.O., and Rowe, J.J., 1966, Estimation of underground temperatures from the silica content of water from hot springs and wet-steam wells: Am. Jour. Sci., v. 264, p. 685-697.

Fournier, R.O., and Truesdell, A.H., 1973, An empirical Na-K-Ca geothermometer for natural waters: Geochim. et Cosmochim. Acta, v. 37, p. 1255-1275.

Fournier, R.O., and Truesdell, A.H., 1970, Chemical indicators of subsurface temperature applied to hot spring waters of Yellowstone National Park, Wyoming, U.S.A.: U.N. Symp. Devel. Util. Geotherm. Res., Pisa., v. 2.

Garrels, R.M., and Christ, C.L., 1965, Solutions, minals, and equilibria: Harper and Row, New York, 450 p.

Garrett, H.L., 1972, Structural geology of the Crazy Mountains basin, in Mont. Geol. Soc. Guidebook 21st Ann. Field Conf.: p. 113-118.

Grim, R.E., 1968, Clay mineralogy, 2nd ed.: McGraw-Hill, New York.

Hadley, H.D., 1972, A philosophical review with some conclusions concerning the search for oil and gas in the Crazy Mountain basin, in Mont. Geol. Soc. Guidebook 21st Ann. Field Conf.: p. 159-163.

Hamilton, Warren, and Meyers, W.B., 1967, The nature of batholiths: U.S. Geol. Survey Prof. Paper 554-C, 30 p.

Hansen, A., 1964, Thermal cycles for geothermal sites and turbine installation at The Geysers power plant, California: Conf. New Sources Energy Proc., Rome 1961, v. 3, p. 365.

Hemley, J.J., 1967, Aqueous Na/K ratios in the system K_2O-Na_2O-Al_2O_3-SiO_2-H_2O: Geol. Soc. America Spec. Paper 115, p. 94.

Huang, W.H., and Kiang, W.C., 1973, Gibbs free energies of formation calculated from dissolution data using specific mineral analysis; III Clay Minerals: Am. Mineralogist, v. 58, p. 1016-1022.

Iler, R.K., 1955, The colloid chemistry of silica and silicates: Cornell University Press, Ithica, N.Y.

Jaeger, J.C., 1965, Application of the theory of heat conduction to geothermal measurements, in Terrestrial Heat Flow: Geophys. Monograph 8, ed. by W.H.K. Lee, American Geophysical Union, Washington, D.C., p. 7-23.

Jaeger, J.C., 1957, The temperature in the neighborhood of a cooling intrusive sheet: Am. Jour. Sci., v. 255, p. 306-318.

James, Russell, 1968, Wairakei and Larderello; geothermal power systems compared: New Zealand Jour. Sci., v. 11, p. 706-719.

Johnson, R.W., Jr., Henderson, J.R., and Tyson, N.S., 1965, Aeromagnetic map of the Boulder batholith area, southwestern Montana: U.S. Geol. Survey Geophys. Inv. Map GP-538.

Kennedy, G.C., 1950, A portion of the system silica-water: Econ. Geology, v. 45, p. 629.

Klepper, M.R., 1973, Geology of the southern part of the Boulder batholith: Soc. Econ. Geol., Butte Field Meeting Guidebook, p. B, abstract.

Klepper, M.R., Robinson, G.D., and Smedes, H.W., 1971, On the nature of the Boulder batholith of Montana: U.S. Geol. Survey Bull. 82, p. 1563-1580.

Klepper, M.R., Weeks, R.A., and Ruppel, E.T., 1957, Geology of the southern Elkhorn Mountains, Montana: U.S. Geol. Survey Prof. Paper 292, 82 p.

Knopf, Adolph, 1963, Geology of the northern part of the Boulder batholith and adjacent area, Montana: U.S. Geol. Survey Misc. Geol. Inv., Map I-381.

Krauskopf, Konrad B., 1956, Dissolution and precipitation of silica at low temperatures: Geochim. et Cosmochim. Acta, v. 10, p. 1-26.

Lewis, Meriwether and Clark, William, 1814, History of the expedition of Captains Lewis and Clark 1804-5-6, with introduction and index by James K. Hosmer: Chicago, Ill., A.C. McClurg & Co., 2 v., v. 1, 500 p., front., 3 maps; v. 2, 583 p., front., 3 maps; 2nd ed., 1903, Cambridge, Mass., Univ. Press.

Mahon, W.A.J., 1970, Chemistry in the exploration and exploitation of hydrothermal systems: U.N. Symp. Devel. Util. Geotherm. Res., Pisa., v. 4.

Mahon, W.A.J., 1966, Silica in hot water discharged from drillholes at Wairakei, New Zealand: New Zealand Jour. Sci, v. 9, p. 135-144.

Marshall, D.C., 1965, Preliminary theory of the Wairakei geothermal field: New Zealand Jour. Sci., v. 9, p. 651-673.

McNitt, James R., 1965, Review of geothermal resources, in Terrestrial Heat Flow: Geophys. Monograph 8, ed. by W.H.K. Lee, American Geophysical Union, Washington, D.C., p. 240-266.

Morey, G.W., Fournier, R.O., and Rowe, J.J., 1962, The solubility of quartz in water in the temperature interval from 29°C to 300°C: Geochim. et Cosmochim. Acta, v. 26, p. 1029.

Muffler, L.J.P., and White, D.E., 1969, Active metamorphism of Upper Cenozoic sediments in the Salton Sea geothermal field and Salton Trough, southeastern California: U.S. Geol. Survey Bull. 80, p. 157.

Mullan, John, Jr., 1855, Report of a reconnaissance from the Bitter Root Valley to Fort Hall, thence to the head of Hell Gate River, thence to the Bitter Root Valley: U.S. War Department, Reports of explorations and surveys***for a railroad from the Mississippi River to the Pacific Ocean: U.S. 33rd Cong., 2nd sess., S. Doc. 78, v. 1. pt. 1, Reports from the field, p. 322-349.

Orville, P.M., 1963, Alkali ion exchange between vapor and feldspar phases: Am. Jour. Sci., v. 261, p. 201-237.

Paces, Thomas, 1972, Chemical characteristics and equilibration in natural water-felsic rock-CO_2 system: Geochim. et Cosmochim. Acta, v. 36, p. 217-240.

Peal, Albert Charles, 1886, Lists and analyses of the mineral springs of the United States (a preliminary study): U.S. Geol. Survey Bull. 32, 235 p.

Perry, Eugene S., 1933, Possibilities of ground-water supply for certain towns and cities of Montana: Montana Bur. Mines and Geol, Misc. Contr., no. 2, p. 23.

Rikitake, T., 1959, Studies of the thermal state of the earth. The second paper: Heat flow associated with magma intrusion: Bull. Earthquake Res. Inst., Tokyo Univ., v. 37, p. 233-243.

Roberts, W.A., and Gude, A.J., 1953, Uranium-bearing deposits west of Clancey, Jefferson County, Montana: U.S. Geol. Survey Bull. 988-F, p. 121-141.

Robertson, E.C., and Bossard, F.C., 1970, Investigation of heat transfer on a deep level in the Butte district: AIME Preprint no. 70-AU-125, p. 27.

Robie, R.A., and Waldbaum, D.R., 1968, Thermodynamic properties of minerals and related substances at 298.15°K (25°C) and one atmosphere (1.013 Bars) pressure and at higher temperatures: U.S. Geol. Survey Bull. 1259, 256 p.

Robinson, G.D., 1967, Geologic map of the Toston quadrangle, southwestern Montana: U.S. Geol. Survey, Map I-486.

Robinson, G.D., 1963, Geology of the Three Forks quadrangle, Montana: U.S. Geol. Survey Prof. Paper 370.

Roy, R.F., Blackwell, D.D., and Decker, E.R., 1972, Continental heat flow, in the nature of the solid earth, edited by E.C. Robertson: McGraw-Hill, N.Y., p. 506-543.

Ryall, A., Slemmons, D.B., and Gedney, L.D., 1966, Seismicity, tectonism, and surface faulting in the western United States during historic time: Bull. Seismolog. Soc. Amer., v. 56, no. 5, p. 1105-1135.

Schoen, Robert and White, D.E., 1965, Hydrothermal alteration in GS-3 and GS-4 drill holes, main terrace, Steamboat Springs, Nevada: Econ. Geology, v. 60, p. 1411-1421.

Schuster, J. Eric, 1973, The search for hot rocks; geothermal exploration, northwest: State Department of Washington, Department of Natural Resources, Division of Mines and Geology, Reprint no. U.

Sclater, John G., and Francueteau, Jean, 1970, The implications of terrestrial heat flow observations on current tectonic and geochemical models of the crust and upper mantle of the earth: Geophys. Jour. Royal Astr. Soc., v. 20, p. 509-542.

Sigualdason, Gudmundure, 1962, Epidote and related minerals in two deep geothermal drill holes, Reykjavik and Hveragerdi, Iceland: U.S. Geol. Survey Prof. Paper 450-E, p. E-77-E79.

Smedes, Harry W., 1973, Regional geologic setting of the Boulder batholith, Montana: Soc. Econ. Geol., Butte Field Meeting Guidebook, p. A, abstract.

Smedes, Harry W., 1966, Geology and igneous petrology of the northern Elkhorn Mountains, Jefferson and Broadwater counties, Montana: U.S. Geol. Survey Prof. Paper 510, 116 p.

Smedes, H.W., Klepper, M.R., and Tilling, R.I., 1973, The Boulder batholith, Montana: Soc. Econ. Geol., Butte Field Meeting Guidebook, p. E-1 - E-3.

Stoll, W.C., and Armstrong, F.C., 1958, Optical calcite deposits in Park and Sweet Grass counties, Montana: U.S. Geol. Survey Bull. 1042-M.

Tilling, R.I., 1973, The Boulder batholith, Montana: Product of two contemporaneous but chemically and isotopically distinct magma series: Soc. Econ. Geol., Butte Field Meeting Guidebook, p. C-1 - C-5.

Tilling, R.L., Klepper, M.R., and Obradovich, J.D., 1968, K-Ar ages and time span of emplacement of the Boulder batholith, Montana: Am. Jour. Sci., v. 266, no. 8, p. 671-689.

Tonani, F., 1970, Geochemical methods of exploration for geothermal energy: U.N. Symp. Devel. Util. Geotherm. Res., Pisa, v. 7.

Weed, Walter Harvey, 1905, Economic value of hot springs and hot-spring deposits: U.S. Geol. Survey Bull. 260, p. 598-604.

Weed, Walter Harvey, 1904, Gypsum deposits in Montana: U.S. Geol. Survey Bull. 223, p. 74-75.

Weed, Walter Harvey, 1900, Mineral vein formation at Boulder Hot Springs, Montana: U.S. Geol. Survey 21st Ann. Rept., pt 2, p. 227-255.

Weed, Walter Harvey, and Pirsson, Louis Valentine, 1896, Geology of the Castle Mountain mining district, Montana: U.S. Geol. Survey Bull. 139, 164 p., 17 pls., 11 figs.

White, D.E., 1970, Geochemistry applied to the discovery, evaluation and exploration of geothermal energy resources: U.N. Symp. Devel. Util. Geotherm. Res., Pisa, sec V.

White, D.E., 1968, Hydrology, activity, and heat flow of the Steamboat Springs thermal system, Washoe county, Nevada: U.S. Geol. Survey Prof. Paper 458-C.

White, D.E., 1965, Saline waters of sedimentary rocks, in subsurface environments: Am. Assoc. Petroleum Geologists Mem., v. 4, p. 342.

White, D.E., 1961, Preliminary evaluation of geothermal areas by geochemistry, geology, and shallow drilling: U.N. Conf. New Sourc. Energy, Rome.

White, D.E., 1957a, Thermal waters of volcanic origin: Geol. Soc. America Bull. 68, p. 1659.

White, D.E., 1957b, Magmatic, connate and metamorphic waters: Geol. Soc. America Bull. 68, p. 1659.

White, D.E., Craig, H., and Begemann, F., 1963, Summary of the geology and isotope geochemistry of Steamboat Springs, Nevada, in "Nuclear geology on geothermal areas",: Pisa, Cons. Naz. Ric., v. 9.

White, D.E., Hem, J.D., and Waring, G.A., 1963, Chemical composition of subsurface waters: U.S. Geol. Survey Prof. Paper 440-F.

White, D.E., Muffler, L.J.P., and Truesdell, A.H., 1971, Vapor dominated hydrothermal systems, compared with hot water systems: Econ. Geology, v. 66, p. 75-97.

White, D.E., and Sigvaldason, Gudmundur E., 1962, Epidote in hot-spring systems, and depth of formation of prophylitic epidotein epithermal ore deposits: U.S. Geol. Survey Prof. Paper 450-E, p. E80-E84.

MONTANA STATE UNIVERSITY LIBRARIES
3 1762 10014609 9

N378
K115
Cop.2